Peers Creek

Hydrotechnical Assessment and Design for Peers Creek Frontage Road Washout Site

Prepared by BGC Engineering Inc. for:

BC Ministry of Transportation and Infrastructure

May 23, 2023

Project 0272097

May 23, 2023 Project 0272097

BC Ministry of Transportation and Infrastructure
310-1500 Woolridge Street
Coquitlam, BC V3K 0B8

Attention: Mr. Chung, P.Eng.

Hydrotechnical Assessment and Design for Peers Creek Frontage Road Washout Site

Please find the above referenced report attached. We appreciate the opportunity to collaborate with you on this challenging and interesting project.

Should you have any questions, please do not hesitate to contact the undersigned.

Yours sincerely,

BGC Engineering Inc.
per:

Evan Shih, M.Eng., P.Eng.
Senior Hydrotechnical Engineer

EXECUTIVE SUMMARY

Flooding on the Coquihalla River in November 2021 caused extensive erosion and damage to infrastructure throughout the river valley, including washouts of Peers Creek Frontage Road (PCFR) near Hope, British Columbia (BC). BC Ministry of Transportation and Infrastructure (MoTI) retained BGC Engineering Inc. (BGC) to provide hydrotechnical engineering support for the reinstatement of PCFR.

BGC completed a detailed hydrological assessment to support design of the road and associated erosion protection. Analysis by BGC suggested that the Water Survey of Canada hydrometric gauge located nearest to the PCFR washout site may have malfunctioned during the November 2021 flood event and failed to capture its full magnitude. To estimate the magnitude of the November 2021 peak flow at the project site, BGC prepared a two-dimensional (2D) hydraulic model and calibrated the modeled water surface elevation to high water marks approximated from post-flood orthoimagery and aerial photographs. A peak flow was estimated by BGC to be approximately 900 m^3/s. The estimated peak flow was used to support flood frequency analysis (FFA) to update flood quantiles at the project site. As the Coquihalla River is subject to both snowmelt- and atmospheric river-related flood events, BGC applied a dual maximum series approach to the FFA.

A climate change assessment was completed using streamflow projections from the Pacific Climate Impacts Consortium (PCIC) to develop a climate change-adjusted FFA. BGC estimated trends in peak flows due to changes in atmospheric rivers and snowmelt independently and then combined the two processes to create an ensemble climate-adjusted model. A 69% increase in the 200-year flood magnitude is predicted within a 75-year timeline extending to 2097. The design flood event, defined by MoTI as the 200-year return period climate adjusted peak flow, was estimated to be 1,813 m^3/s at the project site.

During the detailed design phase, additional 2D hydraulic modelling was conducted to estimate design flood hydraulics for the proposed revetment configuration and to reflect instream works that had been completed by MoTI (for the reconstruction of Highway 5). Based on the modelling results, overtopping of the road is predicted to occur over most of PCFR within the project area. As overtopping of PCFR is also predicted to occur in areas outside of the project area, MoTI ultimately confirmed that overtopping of the reconstructed road is acceptable during the design flood event.

The proposed riprap revetment along PCFR spans an approximate length of 300 m along the previously washed-out section of the road and extending downstream along the natural bankline. The revetment will be constructed along the PCFR embankment at a 2H:1V slope. A launching apron is incorporated into the toe of the revetment to minimize excavation depths during construction. High design velocities estimated throughout the project reach necessitate the use of 2000 kg Class riprap for the majority of the revetment.

TABLE OF REVISIONS

Date	Revision	Remarks
April 12, 2023	0	Draft report
May 23, 2023	1	Final report

CREDITS AND ACKNOWLEDGEMENTS

This work was a collaborative effort conducted by several qualified subject matter experts, each of whom take responsibility for specific technical components and sections of this report. Responsible authors and relevant sections are listed below.

- Evan Shih, M.Eng., P.Eng.: Hydrotechnical assessment and design
- Melissa Hairabedian, M.Sc., P.Geo.: Hydrology and climate change assessment
- Sarah Davidson, Ph.D., P.Geo.: Geomorphic assessment

In addition, technical review was conducted by:

- Robert Millar, Ph.D., P.Eng., P.Geo.: Hydrotechnical assessment and design, geomorphic assessment
- Hamish Weatherly, M.Sc., P.Geo.: Hydrology and climate change assessment

BGC would like to acknowledge the following additional contributors to this report:

- Kenneth Lockwood PhD., P.Eng., Intermediate Hydrotechnical Engineer
- Steven Brazda, M.Sc., EIT, Engineer in Training
- Steven Rintoul, EIT, Engineer in Training
- Martin Devonald, M.Sc., P.Eng., Principal Geotechnical/Geological Engineer

LIMITATIONS

BGC Engineering Inc. (BGC) prepared this document for the account of BC Ministry of Transportation and Infrastructure. The material in it reflects the judgment of BGC staff in light of the information available to BGC at the time of document preparation. Any use which a third party makes of this document or any reliance on decisions based on it is the responsibility of such third parties. BGC accepts no responsibility for damages, if any, suffered by any third party as a result of decisions made or actions based on this document.

As a mutual protection to our client, the public, and ourselves, BGC submits all documents and drawings for the confidential information of our client for a specific project. Authorization for any use and/or publication of this document (or any data, statements, conclusions, or abstracts from or regarding our documents and drawings) through any form of print or electronic media including, without limitation, posting or reproduction of the same on any website, is reserved pending BGC's written approval.

A record copy of this document is on file at BGC. That copy takes precedence over any other copy or reproduction of this document.

TABLE OF CONTENTS

LIST OF TABLES

LIST OF FIGURES

LIST OF APPENDICES

1.0 INTRODUCTION

Flooding on the Coquihalla River in November and December 2021 caused extensive erosion and damage to infrastructure throughout the river valley, including the washout of Peers Creek Frontage Road (PCFR) near Hope, British Columbia (BC) (Figure 1-1 and Figure 1-2). The PCFR washout occurred during two separate flood events:

- November 15-16, 2021: the Coquihalla River eroded through PCFR and removed a small section of Highway 5. The river also avulsed along a portion of PCFR (Figure 1-2a).
- November 28-December 2, 2021: the Coquihalla River eroded further into Highway 5 upstream of the avulsion. The river also avulsed along the original mid-November avulsion path but continued further south, re-entering the mainstem of the Coquihalla River near the Peers Creek Highway 5 Bridge (Figure 1-2b).

BGC Engineering Inc. (BGC) is pleased to provide this document to the BC Ministry of Transportation and Infrastructure (MoTI) presenting our design basis for the hydrotechnical components of the PCFR recovery works. BGC is also providing engineering support to MoTI for recovery works at the Othello Road Washout and Site C project sites (Figure 1-1).

1.1 Project Scope

The scope of the work described in this report includes:

- An overview of the site hydrology and geomorphology (Section 2.0).
- Hydraulic modelling of the Coquihalla River at PCFR (Section 3.0).
- Hydrotechnical design of riprap bank protection along PCFR (Section 4.0).

This report should be read in conjunction with detailed design drawings produced by MoTI's road design and project management consultant, McElhanney Consulting Services Ltd. (McElhanney). BGC has also provided support for geotechnical aspects of the road design, which are discussed under a separate cover (BGC, November 2, 2022).

All work has been completed under the existing As & When Geotechnical Engineering and Design Services contract (Contract No. 861CS1183) between BGC and MoTI, dated September 16, 2021.

Figure 1-1. Site location map (Google Satellite imagery dated July 30, 2022).

Figure 1-2. Photographs from a) November 17, 2021 and b) December 2, 2021 showing the erosion and avulsion at Peers Creek Frontage Road.

Introduction Summary

The November 2021 floods caused extensive damage to PCFR. The current report describes interim works that have been completed within the project area to date, and the hydrotechnical components of the long-term design for PCFR.

2.0 HYDROLOGY AND GEOMORPHOLOGY

2.1 Hydrologic Assessment

Two Water of Survey of Canada (WSC) hydrometric gauges record real-time discharge on the Coquihalla River in the vicinity of the PCFR washout site. Gauge 08MF062 (*Coquihalla River below Needle Creek*) is located approximately 28 km upstream (northeast) from the washout site and Gauge 08MF068 (*Coquihalla River above Alexander Creek*) is located approximately 8 km downstream (southwest). Details for these gauges are provided in Table 2-1.

Table 2-1. WSC hydrometric station information.

Station Name	**Coquihalla River below Needle Creek**	**Coquihalla River above Alexander Creek**
Station ID	08MF062	08MF068
Real Time Gauge	Yes	Yes
Latitude	49° 32' 30" N	49° 22' 06" N
Longitude	121° 07' 11" W	121° 23' 04" W
Drainage Area (km^2)	85.5	720
Record Period	1965-2022	1985-2022
Record Length (complete years of data)	47	26
Regulation Type	Unregulated	Unregulated
Location with Respect to Project Site	28 km upstream	8 km downstream

Based on provisional data, the gauges recorded two flood peaks in November. The first peak was recorded on November 14-15, 2021, and the second on November 28, 2021. The November 14-15 flood peak was the largest flood on record for gauge 08MF062 and the third largest flood on record for gauge 08MF068, which has been in operation since 1985 (Figure 2-1).

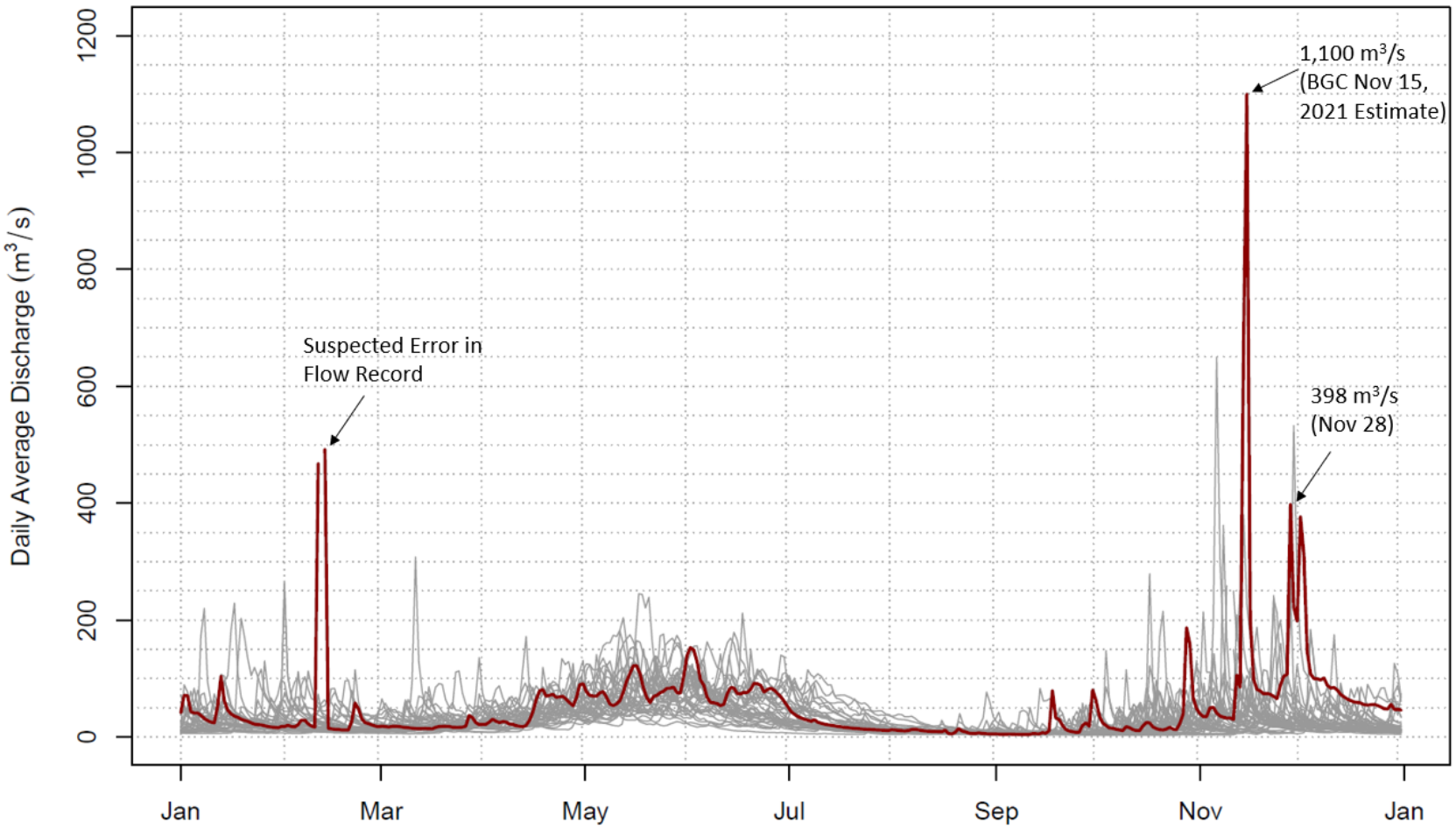

Figure 2-1. Daily flows at gauge 08MF068 from 1981 to 2020 (grey), which is located 8 km downstream of the PCFR washout site. Provisional daily flows for 2021 are shown in dark red and include BGC's estimated value of 1,100 m³/s for November 15, 2021. The peaks recorded in February 2021 are suspected to be an error in the provisional data as the temperature was below freezing from February 11-13 and precipitation fell as snow.

Analysis by BGC suggests that gauge 08MF068 likely malfunctioned during the November 14-15 flood and underreported the full flood peak. BGC used the following approach to estimate flood magnitudes for a range of return periods at the PCFR project site[1]:

- Develop a two-dimensional (2D) hydrodynamic model for the reach using HEC-RAS (Hydrologic Engineering Center – River Analysis System) version 6.3, a publicly available software package developed and distributed by the U.S. Army Corps of Engineers (USACE). The model was first used to estimate the November 14-15 flood discharge at the nearby Othello Road washout site by matching the modeled water surface elevation to high water marks approximated from post-flood orthoimagery and aerial photographs (BGC, February 6, 2023). This resulted in a peak flow estimate of 900 m^3/s at the Othello Road washout site (which corresponds to a flow of 850 m^3/s at the PCFR washout site). Further discussion on development of the hydraulic model is provided in Section 3.0.
- Prorated the estimated November 14-15 peak flood discharge from the Othello Road washout site to gauge 08MF068 using Equation 2-1:

$$\frac{Q_1}{Q_2} = \left(\frac{A_1}{A_2}\right)^n \quad \text{[Eq. 2-1]}$$

  where n is a proration coefficient, Q_1 and Q_2 are the discharge at the gauge 08MF068 and the Othello Road washout site (900 m^3/s), and A_1 and A_2 are the drainage area at the gauge (720 km^2) and the Othello Road washout site (602 km^2). BGC used a proration coefficient (n) of 1.1 based on the observed relationship between gauges 08MF062 and 08MF068 during historical fall and winter peak flows. This produced an estimated peak flow of 1,100 m^3/s at gauge 08MF068 during the November 14-15 flood (Figure 2-1).
- Used the extended dataset for gauge 08MF068 (i.e., including the estimated November 14-15 peak flow) to update the flood frequency analysis (FFA) for the gauge. As the Coquihalla River is subject to both snowmelt- and atmospheric river-related flood events, BGC applied a dual maximum series approach to the FFA (Appendix B). The estimated November 14-15 peak flow of 1,100 m^3/s at gauge 08MF068 has a return period of approximately 90 years (Table 2-2).
- Used streamflow projections from the Pacific Climate Impacts Consortium (PCIC), based on six Global Climate Models (GCMs), to develop a climate change-adjusted FFA. BGC estimated trends in peak flows due to changes in atmospheric rivers and snowmelt independently and then combined the two processes to create an ensemble climate-adjusted model. The atmospheric river-driven peak flows are expected to increase rapidly later in the century, resulting a 69% increase in the 200-year (i.e., 0.5% annual exceedance probability) flood magnitude within a 75-year timeline extending to 2097 (Table 2-2).

[1] Hydrologic assessment for the PCFR project site was preceded by similar assessment and design work completed for the Othello Road washout site located approximately 4 km downstream. The November 2021 flood peak discharge estimated at the Othello Road washout site was used to extend the flood record at gauge 08MF068 for the FFA. Flood quantiles were then prorated from gauge 08MF068 to the PCFR project site.

- Prorated the climate change adjusted flows to the PCFR project site

Detailed discussion on the estimation of flood magnitudes in the Coquihalla River are provided in Appendix B. A MoTI Design Criteria Sheet for Climate Change Resilience is provided at the end of Appendix B. The climate change-adjusted 200-year return period peak flow estimate has been selected by MoTI as the 'design' event for the hydrotechnical design of PCFR.

Table 2-2. Peak flow estimates for a range of return periods at gauge 08MG068 and the PCFR washout site.

Return Period	Stationary Flow		Climate Change-Adjusted Flow	
	Gauge 08MF068 (m^3/s)	PCFR Washout Site (m^3/s)	Gauge 08MF068 (m^3/s)	PCFR Washout Site (m^3/s)
2	240	190	310	240
5	395	305	615	475
10	540	420	865	670
20	700	500	1,140	880
50	930	720	1,555	1,200
100	1,135	880	1,920	1,485
200	1,380	1,070	2,345	1,815
500	1,785	1,380	3,035	2,345

2.2 Geomorphic Assessment

The Coquihalla River has a low sinuosity meandering to wandering planform in the vicinity of the PCFR site. The river contains a mid-channel island and large exposed bars composed of gravel- to boulder-sized sediment. Wandering rivers are transitional between more stable meandering rivers and highly unstable braided rivers and are susceptible to sudden widening, lateral shifting, and avulsion during flood events (Rice, Church, Woolridge, & Hickin, 2009). Wandering planforms typically develop in aggrading environments with coarse bedload, as the banks lack cohesion and the wide and shallow channel promotes avulsion (Desloges & Church, 1989).

The November 2021 flood events caused extensive bank erosion at the PCFR site; bank erosion was the primary mechanism for damage to infrastructure within the project area. BGC used historical air photographs, satellite imagery, orthoimagery, and lidar to characterize historical geomorphic change within a 1.5 km-long erosion assessment reach that encompasses the project area using imagery from 1968 to December 2021 (Table 2-3).

Table 2-3. Air photographs, satellite imagery, and lidar used to assess geomorphic change along the Coquihalla River within the 1.5 km-long erosion assessment reach.

Year[1]	Type	Flight Line	Frame	Scale	Source
1968	Air Photo	BC5286	170, 174-176	1:24000	Government of BC
2015	Satellite Imagery	-	-	-	ESRI World Imagery
2021	Orthoimagery (Nov 19, 2021)	-	-	-	McElhanney
2021	Lidar (April 20, 2022)	-	-	-	McElhanney

1. All photo years cover the 3.5 km-long erosion assessment reach. Imagery from 1968, 2015/2016 (combined), and lidar from 2021 covers the entire 6.1 km-long reach shown in Figure 2-2, which includes the landslide upstream from the Peers Creek Highway 5 Bridge.

BGC delineated the channel banks and islands throughout the 1.5 km-long erosion assessment reach for the three years using GIS software (Figure 2-2). The measurement error associated with the channel mapping estimated to be ±5 m. Between 1968 and 2021, the sinuosity of the Coquihalla River generally increased at the PCFR site.

For this qualitative assessment, the reach was split into two sections herein referred to as the “Upstream Section” and “Landslide Section”. The Upstream Section encompasses a section of the project reach where the river flows directly alongside the PCFR. In this section the river bend migrated downstream (south) by approximately 50 m to 100 m from 1968 to 2015 (Figure 2-2). In 1968, the main stem of the river in the upstream section was located on the left (east) side of the floodplain and a side channel was present on the right (west) side of the floodplain. Between 1968 and 2015, the main stem of the river migrated west toward the right side of the floodplain and occupied the historical side channel (Figure 2-2). Following construction of Highway 5 in the mid 1980s the progression of the eroding right bank was limited by the riprap armouring placed along PCFR. By 2015 the east side of the floodplain had become vegetated, with only a small side channel present.

Within the Upstream Section the 2021 flood event damaged the riprap along the PCFR (and Highway 5) as the river eroded toward the west. The damage was enhanced by the avulsion along the PCFR south of the washed-out section of the road and parallel to Highway 5 (Figure 2-2). The side channel along the east side of the floodplain was reactivated and enlarged during the flood event but did not convey the majority of the flow (Figure 1-2). The vegetated mid-channel bar remained intact through the flood event.

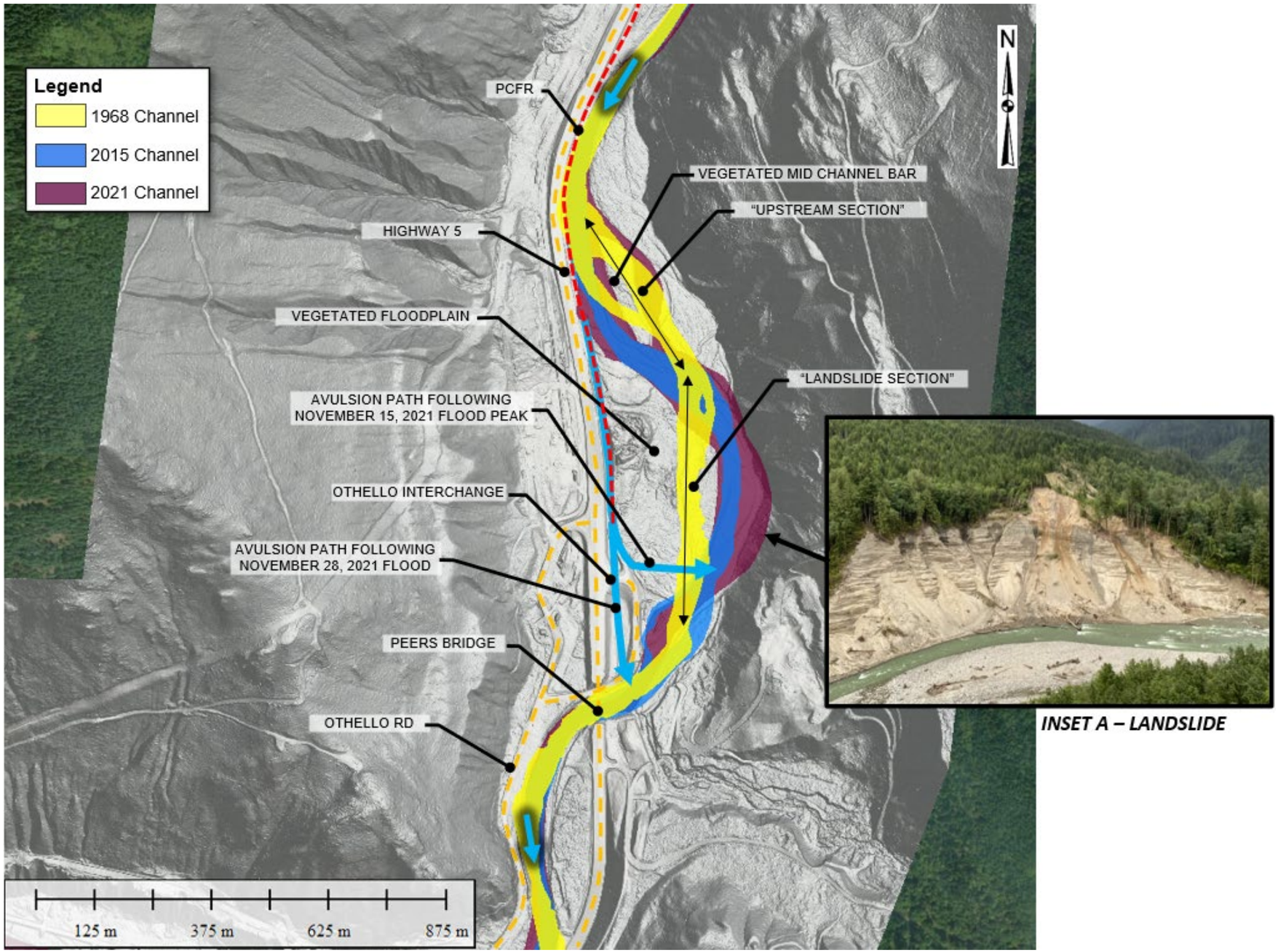

Figure 2-2. Overview of the PCFR project reach. Inset A photograph taken by BGC on June 21, 2022. Base imagery source is ESRI (August 11, 2015) overlain with post-flood lidar obtained by McElhanney (April 22, 2022).

The Landslide Section is located immediately downstream from the Upstream Section, where the river diverges from the PCFR and flows along the eastern side of the floodplain. In the Landslide Section, the river migrated to the east by approximately 85 m between 1968 and 2015, abutting against the toe of the east valley slope (Figure 2-2). During the 2021 flood events the east bank eroded an additional 110 m to the east, destabilizing the valley side and triggering the landslide (Inset A, Figure 2-2). It is suspected that the majority of this erosion occurred during the mid-November 2021 flood event and that partial blockage of the river by the deposited landslide material contributed to the avulsion along the PCFR during the subsequent flood, as the majority of the avulsion occurred during the late-November event (Figure 1-2 and Figure 2-2). The Coquihalla River is confined both up- and downstream from the erosion assessment reach and did not migrate significantly between 1968 and 2021.

In the future erosion could progress in a similar pattern to the observed erosion from 1968 to 2021, with the reach sinuosity increasing as the river erodes toward the west in the Upstream Section and toward the east in the Landslide Section, triggering additional landslide activity. However, armouring along the PCFR and Highway 5 is likely to limit erosion toward the west . Alternatively, flow may increasingly occupy the side-channel along the east side of the floodplain in the Upstream Section (similar to the 1968 configuration in Figure 2-2). This shift has the potential to reduce velocities along the PCFR and could also reduce the potential for landslide activation in the future by directing flow at a less severe angle toward the toe of the landslide.

Climate change may also change the erosion potential in the future; at the downstream Othello Road reach BGC predicted that erosion could increase by 100 m (to 160 m) during a 200-year flood event due to a large increase in the 200-year flood magnitude (BGC, February 6, 2023). Erosion magnitude at the PCFR site is likely to be similar.

However, the potential effects of climate change on geomorphologic processes are complex as changes in hydrology may impact the long-term width of the Coquihalla River as well as the frequency and magnitude of erosion events. As flood magnitude and year-to-year variability increase there is likely to be an increase in the average width of the many rivers (e.g., Davidson & Eaton, 2018; EGBC, 2020; Mauger et al., 2021; Eaton & Davidson, 2022). Modelling for rivers in the Fraser River basin for example showed a 25% increase in mean (long-term) river width in the period from 2055-2094 relative to a baseline period from 1955-1994, as well as less frequent (but higher magnitude) bank erosion (Davidson et al., 2019).

Hydrology and Geomorphology Summary

BGC estimated a peak flood discharge of 850 m^3/s for the November 14-15, 2021 flood event at the PCFR washout site, which corresponds to a discharge of 1,100 m^3/s at gauge 08MF068 (approximately a 90-year flood event). The Coquihalla River has been laterally active within the project area since 1968. Upstream of the Othello Interchange, the right (south) bank migrated 50-100 m between 1968 and 2015, and the November 2021 flood events caused additional erosion leading to a severe washout and avulsion along PCFR and Highway 5. Across the river from the Othello Interchange, the river migrated to the east by approximately 85 m between 1968 and 2015, abutting against the toe of the east valley slope, and then destabilized during the November 2021 flood events.

The selected design discharge of 1,813 m^3/s at the PCFR washout site or 2,345 m^3/s at gauge 08MF068 (i.e., the 200-year climate change-adjusted flow) is predicted to cause up to 160 m of erosion on average within the erosion assessment area based on the historical assessment. However, the potential effects of climate change on geomorphologic processes are complex as changes in hydrology may impact the long-term width of the Coquihalla River as well as the frequency and magnitude of erosion events. At the PCFR site a change in the channel configuration in the future (with more flow occupying the side channel) could also limit erosion and landsliding, reducing erosion in the future.

3.0 HYDRAULIC MODELLING OF COQUIHALLA RIVER AT PCFR

Flood hydraulics along the PCFR project reach of the Coquihalla River were evaluated using the 2D model that was initially developed to estimate the November 2021 flood peak flow at the Othello Road washout site (Section 2.1). The model results were used to: (i) simulate hydraulic conditions in the vicinity of the planned mitigation work for a range of flows (ii) assess inundation extents along the project reach, and (iii) estimate hydrotechnical design parameters.

The 2D model was developed using a digital elevation model (DEM) that combined bathymetric survey data collected by McElhanney from August 29-31 and September 16, 2022, with lidar data collected by McElhanney on April 22, 2022. The upstream model boundary was located approximately 1.5 km upstream of the project area. The downstream model boundary was set approximately 5 km downstream of the project area, just upstream of the Coquihalla River canyon. The parameters used in the 2D model simulations are summarized in Table 3-1.

Table 3-1 Parameters used for 2D hydrodynamic modelling using HEC-RAS.

Hydraulic Parameter	Value
Manning's n roughness coefficient in the channel	0.035
Manning's n roughness coefficient in the floodplain	0.1
Manning's n roughness coefficient over roads	0.025
Slope at the downstream model boundary (m/m)	0.016
General mesh spacing (m)	25 m x 25 m
Grid spacing at breaklines (m)	5 m x 5 m
Model time step	Variable based on Courant condition

Insufficient information exists to calibrate the hydraulic model given that the November flood discharge was back-estimated and high-water marks were not surveyed. BGC matched the modelled inundation extents as closely as possible to the observed inundation extents and high-water marks from the November 14-15, 2021 flood peak at the Othello Road washout site by adjusting the downstream boundary location, the downstream model boundary slope, and the Manning's n values (Table 3-1). The modelled inundation extents were then compared to observed inundation extents in the vicinity of the PCFR project site and also found to match well. Model results were used to inform hydrotechnical design recommendations for interim road repair works completed by Kiewit Corporation (Kiewit) from late fall 2022 through spring 2023 (Section 4.0), and detailed design of the long-term solution (Section 5.0).

Hydraulic Modelling Summary

Hydraulic modelling was completed to simulate hydraulic conditions along the PCRF project reach of Coquihalla River over a range of flows. Modelling results were used to inform hydrotechnical design recommendations for interim road repair works and detailed design of the long-term solution.

4.0 INTERIM CONSTRUCTION

Two phases of repair work have occurred at the PCFR project site since the November 2021 flood event:

Phase 1: Emergency repairs completed by MoTI to reinstate and protect Highway 5

Phase 2: Interim repairs along PCFR by Kiewit for the Trans Mountain Expansion Project

Emergency repairs were completed by MoTI in December 2021 involving temporary placement of riprap along the approximately 140 m washed-out section of PCFR to provide bank stabilization for Highway 5 (Figure 4-1and Figure 4-2). As the PCFR was not reinstated at this time, access along the along the road was provided through temporary offramps from Highway 5 north and south of the washout. An additional 170 m of riprap bank protection was installed along the natural bankline downstream of washout. Limited documentation of the emergency repairs is available. Based on visual inspection, BGC estimates that the installed riprap consisted of a range of sizes of approximately 500 kg Class and larger.

Figure 4-1. Looking downstream along emergency bank protection place on the right bank of the Coquihalla River. Photo Source: BGC, May 9, 2022

Figure 4-2. Overview of emergency repair extents along PCFR and Highway 5. Base Imagery Source: McElhanney, April 20, 2022

On September 30, 2022, Kiewit requested that MoTI's project team provide highway and hydrotechnical design recommendations to inform Kiewit's overall design of interim repairs to the road. The purpose of the interim repairs was to reinstate the road and provide construction access for the Trans Mountain Expansion Project until a long-term solution can be implemented by MoTI. BGC submitted a memo to MoTI that was subsequently shared with Kiewit titled "Preliminary Hydrotechnical Assessment for Interim Repairs of Peers Creek Frontage Rd" (BGC, October 25, 2022) (Appendix B). Given the interim nature of the repairs, and to allow Kiewit to reuse riprap previously installed during emergency repairs, MoTI selected the 10-year return period peak flow as the design flood. Based on a preliminary hydrotechnical analysis, BGC's recommendations for the interim repairs are summarized as follows:

- Ideally, the top elevation of the riprap revetment would be installed above the water surface elevation associated with the 10-year return period peak flow, although this may not be feasible given site constraints. Based on discussions with McElhanney and MoTI, BGC understands that overtopping of the revetment may be tolerated given that the interim works will repair the site to an improved condition.
- A minimum riprap size of 500 kg Class is required for hydraulic stability of the proposed riprap revetment. BGC has not estimated the gradation of riprap that was installed onsite immediately following the November 2021 flood. However, based on visual inspection, the riprap appeared to consist of a range of sizes of approximately 500 kg Class and larger. BGC understands that Kiewit will be repurposing existing riprap onsite to construct the temporary revetment. BGC recommends that a sorting of riprap onsite be completed to the extent possible such that the temporary revetment is constructed of 500 kg Class riprap or larger, while meeting the gradation specifications provided in Section 205 of the MoTI Standard Specifications (MoTI, 2020). The revetment should be constructed at slopes no steeper than 2H:1V and the minimum thickness of the riprap should align with the riprap size selected (i.e., if a larger class of riprap is used, it should match the corresponding thickness indicated in Table 205-D of MoTI (2020)).
- Geotextile filter fabric should be installed beneath all riprap to reduce the potential for migration of soil particles from the underlying insitu soils. Mirafi 1100N or equivalent is recommended and overlain with a 150 mm gravel bedding layer.
- The riprap revetment should be blended into the existing revetments upstream and downstream to provide smooth transitions, and keyed into the channel bed to an elevation of 216.0 m.

BGC and McElhanney completed a site visit of the interim repair works with Kiewit and their subcontractor Tuya Construction Ltd. (Tuya) on March 23, 2023. Although interim repairs were ongoing at the time of the site visit, the riprap bank protection had been fully installed. BGC's site observations and understanding of the construction sequence, based on discussions with Tuya, are summarized as follows:

- Riprap previously installed during emergency repairs was reused. Riprap installed along the repaired road embankment was 500 kg Class and larger (Figure 4-3 and Figure 4-4).
- Some oversized rocks were relocated to the downstream end of the washout area where the riverbank departs from the road embankment towards the southeast (Figure 4-3 and Figure 4-4). At this location, the riprap size was estimated to be approximately 1000 kg Class.
- The riprap revetment was keyed into the riverbed to an elevation of 216.0 m. An additional approximately 5 m wide launching apron was incorporated along the toe of the revetment at elevation 216.0 m.
- Natural boulders and cobbles encountered during excavation were placed and spread along the river bar adjacent to the road (Figure 4-3 and Figure 4-4).
- Riprap (approximately 100 kg Class) was placed intermittently along both the PCFR and Highway 5 embankments towards the south end of the project extents near the Othello interchange (Figure 4-5 and Figure 4-6).

Figure 4-3. View of interim road repairs looking downstream (south). Photo Source: BGC, March 21, 2023.

Figure 4-4. View of interim road repairs looking upstream (north). Photo Source: BGC, March 21, 2023.

Figure 4-5. View of interim road repairs looking north near the Othello interchange. Photo Source: BGC, March 21, 2023.

Figure 4-6. View of interim road repairs looking south near the Othello interchange. Photo Source: BGC, March 21, 2023.

Interim Construction Summary

Interim construction within the PCFR project area has been completed in two phases: 1.) emergency repairs to reinstate and protect Highway 5 in December 2021 and 2.) interim repairs by Kiewit to provide access for the Trans Mountain Expansion Project from late fall 2022 to spring 2023.

5.0 DETAILED HYDROTECHNICAL DESIGN

5.1 Design Flood Event

The design flood adopted by MoTI for the PCFR project is the climate change-adjusted 200-year peak flow (1,815 m^3/s).

5.2 Hydrotechnical Design Components

The hydrotechnical design for PCFR consists of four main components as shown on Figure 5-1. These components have been developed in coordination with the MoTI project team and are summarized as follows:

- Riprap Revetment – A riprap revetment is proposed along the previously washed-out section of PCFR and extending downstream along the natural riverbank. Details regarding the sizing and configuration of the riprap revetment are provided in Section 5.5. A decision was made in coordination with the project team to avoid embedment of large wood directly into the riprap revetment as this could negatively impact its long-term integrity.
- Deflection Berm – An approximately 1 m high deflection berm is proposed near the downstream end of the riprap revetment. The purpose of the berm is to partially deflect flows from PCFR and Highway 5, which are predicted to overtop during design flood conditions (discussed further in Section 5.3). The berm will function to reduce inundation extents along PCFR and Highway 5, but not eliminate overbank flows in those areas. The berm is armoured with riprap and designed to be overtopped during the design flood event.
- Overbank Armouring (Ditch, Road Embankment and Knickpoint Armour) – As inundation of both PCFR and Highway 5 is anticipated during the design flood event, riprap armouring is proposed within the ditch that runs between PCFR and Highway 5, and along the eastern PCFR embankment including an area where there is a potential for knickpoint erosion immediately south of the previously washed-out section of the road (Figure 5-2). Details regarding the sizing and configuration of the riprap armour are provided in Section 5.5.
- Stability Seeding – Stability seeding is an experimental approach whereby sediment similar in size to the D_{84} to D_{90} (or the 84th to 90th percentile of the grain size distribution) of sediment observed on a riverbed is strategically placed on or adjacent to the riverbanks. Results from laboratory experiments indicate that stability seeding has the potential to provide various channel stability and fish habitat benefits as discussed in further detail in Appendix C. At the PCFR project site, stability seeding is proposed along the river bar adjacent to the previously washed-out section of the road. The long-term performance of the stability seeding measures will be monitored through various research programs through the University of British Columbia (UBC).

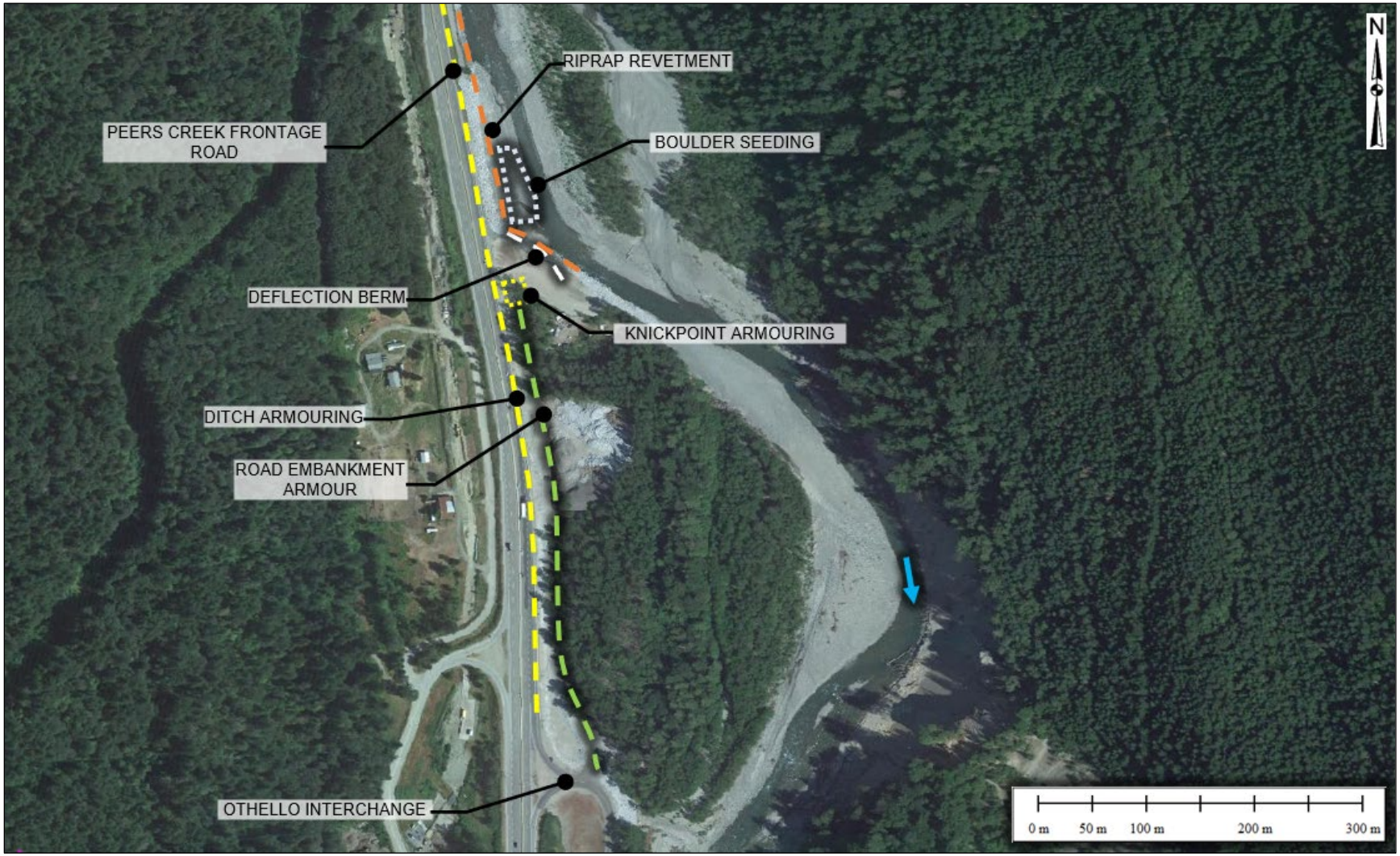

Figure 5-1. Detailed Design Components

Figure 5-2. View of potential knickpoint immediately south of previously washed-out section of PCFR. Photo Source: BGC, March 21, 2023.

5.3 Hydraulic Model Updates

5.3.1 Terrain Modifications

BGC modified the DEM of the hydraulic model in the following ways to represent the design condition of the project reach:

- The proposed PCFR alignment was incorporated. Road elevations were based on the 50% design surface provided by McElhanney.
- The channel bathymetry adjacent to the proposed riprap revetment was modified such that it maintained the same width before and after incorporation of the road.
- Road barriers along the side and centerline of Highway 5 which were not captured in the lidar were added to the DEM. These barriers were assumed to be impermeable for simplicity of modelling. The barrier along the center of the highway was raised 0.8 m above the surface of the lidar and the barrier along the east side of the road was raised 0.7 m above the surface of the lidar.
- An approximately 1 m high deflection berm was added along the right riverbank near the downstream end of the riprap revetment.

The terrain modifications are shown in Figure 5-3.

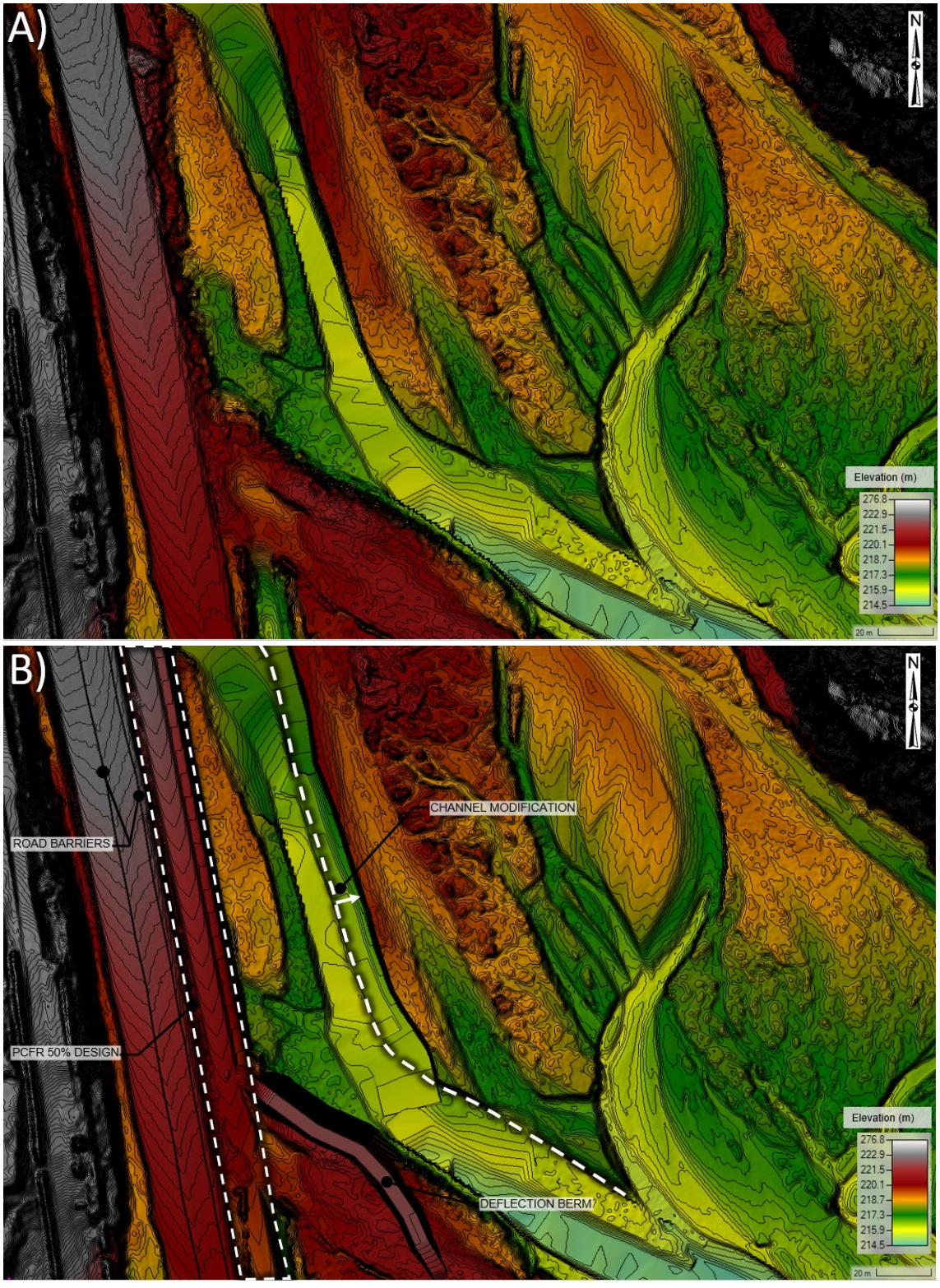

Figure 5-3. Model terrain of existing conditions (A) and design conditions (B).

5.3.2 Results

Modelled water surface elevations (WSE), flow velocities, and flow depths were evaluated throughout the project reach for the design flood event and used to inform design of the components described in Section 5.2. at the design peak flow, overbank flooding is predicted to occur, resulting in inundation of PCFR and Highway 5 south of the previously washed-out section of PCFR (Figure 5-4a). Inclusion of the deflection berm results in a reduction in the inundated extent of Highway 5 (Figure 5-4b). Model simulations indicate that raising the berm higher than 1 m provides little additional benefit with regards to reducing inundation along PCFR and Highway 5. Simulated overbank flow velocities were observed to be similar with and without inclusion of the berm.

Final modelling results along the entire project reach indicate that the majority of PCFR will be inundated during the design flood event (Figure 5-5). Main channel velocities in excess of 7 m/s are simulated. Maximum overbank flow velocities of up to approximately 3.5 m/s are simulated along the road surface where lower Manning's n values were assumed (Table 3-1).

Flooding over Highway 5 is limited by Jersey barriers that run along the eastern side of the highway as well as between northbound and southbound highway lanes. As mentioned in Section 5.3.1, the Jersey barriers were assumed to be impermeable within the model. Actual flood extents may be greater than what is represented by the modelling results, particularly if the barriers are damaged during flooding.

Key parameters for hydraulic design of the various hydrotechnical components were extracted from the model as discussed further in Section 5.5.

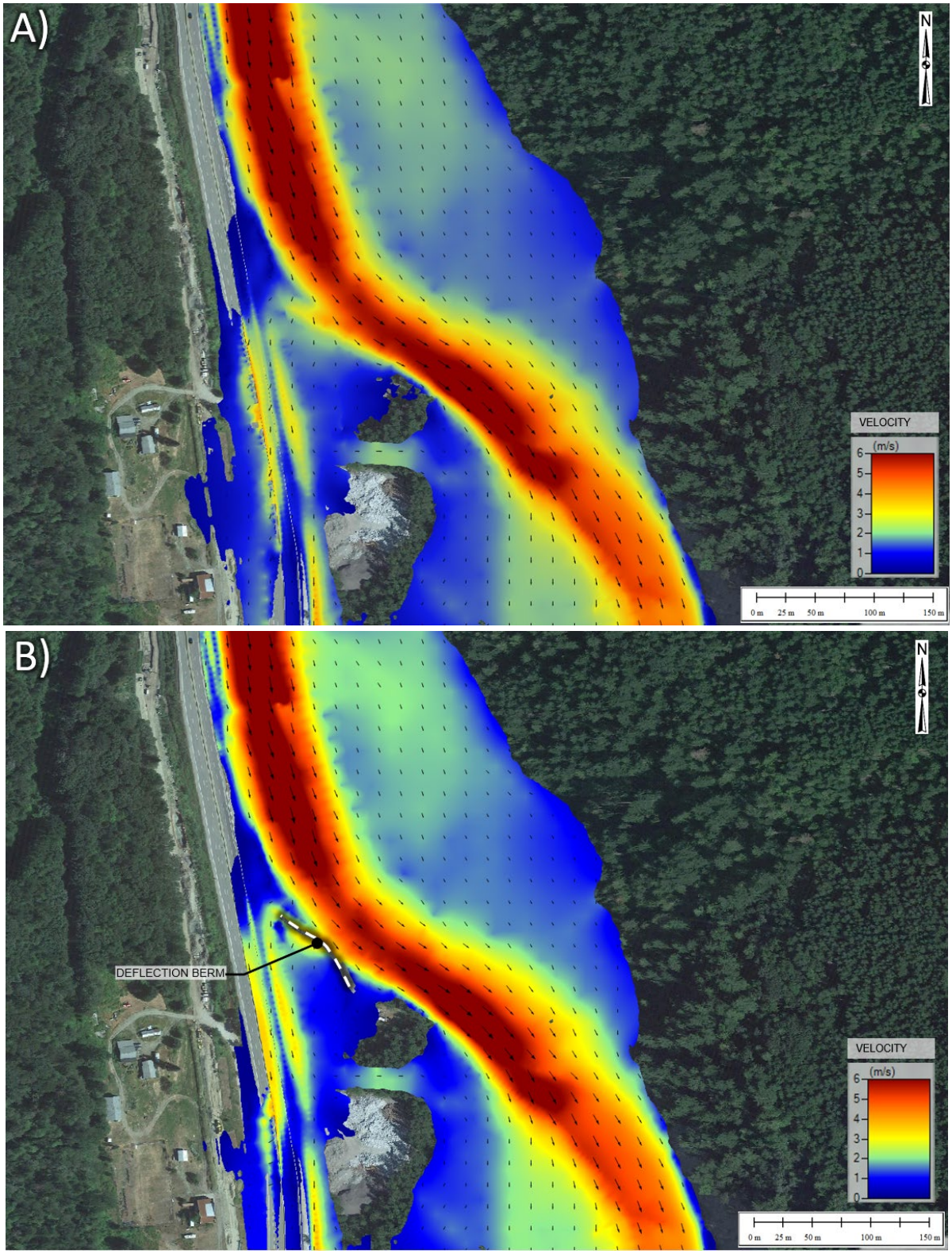

Figure 5-4. Model results demonstrating the effect of the 1.0 m deflection berm. A: No deflection berm. B: With deflection berm installed.

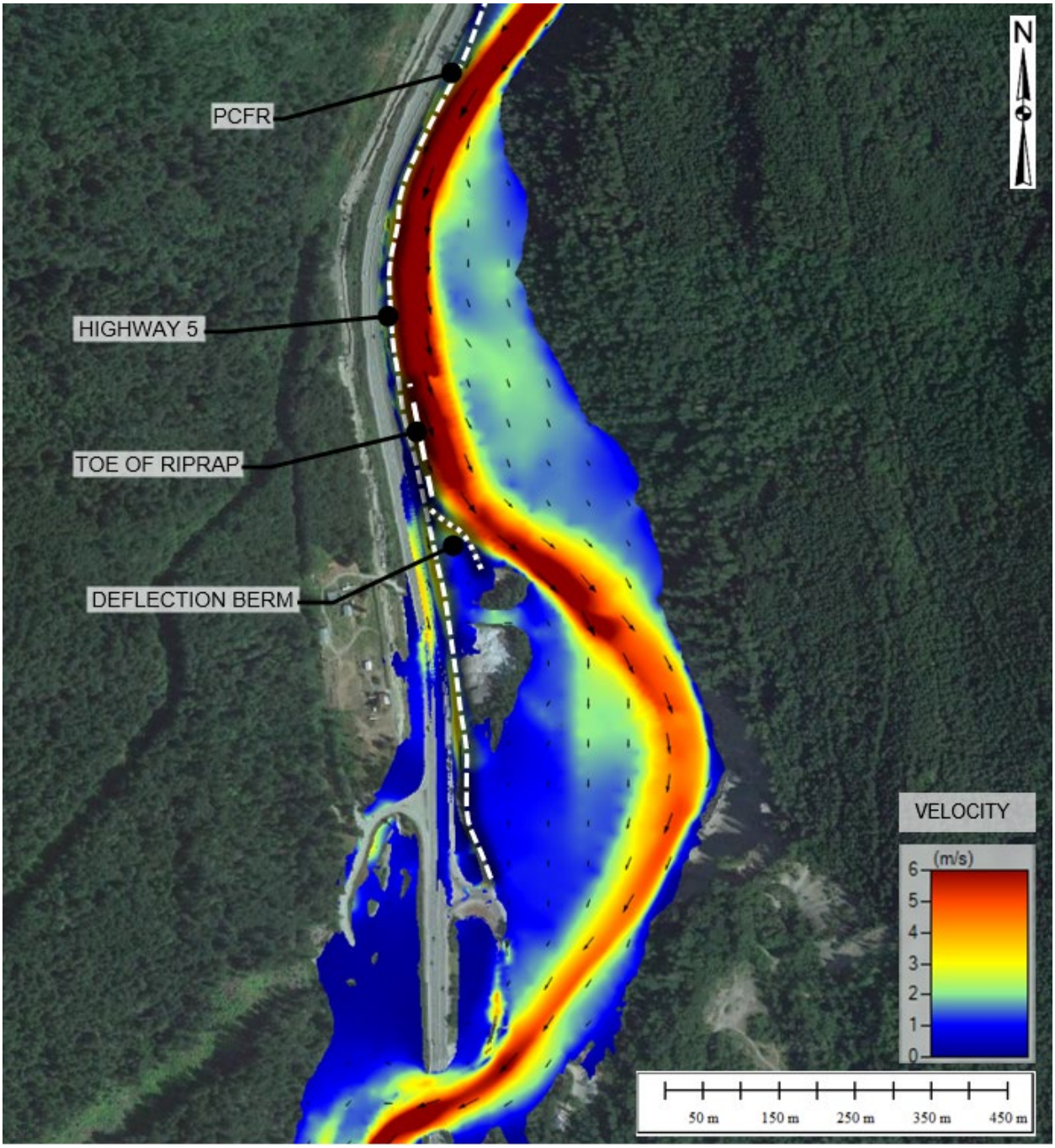

Figure 5-5. Velocity and inundation results within the project reach during design flood conditions (Q = 1,815 m^3/s).

5.4 Scour Analysis

A scour assessment was performed to support design of the riprap revetment using results from the hydraulic model taken at the cross section shown in shown in Figure 5-6.

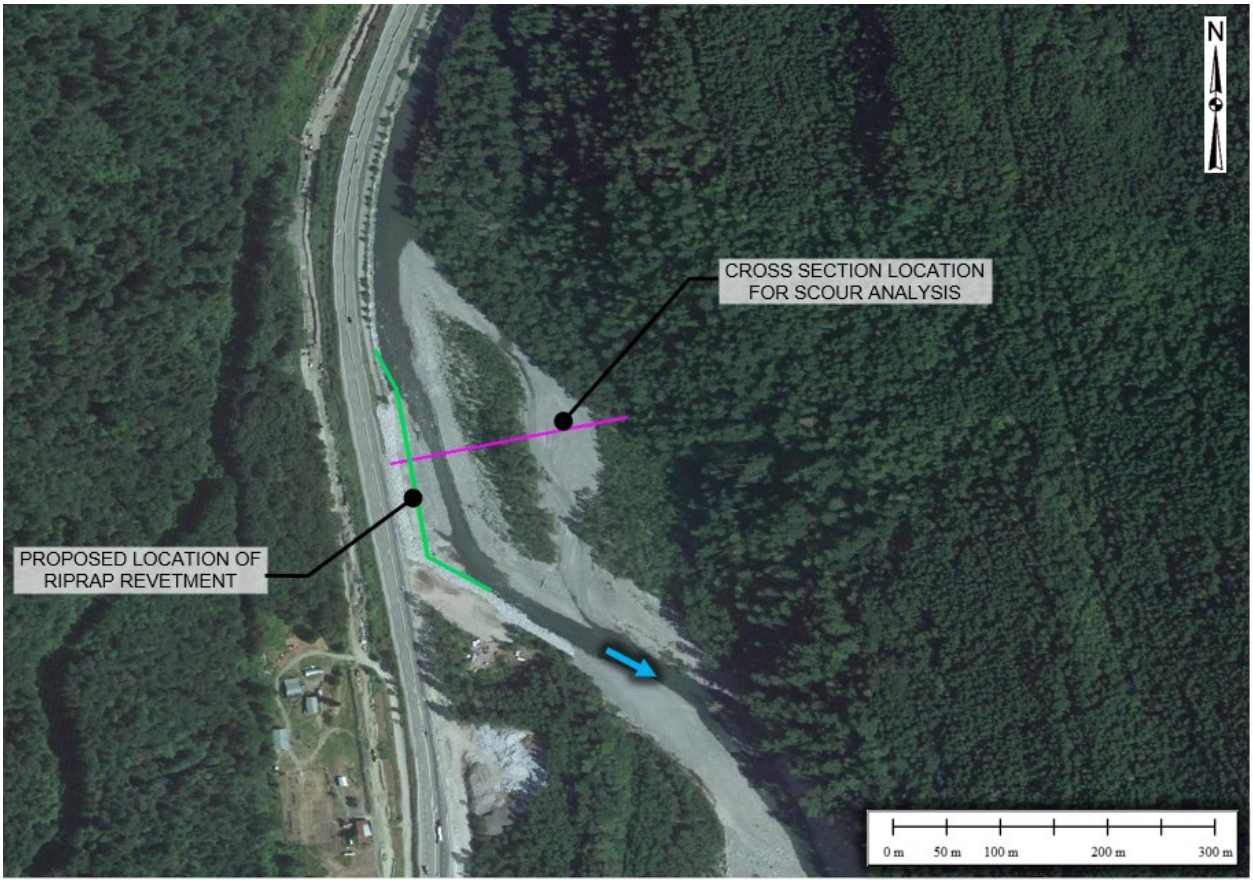

Figure 5-6. Location of cross section used for scour analysis.

Natural scour was estimated using the Blench regime method (Blench, 1969). The Blench method extended previous regime methods to include cases of different bank material. Blench defined the regime depth as follows:

$$d_r = q^{2/3}/F_b^{1/3}$$

Where d_r is the regime depth (m), q is the unit discharge (m^2s^{-1}) found by taking the return period discharge of interest and dividing by the water surface width, and F_b is the bed factor (m/s^2).

Estimation of F_b involves an iterative calculation using the regime depth, bed load charge, C (parts per hundred thousand), and the median bed material particle size, D_{50} (mm). The first approximation of regime depth is the average flow depth for the given flood (e.g., 200-year). The estimated bed load charge is used when significant bed load transport occurs, such that a portion of the stream's energy is committed to sediment transport rather than the scouring of the channel bed. Essentially, it is an adjustment factor to dampen estimated scour depths.

A Z factor is then applied to the regime depth to account for the channel morphology. The final scour depth (d_s) is estimated relative to the estimated design water surface elevation (Equation 4-2):

$$d_s = Z \times d_r \quad \text{[Eq. 4-2]}$$

The Z factor used is unique to the channel morphology at the project site (Table 5-1). Given that the site is at a moderate bend in the river, a Z factor of 1.6 was adopted A mean scour depth of 1.8 m is estimated below the channel thalweg during the design flood event.

Table 5-1. Typical Z factors for estimation of scour depth.

Channel Morphology	Z Factor
Straight Reach	1.3 - 1.4
Moderate Bend	1.5
Severe Bend	1.75
Right Angle Bend	2.0
Vertical Rock Bank or Wall	2.25

Table 5-**2** provides the input parameters used in the natural scour estimate and the mean scour depth below the design water surface elevation.

Table 5-2. Input parameters and results for natural scour estimates.

Parameter	Value
F_b	6.27
q	19.5
d_r	3.9
Z	1.6
d_s	6.3

5.5 Riprap Design

5.5.1 Riprap Sizing and Filter Requirements

Riprap sizes for the design components discussed in Section 5.2 were estimated using the hydraulic modelling results. Riprap sizing for slopes with gradients shallower than ~5% were completed based on methods provided in USACE EM 1110-2-1601 (USACE, 1994), and the TAC Guide to Bridge Hydraulics (TAC 2004). Riprap sizing for slopes with gradients steeper than ~5% were estimated based on Equation 4-3 provided in Robinson et al. (1998).

$$D_{50} = \left[\frac{qS^{0.58}}{8.07 \times 10^{-6}}\right]^{1/1.89} \quad \text{[Eq. 4-3]}$$

Where:

D_{50} is the median riprap particle size (mm)
q is the design flood discharge per unit bottom width ($m^3/s/m$)
S is the energy gradient

Key design parameters for riprap sizing of the various design components are provided in Table 5-3. Recommended riprap sizes are provided in Table 5-4.

Table 5-3. Key design parameters for riprap sizing.

Riprap Sizing Method	Parameter	Riprap Revetment[1]	Ditch Armour[2]	Knickpoint Armour	Road Embankment Armour[2]	Deflection Berm[3]
USACE (1994)	Design Velocity (m/s)	5.2	2.5	-	3.5	-
	Average Flow Depth (m)	2.7	1.1	-	1.5	-
Robinson et al. (1998)	Design Flood Discharge per Unit Bottom Width ($m^3/s/m$)	-	-	2.7		2
	Energy Gradient (m/m)	-	-	0.15		0.33

1. Design flow velocities for the riprap revetment were approximated as the maximum depth-averaged velocity at a point measured 20% of the way up the slope length from the bank toe based on the hydraulic modelling results.
2. Design flow velocities for the ditch and road embankment armour were approximated as the maximum depth-averaged velocity along the proposed ditch line based on the hydraulic modeling results.
3. Riprap sizing for the deflection berm was estimated using both the USACE (1994) method (based on flow parallel to the berm) as well as the Robinson et al. (1998) method (based on flow overtopping the berm). Results from the Robinson et al. (1998) method govern riprap sizing for the deflection berm.

Table 5-4. Recommended riprap sizes for design components.

Design Component	Minimum Recommended Riprap Sizing and Thickness
Riprap Revetment	2000 kg Class (D_{50} ~ 1,150 mm) 2.3 m Thick
Ditch Armour	10 kg Class (D_{50} ~ 200 mm) 0.35 m Thick
Knickpoint Armour	250 kg Class (D_{50} ~ 575 mm) 1.0 m Thick
Road Embankment Armour	100 kg Class (D_{50} ~ 425 mm) 0.7 m Thick
Deflection Berm	250 kg Class (D_{50} ~ 575 mm) 1.0 m Thick

1. A factor of safety of 1.2 was applied to the riprap sizing and a specific gravity of 2.5 was assumed. The actual specific gravity of the available quarry material is expected to be higher than 2.5 (likely between 2.6 and 2.7); however, specific gravities in this range are not expected to reduce the recommended riprap sizing.

Non-woven geotextile filter fabric will be required beneath all riprap to reduce the potential for migration of soil particles from the underlying road fill or in situ soils. Geotextile filter fabric shall meet the specifications of Mirafi 1100N or an equivalent product. A 300 mm thick layer of well-graded cobble bedding material will be required between the geotextile and 2000 kg Class riprap layers. The cobble bedding material should meet the gradation specification provided in Table 5-5. A 100 mm thick gravel bedding layer will be required between the geotextile and 250 kg Class riprap layers.

Table 5-5. Recommended granular bedding material gradation.

Intermediate Dimension (mm)			
Percent Smaller than Intermediate Dimension			Maximum Size
15%	50%	85%	
50	150	250	300

5.5.2 Riprap Configuration

Riprap Revetment: The proposed riprap revetment consists of 2000 kg Class riprap spanning an approximate length of 300 m along the previously washed-out section of the road and extending downstream along the natural bankline (Figure 5-1). The proposed revetment would be installed to a thickness of 2.3 m, at a maximum slope of 2H:1V, overtop of the interim

revetment installed by Kiewit (Figure 5-7). The toe of the revetment will be configured as a launching apron to minimize overall excavation requirements. BGC understands that MoTI and McElhanney intend to constrain the extents of the riprap revetment such that flow isolation will not be required at the time of construction. Therefore, the downstream end of the revetment (i.e., section extending east of PCFR along the natural bankline) will be setback from the existing bankline. The launching apron at the upstream end of the revetment will gradually reduce in width as it transitions into the existing riprap revetment upstream from the project area. The riprap revetment will not contain a sufficient volume of material to launch to the design scour elevation within this transition area; however, the hydraulic stability of the bank armour will be improved compared to the existing condition.

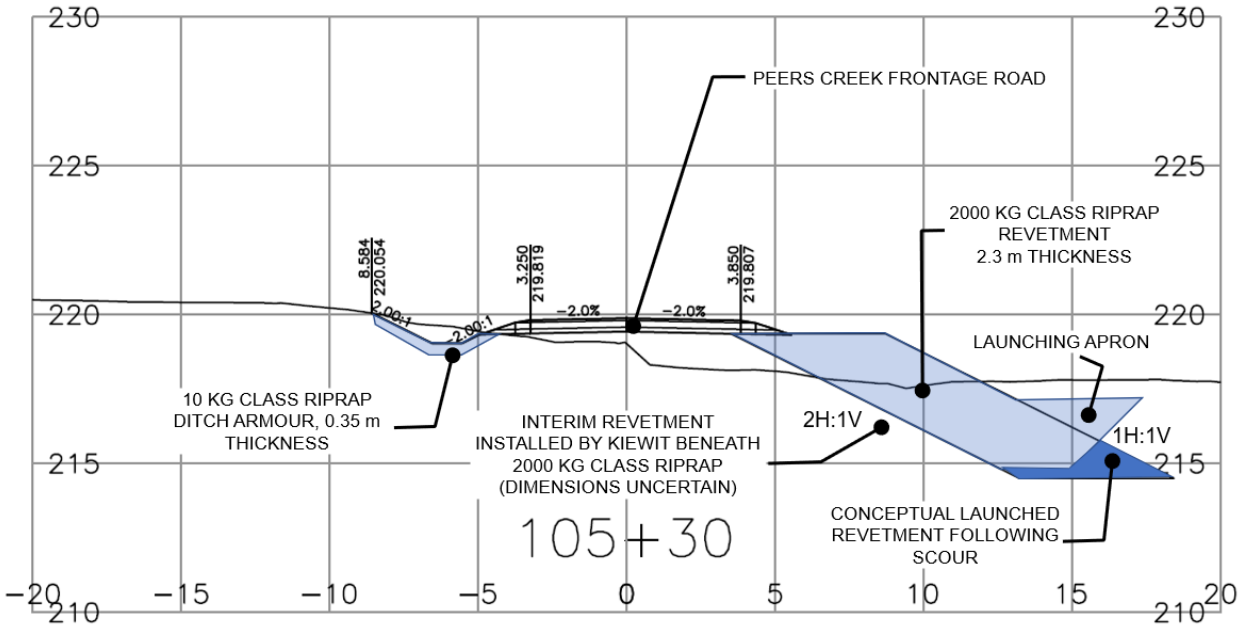

Figure 5-7. Typical cross section for riprap revetment along PCFR.

Deflection Berm: The proposed deflection berm spans a length of approximately 80 m along the downstream end of the riprap revetment. The berm should have a height of 1 m and a top width of 4 m. The road side slope of the berm should be 3H:1V whereas the river side slope should be 2H:1V. The core of the berm may consist of compacted fill. The sides and end of the berm should be armoured with 250 kg Class riprap. If setback from the Coquihalla River, the armour on both sides of the berm should be keyed into the surrounding terrain to a depth of 1 m Figure 5-8a. If set directly adjacent to the Coquihalla River, the riprap armour on the river side slope may be placed directly over the 2000 kg Class riprap revetment Figure 5-8b.

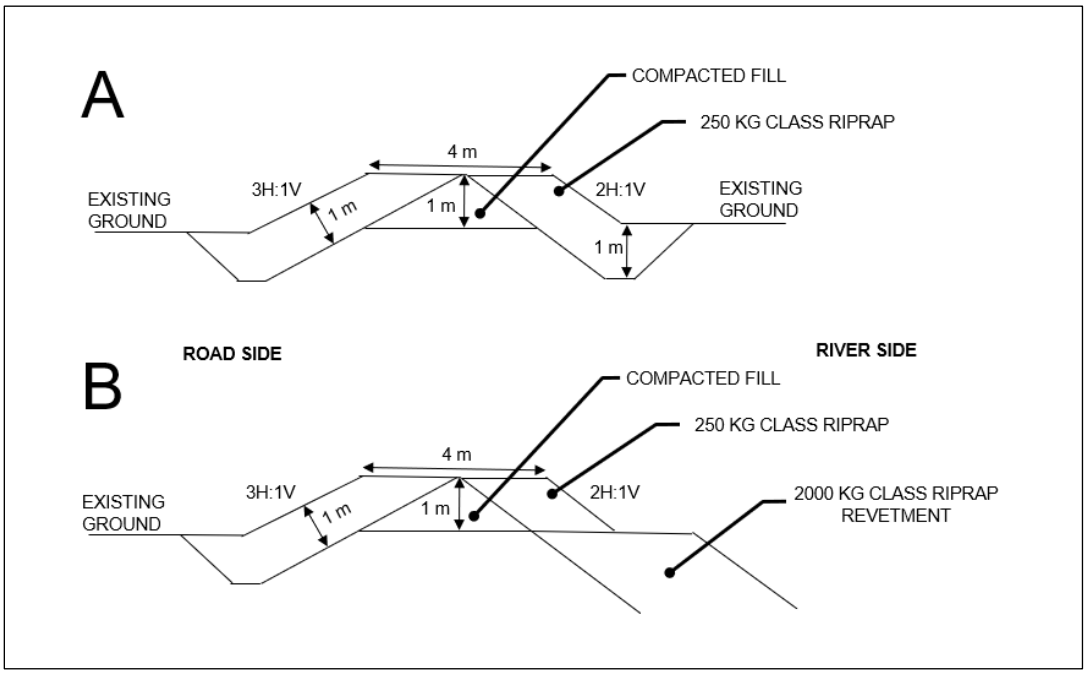

Figure 5-8. Typical cross sections for deflection berm setback from the Coquihalla River riprap revetment (A) and adjacent to riprap revetment (B), (not to scale).

Overbank Armouring: The ditch armour consists of a 0.35 m thick layer of 10 kg Class riprap extending from the upstream end of the project area south to the Othello interchange. The armour should line the entire ditch between Highway 5 and PCFR such that no road fill remains exposed (Figure 5-7).

The potential knickpoint located immediately south of the previously washed-out section of the road (Figure 5-2) should be armoured using a 1 m thick layer of 250 kg Class riprap. The knickpoint area should be graded as a trapezoidal channel with a minimum base width of 3 m, and 2H:1V side slopes. Grading of the area should be completed so that the maximum slope parallel to the direction overbank stream flow is no steeper than 15%.

Riprap should be placed along the full PCFR road embankment so that no road fill remains exposed. The road embankment armour consists of a 0.7 m thick layer of 100 kg Class riprap. The upstream end of the road embankment armour should tie in with the 250 kg armour placed in the knickpoint area and the downstream end of the armour should tie in with the 100 kg Class riprap placed by Kiewit as part of the interim road repairs near the Othello interchange (Figure 4-6).

Detailed Hydrotechnical Design Summary

Hydraulic modeling results indicate that both Highway 5 and PCFR will become inundated during the design flood event (the climate change-adjusted 200-year peak flow, 1,815 m^3/s). Due to high flow velocities modelled within the main channel of the Coquihalla River, and the extent of overbank flooding observed, various hydrotechnical design components are recommended including a riprap revetment along the right riverbank, a deflection berm to reduce potential inundation of Highway 5 and PCFR, and additional armouring in select overbank areas to reduce the potential for erosion of road and highway fill. Riprap of minimum sizes ranging from 10 kg to 2000 kg Class are recommended throughout the project area.

6.0 CLOSURE

We trust the above satisfies your requirements. Should you have any questions or comments, please do not hesitate to contact us.

Yours sincerely,

BGC Engineering Inc.
per:

Evan Shih, M.Eng., P.Eng.
Senior Hydrotechnical Engineer

Reviewed by:

Robert Millar, Ph.D., P.Eng.
Principal Hydrotechnical Engineer

EGBC Permit to Practice, BGC Engineering Inc. 1000944

SD/RGM/md/sjk

REFERENCES

BGC Engineering Inc. (March 13, 2023). Stability Seeding at Peers Creek Frontage Road [Report]. Prepared for MoTI.

BGC Engineering Inc. (February 6, 2023). Hydrotechnical Assessment and Design for Othello Road Washout Site [Draft Report]. Prepared for MoTI.

BGC Engineering Inc. (November 2, 2022). Peers Creek Frontage Road Geotechnical Assessment and Recommendations [Draft Report]. Prepared for MoTI.

BGC Engineering Inc. (October 25, 2022). Preliminary Hydrotechnical Assessment for Interim Repairs of Peers Creek Frontage Road [Memo]. Prepared for MoTI.

Booker, W.H. & Eaton, B.C. (2020). Stabilizing large grains in self-forming steep channels. *Earth Surface Dynamics, 8(1),* 51-67. https://doi.org/10.5194/esurf-8-51-2020

Davidson, S.L., Eaton, B.C. (2018). Beyond regime: A stochastic model of floods, bank erosion, and channel migration. *Water Resources Research, 54(9),* 6282-6298.

Davidson, S.L., Eaton, B.C., & Jakob, M. (2019). Modeling floods and channel migration in a changing climate. AGU Fall 2019 Annual Meeting, San Francisco, USA.

Desloges, J.R. & Church, M.A. (1989). Wandering gravel-bed rivers. *The Canadian Geographer 33*, 360-364.

Eaton, B.C., Mackenzie, L.G., & Tatham, C. (2022). Modulating the lateral migration of a gravel bed channel using the coarse tail of the bed material distribution. *Earth Surface Processes and Landforms, 42(8),* 1304-1321. **https://doi.org/10.1002/esp.5318**

Eaton, B.C., & Davidson, S.L. (2022). *Hydraulic Geometry: Empirical Investigations and Theoretical Approaches*. In: Shroder, J.J.F [Editor], Treatise on Geomorphology. Elsevier, Academic Press, 461-479.

Engineers & Geoscientists British Columbia. (2020, July 9). *Professional Practice Guidelines – Developing Climate Change-resilient Designs for Highway Infrastructure in British Columbia*. Version 2.0.

Mackenzie, L.G. & Eaton, B.C. (2017). Large grains matter: Contrasting bed stability and morphodynamics during two nearly identical experiments. *Earth Surface Processes and Landforms, 42(8),* 1287-1295. **https://doi.org/10.1002/esp.4122**

Mauger, G., Liu, M., Adam, J., Won, J., Wilhere, G., Dulan, D., Atha, J., Helbrecht, L, & Quinn, T. (2021). *New Culvert Projections for Washington State: Improved Modeling, Probabilistic Projections, and an Updated Web Tool.* Prepared for the Northwest Climate Adaptation Science Center. Climate Impacts Group, University of Washington.

Rice, S.P., Church, M., Woolridge, C.L., & Hickin, E.J. (2009). Morphology and evolution of bars in a wandering gravel-bed river; lower Fraser River, British Columbia. *Sedimentology, 56,* 709-736. https://doi.org/10.1111/j.1365-3091.2008.00994.x

Robinson, K.M., Rice, C.E., & Kadavy, K.C. (1998). Design of rock chutes. *Transactions of the American Society of Agricultural Engineers, 41*, 621 – 626.

Transportation Association of Canada (TAC). (2004). *Guide to Bridge Hydraulics* (2nd ed.).

US Army Corps of Engineers (USACE). (1994). *Hydraulic Design of Flood Control Channels. Engineering Manual* (EM) 1110-2-1601. June 30, 1994.

APPENDIX A
FREQUENCY-MAGNITUDE RELATIONSHIP FOR THE COQUIHALLA RIVER

1.0 INTRODUCTION

BGC Engineering Inc. (BGC) conducted a flood frequency analysis (FFA) to characterize the flood hydrology for the Coquihalla River, British Columbia (BC). The standard practice to conduct an FFA is to fit a statistical model to the annual maxima series (AMS), a dataset consisting of the largest flood per year, to estimate the probability of different flood magnitudes based on a frequency-magnitude (FM) relationship. A typical AMS approach does not consider that floods in the watershed may be driven by different process, like snowmelt or rainfall, resulting in two different populations of flood events. As a result, this method may not be appropriate for watersheds where floods are caused by more than one hydrological process (Waylen and Woo, 1982; Waylen and Woo, 1983; Bobotas and Koutras, 2019).

The Coquihalla River being subject to both rainfall-related floods caused by atmospheric rivers (ARs[1]) in the fall and winter and snowmelt-related floods in the spring, is an example of a watershed with mixed flood-generating processes. ARs are related to the largest ten floods on record, not including the November 2021 flood event, indicating that AR-related floods exert an important control on the distribution of floods in the watershed (Figure 1-1). Snowmelt-related floods dominate the smaller floods. On occasion, a rain-on-snow event occurs in the spring, but these events do not dominate the historical record[2].

Given the presence of multiple processes driving floods, BGC constructed a combined statistical model using a dual maxima series (DMS) approach of AR-related and snowmelt-related floods to develop an updated FM relationship in the Coquihalla River watershed. This report includes a description of the data that was used to compile the dataset for analysis (Section 2.0). A description of the methodology that pertains specifically to the Coquihalla River is included in Section 3.0. The results include the FM relationship (stationary and climate-adjusted) for the lower (between Hope and above Alexander Creek) and upper (below Needle Creek) gauged watersheds as well as an ungauged location in the watershed (Jessica Bridge as an example) (Section 4.0). A discussion on the implications for hydrotechnical design (Section 5.0), limitations, assumptions, and sources of uncertainty (Section 6.0), as well as conclusions (Section 7.0) are included at the end of the report.

This report is intended to provide a high-level description of how the FM relationship was developed for the Coquihalla River. The reader is referred to BGC's recently completed FFA study of the Coldwater River for additional methodology details (BGC, May 20, 2022).

[1] ARs are long, conveyor belts of warm, moist air typically occurring in the atmosphere during the late fall and early winter.

[2] Floods were separated into two populations based on the time of year they occurred, recognizing that floods are typically a combination of snowmelt and rainfall in the Nicola River watershed.

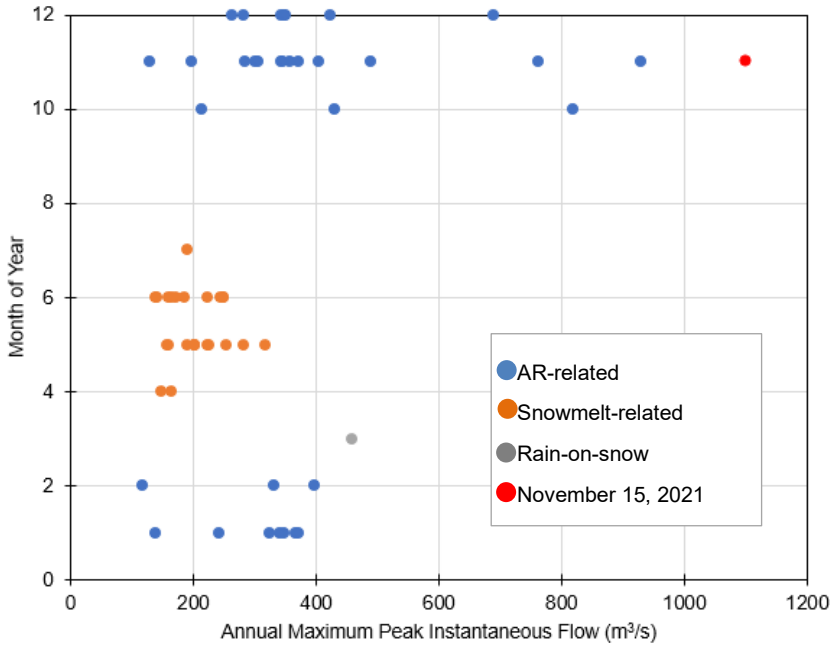

Figure 1-1. Timing of the historical floods recorded at the *Coquihalla River near Hope* (08MF003) and the *Coquihalla River above Alexander Creek* (08MF068) hydrometric stations over the 1958 to 2021 period.

2.0 DATA ACQUISITION AND COMPILATION

2.1. Historical Streamflow

The Water Survey of Canada (WSC) maintains three hydrometric stations in the Coquihalla River watershed (Figure 2-1,Table 2-1).

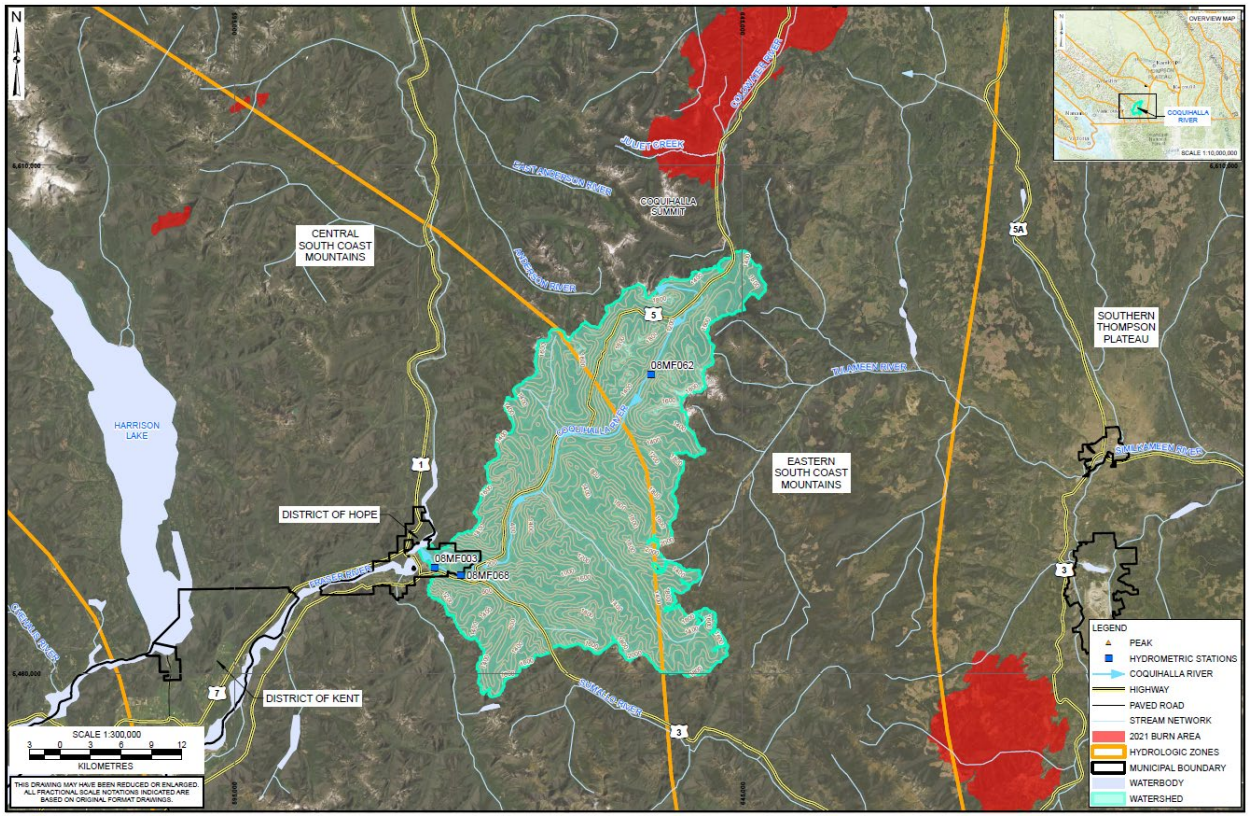

Figure 2-1. Coquihalla River watershed at Hope showing the location of the three hydrometric stations.

The *Coquihalla River near Hope* (08MF003) and the *Coquihalla River above Alexander Creek* (08MF068) hydrometric stations are located in the lower Coquihalla watershed. The streamflow record at Alexander Creek station essentially represents an extension of the Hope station, which was destroyed in 1984 during a large flood event. Due to concerns that the rating curve at Hope would not be stable in the long-term, the hydrometric station was re-located upstream by the WSC in 1987 to the vicinity of Alexander Creek. Given their proximity and similar watershed area, records from these two stations were combined by BGC, providing 59 years of streamflow data. Out of this 59-year dataset, 40 annual instantaneous peak flows (Q_{IPF}) are available, of which 19 occurred between October and February. The remaining 21 occurred following snowmelt in the spring.

The *Coquihalla River below Needle Creek* (08MF062) hydrometric station records streamflow in the upper watershed. A total of 54 years of data are available from this station, including 21 Q_{IPF} values. Of these instantaneous values, 7 occurred from October through February and the remaining 14 are associated with spring snowmelt.

Table 2-1. Hydrometric station information for the Coquihalla River.

Station Information	Lower Watershed		Upper Watershed
	Coquihalla River near Hope	Coquihalla River above Alexander Creek	Coquihalla River below Needle Creek
Station ID	08MF003	08MF068	02MF062
Latitude (°)	49.37527	49.36833	49.54189
Longitude (°)	-121.41944	-121.38444	-121.11997
Watershed Area (km^2)	741	720	85.5
Approximate elevation (m)	60	105	810
Hydrologic regime	Natural	Natural	Natural
Real-time recording	Yes	Yes	Yes
Record Period	1911-1983[1]	1987-2021[3]	1965-2021
Record Length (years)	27	38[4]	56
Missing Years on Record	1	5	3
Number of published instantaneous peak flows[2]	40		21
Number of published instantaneous peak flows that are rainfall-related	19		7
Number of published instantaneous peak flows that are snowmelt-related	21		14

Notes:
1. Early data from 1911-1922 at the Coquihalla River near Hope (08MF003) hydrometric station was not considered because there is no historic AR event data for that time period.
2. Records do not all have both the daily mean and daily instantaneous values.
3. The November 15, 2021, flood was estimated by BGC.
4. Instantaneous peak flows for 2020 was included in the analysis but considered provisional by the WSC. The estimate of the November 15, 2021 made by BGC was included in the analysis but is not published by the WSC.

2.2. Historical Dataset Compilation

A Dual Maximum Series (DMS) dataset was compiled where one snowmelt-related flood and one rainfall-related flood (if present) were included for each year on record. A DMS dataset was built for both the lower and upper watershed stations.

The WSC publishes the Q_{IPF} for the annual maximum and the daily mean streamflow time series for all years on record. The DMS was constructed by using available Q_{IPF} data first. The years with missing Q_{IPF} were filled in using the annual maximum mean daily flow (Q_{MDF}) value from April through August for snowmelt-related floods and from September through March for rainfall-related floods if present. The methodology used for this fill-in procedure is described in Section 3.2.

The timing of the rainfall-related floods was cross-referenced with AR events using a historical dataset. Historical AR events have been catalogued by the Scripps Institute of Oceanography (SIO-R1-AR), which is available at http://cw3e.ucsd.edu/Publications/SIO-R1-Catalog/. This AR catalogue provides the frequency, duration, and landfalling location of ARs along the North American West Coast from 20° to 60°N from 1948 to 2017 (Gershunov, Shulgina, Ralph, Lavers, and Rutz., 2017). This dataset has been used by a number of researchers to characterize changes to AR characteristics over time (Sharma and Déry, 2019; 2020a; 2020b). Rainfall-related floods were defined as AR-related if the hydrological response occurred on or up to five days after the AR event.

2.3. Missing Historical Floods

In 1984, the *Coquihalla River near Hope* (08MF003) hydrometric station was destroyed during a flood event. The hydrometric station was rebuilt further upstream above Alexander Creek (08MF068) and made operational in 1987. The 1984, 1985, and 1986 floods are thus missing from the WSC record. Furthermore, AR-related floods in the fall of 1989 and 1990 are also missing from the WSC record.

In 1994, Northwest Hydraulics Consultants (NHC) published estimates of the magnitude of the winter 1984 flood as well as the fall floods of 1989 and 1990 (NHC, 1994) (Table 2-2). Unfortunately, the methodology supporting these estimates was not published. Based on the lack of supporting information and absence of corresponding WSC estimates, the NHC values were not included in the analysis here-in.

Table 2-2. Estimated missing instantaneous peak flows (Q_{IPF}) in the Coquihalla River (NHC,1994).

Hydrometric Station	Date (mm-dd-yyyy)	Peak Flow Estimate (m^3/s)
08MF003	01-04-1984	779
08MF068	10-11-1989	475
08MF068	10-11-1990	725

2.4. Projected Streamflow

The FM relationship for floods on the Coquihalla River is projected to increase in the future as the atmosphere warms. Projected daily mean streamflow at the *Coquihalla River above Alexander* (08MF068) hydrometric station have been modelled from 1945 to the end of the century by the Pacific Climate Impacts Consortium (PCIC, 2020) for two emission scenarios and six global circulation models (GCMs). The simulation used for the analysis here-in assumes a radiative forcing of +8.5 Watts/m^2 by 2100 with negligible carbon emission reduction[3]. Six GCMs were

[3] Since 2006, this scenario has tracked most closely to observed emissions and warming and, given that many governments are falling short of their greenhouse gas emission reduction targets, it can be assumed that 8.5 is presently the most realistic scenario for future climate projections. http://www.iiasa.ac.at/web-apps/tnt/RcpDb (retrieved June 22, 2022).

selected for analysis. The projected daily mean streamflows from the six GCMs were used by BGC to infer the impacts of climate change in the Coquihalla River watershed. The future trends in floods were characterized by extracting a DMS with one annual maximum rainfall-related (AR and non-AR) flood from September to March and one annual maximum snowmelt-related flood from April to August. The September to March floods were not differentiated between AR-related and those related with other types of rainfall systems.

Information on the climate models and calibration performance are detailed further in BGC (June 4, 2021).

3.0 METHODS

3.1. November 15, 2021 Event

The *Coquihalla River below Needle Creek* (08MF062) hydrometric station recorded the peak flow of the November 15, 2021 event. However, the *Coquihalla River above Alexander Creek* (08MF068) station stopped working before the peak of the event with the hydrograph being updated months later (Figure 3-1). Therefore, BGC estimated the Q_{IPF} of the November 2021 flood in the lower watershed using available data from other WSC gauges during the event, historic gauge data and a two-dimensional (2D) hydraulic model developed in the HECRAS 6. Additional information on the estimate of the November 15, 2021 flood magnitude at the *Coquihalla River above Alexander Creek* (08MF068) hydrometric station is included in Attachment I.

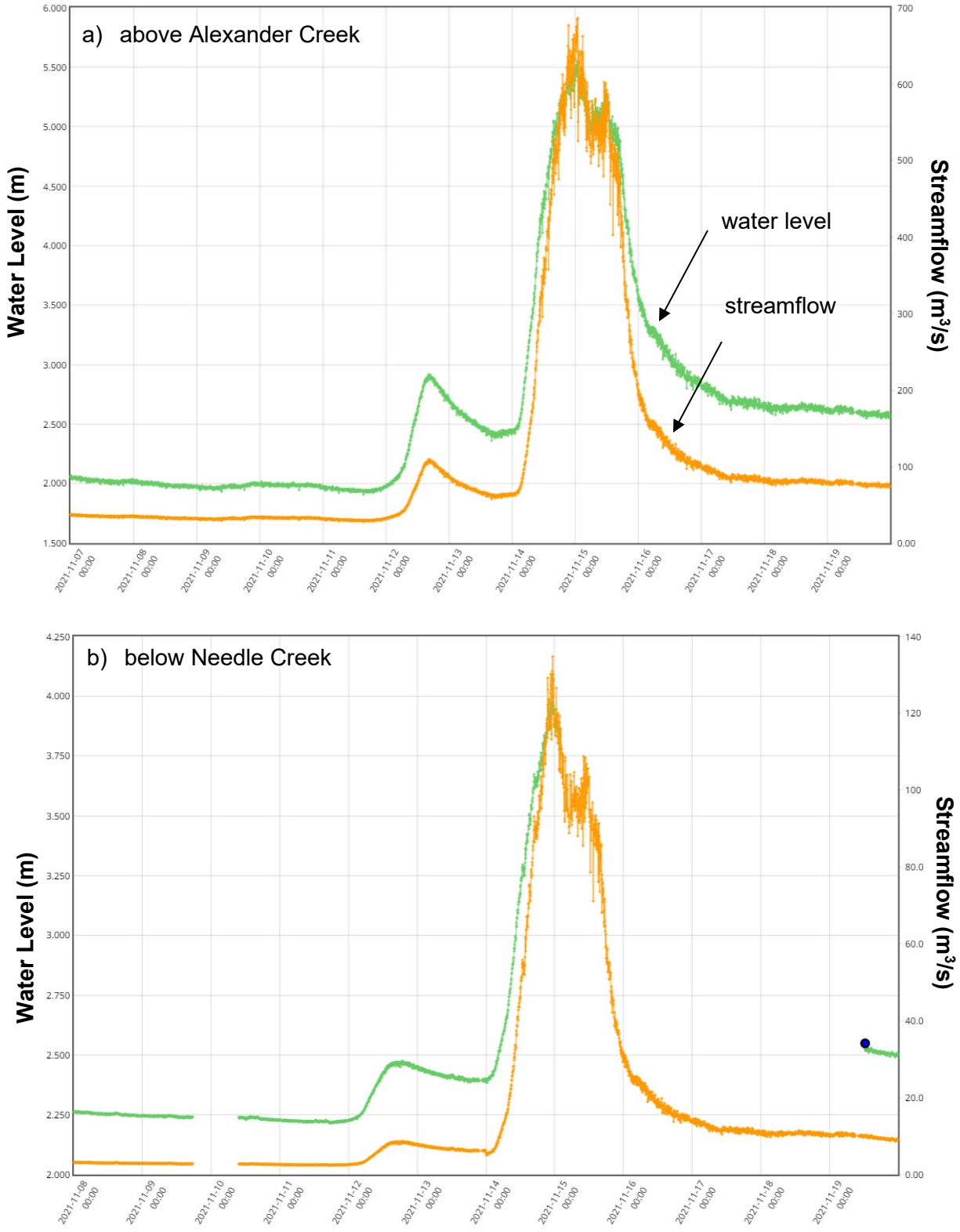

Figure 3-1. Hydrograph for the November 15, 2021 event recorded at the a) *Coquihalla River above Alexander Creek* (08MF068) and the b) *Coquihalla River below Needle Creek* (08MF002) hydrometric stations.

3.2. From Q_{DMF} to Q_{IPF}

A flood type-specific linear regression was built to estimate missing Q_{IPF} from available daily mean Q_{DMF} records[4]. The regression was built using paired observations of Q_{IPF} and Q_{DMF} from the historical record. The slope of the regression was calculated by minimizing the difference between observed value and the fitted value (provided by the regression) using the least squares estimate fitted through the origin. The overall fit of the regression was assessed using the coefficient of determination (R^2).

3.3. Historical Trend Assessment

A historical trend was evaluated for both snowmelt- and AR-related floods to determine whether a non-stationary approach was warranted. The trends were estimated using the Sen's[5] slope and the Mann-Kendall[6] test. The alpha threshold level was selected to be 0.01 for statistical significance to increase our confidence that the trend is not due to random chance.

3.4. Statistical Model Development

The FM relationship was built by first developing statistical models for snowmelt-related floods and AR-related floods separately. Seven[7] different probability distributions were compared to determine which had the best fit, particularly how well the distribution fit the larger floods. Three statistical tests[8] were used to determine best choice of distributions for AR-related and snowmelt-related floods. The Generalised Extreme Value (GEV) and the Log Pearson Type III were considered regardless of test score given their prominent use in Canada (Zhang et al., 2019) and the United States (England et al., 2018). Several methods[9] were considered to fit the model to the data.

A "leave one out" cross validation based on the quantile score was used to inform the final distribution selection for analysis. The quantile score is a specific way of evaluating how well the quantile estimate from the statistical model compares to the annual maximum Q_{IPF} recorded at the hydrometric station over all years on record with a penalty depending on whether the quantile estimate is above or below. The overall quantile score was obtained by averaging each year's quantile score. The best distributions were defined by the lowest quantile scores. This process was done for all return periods.

---

4 Q_{DMF} is defined as the average streamflow over the course of the day from midnight to midnight the following day.

5 The Sen's Slope is a non-parametric estimate of the slope of the line practical when the data elements don't fit a straight line.

6 The non-parametric Mann-Kendall test is widely used to detect consistently increasing or decreasing trends through time.

7 The seven distributions include Normal, Log Normal, Gumbel (EV1), Freshet (EV2), GEV, Pearson Type III, and Log Pearson Type III. The GEV and Log Pearson Type III were included regardless of their test scores due to their standard use in Canada and the US, respectively.

8 The tests include the Akaike Information Criterion (AIC), Bayesian Information Criterion (BIC) and Anderson-Darling Criterion (ADC).

9 The maximum likelihood estimate (MLE) method, the maximum goodness-of-fit estimates (MGE), the method of moments (MM), and linear moments (l-moments).

The snowmelt-related and AR-related statistical models were subsequently combined by a maximization process where floods from each distribution was randomly generated and the highest value between the two estimates was selected to build the combined model. The combined model was based on the collection of maxima of randomly drawn pairs between both models and was calculated using the distplyr R package (Coia, Joshi, Tan, and Zhu, 2022).

The FM relationship was built for the following return periods (% AEP): 2-year (50% AEP), 5-year (20% AEP), 10-year (10% AEP), 20-year (5% AEP), 50-year (2% AEP), 100-year (1% AEP), 200-year (0.5 % AEP), and 500-year (0.2 % AEP).

3.5. Sensitivity Analysis

A sensitivity analysis was conducted to assess the influence of a range of 2021 peak flow estimates on the FM relationship. The sensitivity of the FM relationship was assessed using flood magnitudes of 900 m^3/s and 1300 m^3/s for the November 15, 2021 flood at the lower hydrometric station and flood magnitudes of 100 m^3/s and 150 m^3/s at the upper station.

3.6. Future Trend Characteristics

Curves were fit to the PCIC generated rainfall-related (AR and non-AR) and snowmelt-related floods separately to infer the potential impacts of climate change. The curve consisted of the geometric mean across time of the pooled data from the six GCMs (i.e., LOESS[10] regression). The scales were removed from each curve by dividing out the current (2022) value of the curve, and then capturing how many times greater each future year's geometric mean (of the pooled data from the six GCMs) is compared to the geometric mean in 2022. The end result is “dimensionless scaling factors”.

The dimensionless scaling factors were subsequently used to re-scale the flood distributions (snowmelt-related, and rainfall-related [AR and non-AR]), so that future flood distributions compare to the current flood distribution by the same multiple that future geometric means compare to the current geometric mean in PCIC’s projections. A distribution for the annual maximum was obtained for each future year, from which a single climate-adjusted FM relationship was obtained.

The variability in the six GCMs was characterized using a bootstrap statistical approach. The floods generated from the different GCMs were pooled, from which many resamples (more than just six) were drawn. This variability was taken together with the uncertainty in the distribution fitting method to get overall confidence intervals for the climate-adjusted FM relationship. The 90% confidence intervals were calculated using 1000 bootstrap iterations.

The magnitude shift due to climate change is not likely to be the same for different quantiles (e.g., 2-year [50% AEP] and 200-year [0.5% AEP] events). The reliability of the scaling assumption was verified using PCIC’s projected streamflow data by observing the residuals (as

[10] Loess regression is a nonparametric technique that uses local weighted regression to fit a smooth curve.

defined as a ratio of simulated peak flows to the LOESS geometric mean) of the simulated maxima about the fitted geometric mean curves. The residuals appear to be stationary over time for the rainfall-related (AR and non-AR) peak flows suggesting that the distribution is not changing due to climate change aside from this scaling factor. Additional information on the validity of the scaling factors is discussed in BGC (June 4, 2021).

3.7. Transfer to Ungauged Watersheds

Flood information was transferred from the hydrometric stations to Jessica Bridge (Latitude: 49.447651° and Longitude: -121.270165°) above Sowoqua Creek (watershed area 373 km^2) on the Coquihalla River using a weighted function. The lower and upper watershed of the Coquihalla River are hydro-climatically different reflecting the elevation gradient of the Coast Mountains. The mean temperature averaged across the upper watershed below Needle Creek is lower given its higher mean elevation compared to the watershed above Alexander Creek. As a result, the upper watershed receives 13% more precipitation as snow based on data from Wang, Hamann, Spittlehouse, and Carroll (2016).

Given Jessica Bridge is located between the hydrometric stations (08MF003/08MF068 and 08MF062) in the watershed, a weighted function was used estimate floods at the bridge location based on the following three equations:

$$Q_c = Q_{c,d} + Q_{c,u}\beta \quad \text{[Eq. 3-1]}$$

$$\alpha = \frac{\log A_c - log\ A_u}{log A_d - log\ A_u} \quad \text{[Eq. 3-2]}$$

$$\beta = 1 - \alpha \quad \text{[Eq. 3-3]}$$

where Q_c is the flood estimate at Jessica Bridge, $Q_{c,d}$ and $Q_{c,u}$ are the flood estimates pro-rated from the downstream and upstream hydrometric stations to the ungauged location, α and β are the weighting factors, and A_c, A_d, A_u are the watershed areas at the ungauged location (c), at the downstream hydrometric station (d) (08MF003/08MF068), and the upstream hydrometric station (u) (08MF062).

The flood estimates were pro-rated to Jessica Bridge from the downstream and upstream hydrometric stations using the following equation:

$$\frac{Q_U}{Q_G} = \left(\frac{A_u}{A_G}\right)^n \quad \text{[Eq. 3-4]}$$

where Q_U is the flow (m^3/s) at Jessica Bridge, Q_G is the flow (m^3/s) at the hydrometric station, A_U is the watershed area (km^2) at the Jessica Bridge, and A_G is the watershed area at the hydrometric station, and *n* is a site-specific exponent related to peak flow data at both locations.

Typically, a value for *n* is chosen based on the watershed area size and takes on a value between 0.2 to 0.8 (Watt, 1989). A higher *n* is recommended for smaller watershed and indicates that streamflow will approach a value almost proportional to watershed area. An exponent of 1.0 was

adopted for the Coquihalla River. The average exponent when comparing flood estimates between the two hydrometric stations is 1.15 for AR-related floods. Similar results are obtained when an *n* value of 1.15 is used in the weighted calculation.

4.0 RESULTS

4.1. The November 15, 2021 Event

BGC's best estimate of the November 15, 2021, Q_{IPF} at the *Coquihalla River above Alexander Creek* (08MF068) hydrometric station is 1100 m^3/s. The November 15, 2021 Q_{IPF} at the *Coquihalla River below Needle Creek* (08MF062) hydrometric station is 135 m^3/s, which was recorded at the gauge.

4.2. From Q_{DMF} to Q_{IPF}

The linear regression shows that AR-related Q_{IPF} are typically larger than their corresponding Q_{DMF} compared to the relationship for snowmelt-related floods at both the lower (Figure 4-1) and upper (Figure 4-2) stations. The database of AR-related and snowmelt-related Q_{IPF} for the lower and upper watershed is shown in Table 4-1.

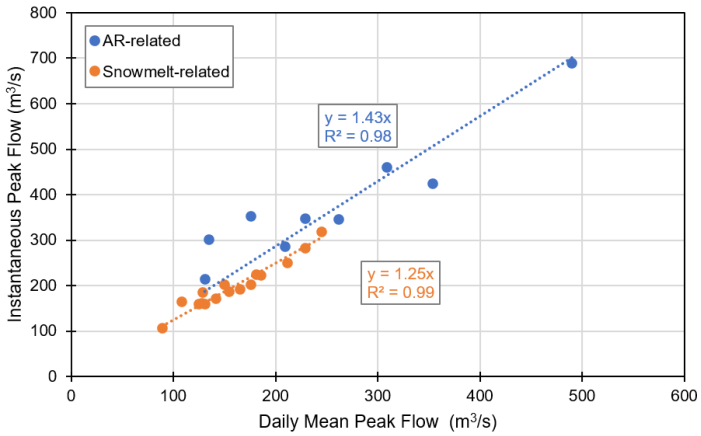

Figure 4-1. The linear regression between paired observation of Q_{IPF} and Q_{DMF} for AR-related (blue) and snowmelt-related (orange) floods in the lower watershed.

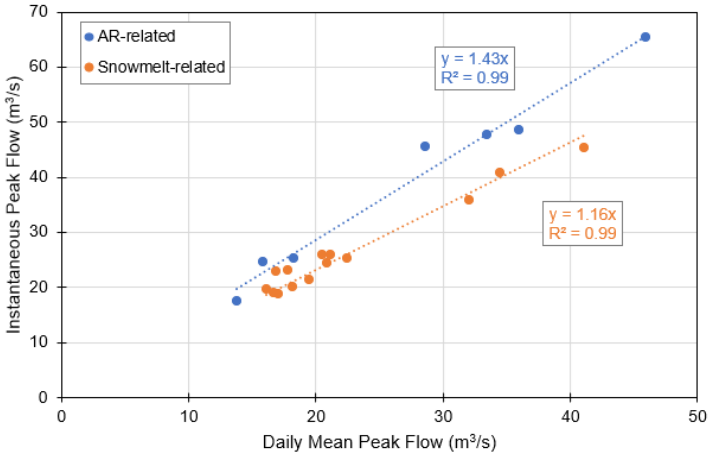

Figure 4-2. The linear regression between paired observation of Q_{IPF} and Q_{DMF} for AR-related (blue) and snowmelt-related (orange) floods in the upper watershed.

Table 4-1. Q_{IPF} for AR-related and snowmelt-related floods in the lower (08MF003/08MF068) and upper (08MF062) watershed. Values in bold and highlighted are estimated using the linear regression.

Date	Lower Watershed (08MF003/08MF068)		Upper Watershed (08MF062)	
	AR-related (m^3/s)	Snowmelt-related (m^3/s)	AR-related (m^3/s)	Snowmelt-related (m^3/s)
1957	**73**	Na	Na	Na
1958	**283**	**150**	Na	Na
1959	**343**	**262**	Na	Na
1960	**71**	**249**	Na	Na
1961	**242**	**173**	Na	Na
1962	**332**	**120**	Na	Na
1963	**406**	**127**	Na	Na
1964	**159**	**244**	Na	Na
1965	**155**	**165**	Na	Na
1966	**348**	**185**	**24**	**17**
1967	**819**	**238**	46	**24**
1968	**367**	**283**	**20**	19
1969	**38**	**227**	**4.5**	**23**
1970	**107**	**202**	**3.1**	21
1971	**152**	192	**12**	24
1972	**196**	283	**28**	45
1973	**121**	159	**9.0**	20
1974	**206**	223	**19**	**28**
1975	425	**237**	**27**	**22**
1976	**78**	187	**8.7**	**20**
1977	348	**155**	18	**14**

Date	Lower Watershed (08MF003/08MF068)		Upper Watershed (08MF062)	
	AR-related (m^3/s)	Snowmelt-related (m^3/s)	AR-related (m^3/s)	Snowmelt-related (m^3/s)
1978	390	**173**	**29**	**20**
1979	345	**133**	25	**20**
1980	689	**133**	65	**27**
1981	Na	Na	**3.9**	23
1982	**86**	161	**5.4**	**24**
1983	**191**	185	**16**	23
1984	Na	Na	48	**21**
1985	Na	Na	**18**	**27**
1986	Na	Na	**27**	**27**
1987	**81**	202	**4.1**	26
1988	Na	Na	**36**	Na
1989	**264**	**168**	**34**	**24**
1990	**371**	**119**	**6.3**	**15**
1991	**160**	171	**9.7**	**18**
1992	**140**	**131**	**6.6**	**17**
1993	**67**	225	**69**	**11**
1994	130	**128**	**12**	**16**
1995	**764**	**197**	**22**	**17**
1996	138	**142**	**6.4**	Na
1997	**181**	203	**19**	41
1998	**132**	160	**5.2**	**31**
1999	286	**223**	**17**	**44**
2000	**75**	**138**	**31**	26
2001	199	**151**	**41**	**24**
2002	372	**217**	**18**	**48**
2003	432	**128**	**27**	**19**
2004	352	**132**	25	**15**
2005	342	**82**	**22.7**	**10**
2006	**931**	**206**	**69**	**26**
2007	460	**195**	**45**	**22**
2008	**205**	319	**23**	**39**
2009	214	**147**	**17**	**21**
2010	**121**	165	**9.7**	19
2011	326	**203**	**21**	25
2012	**116**	250	**17**	36
2013	**94**	**254**	**7.5**	**35**
2014	**357**	**192**	**41**	**26**

Date	Lower Watershed (08MF003/08MF068)		Upper Watershed (08MF062)	
	AR-related (m^3/s)	Snowmelt-related (m^3/s)	AR-related (m^3/s)	Snowmelt-related (m^3/s)
2015	301	**52**	**31**	**8.2**
2016	**119**	107	**23**	20
2017	**346**	176	49	**24**
2018	**307**	171	**28**	**29**
2019	Na	148	**11**	**17**
2020	399	207[2]	**35**	**33**
2021	1100[1]	152[2]	135[2]	Na

Notes:
1. Estimated by BGC using a hydraulic model.
2. Considered provisional by the WSC.

4.3. Historical Trend Characteristics

There is no significant trend in the magnitude of historical AR-related and snowmelt-related floods in either the lower or upper watershed of the Coquihalla River, with or without the November 15, 2021 event (Table 4-2). Though, the snowmelt-related floods are approaching are approaching significance. The relatively flat 10-year moving average is consistent with this finding (Figure 4-3 and Figure 4-4). The absence of a significant trend supports the use of a stationary frequency analysis based on the historical data in the Coquihalla River watershed.

Table 4-2. Significance of historical trend as shown by the p-value.

Flood type	Lower Watershed	Upper Watershed
AR-related peak flows *with* November 15, 2021, event	0.31	0.22
AR-related peak flows *without* November 15, 2021, event	0.52	0.16
snowmelt-related peak flows	0.13	0.05

Note: The alpha threshold level was selected to be 0.01 for statistical significance to increase our confidence that the trend is not due to random chance

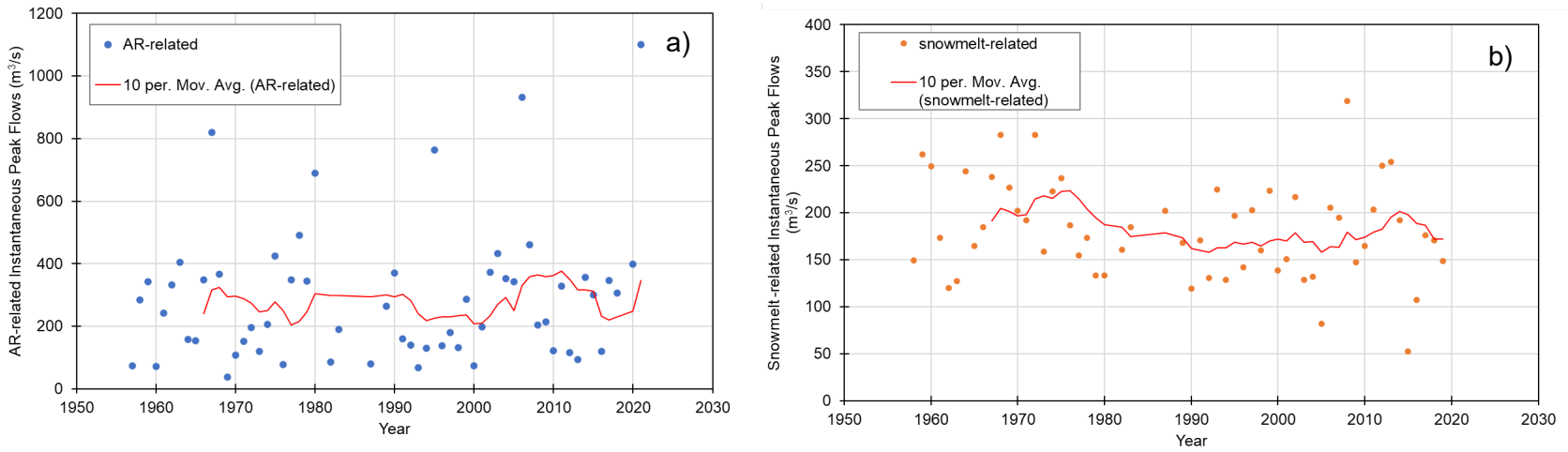

Figure 4-3. Temporal change in AR-related floods a) and snowmelt-related floods b) in the lower Coquihalla watershed over 1958 to 2021.

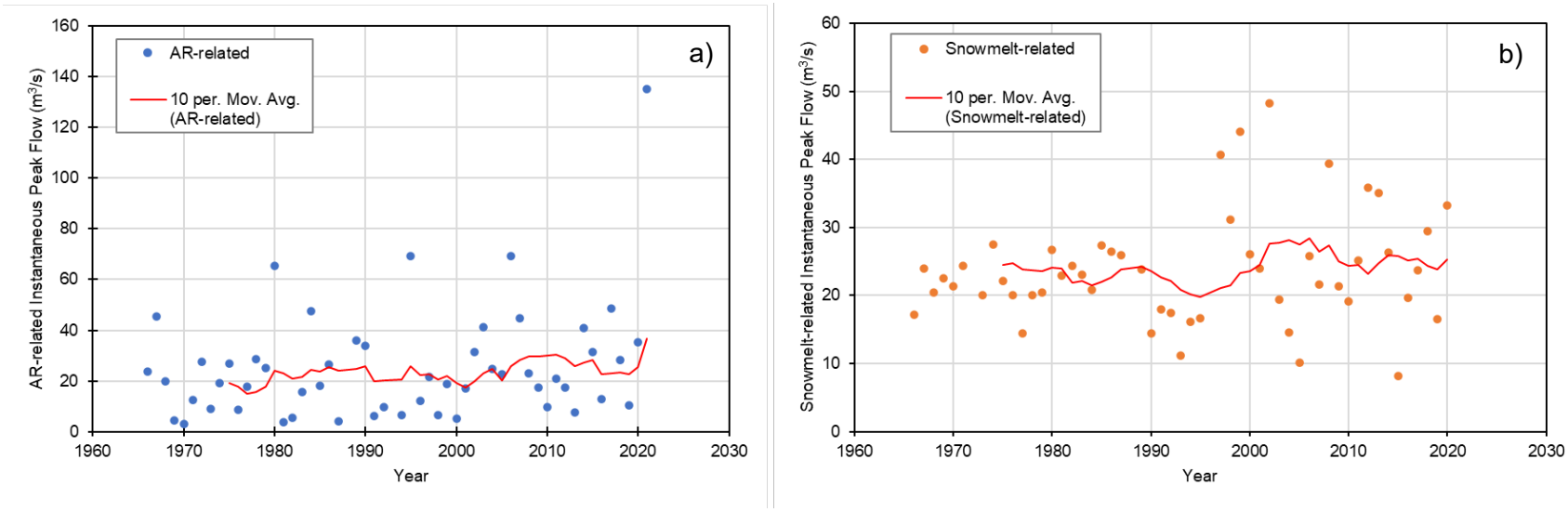

Figure 4-4. Temporal change in AR-related floods 2) and snowmelt-related floods b) in the upper Coquihalla watershed over 1966 to 2021.

4.4. Stationary FM Relationship

While the statistical model for snowmelt-related floods was relatively insensitive to the choice of distribution, the GEV distribution was ultimately selected because of its flexibility when extrapolating to longer return periods (lower % AEPs).

Unlike the snowmelt-related floods, the different distributions resulted in a range of options to characterize the largest AR-related floods (Figure 4-5). As a result, an ensemble of the best three distributions (as defined by the lowest quantile scores) was used to define them: the GEV, Log Normal, and Pearson Type III.

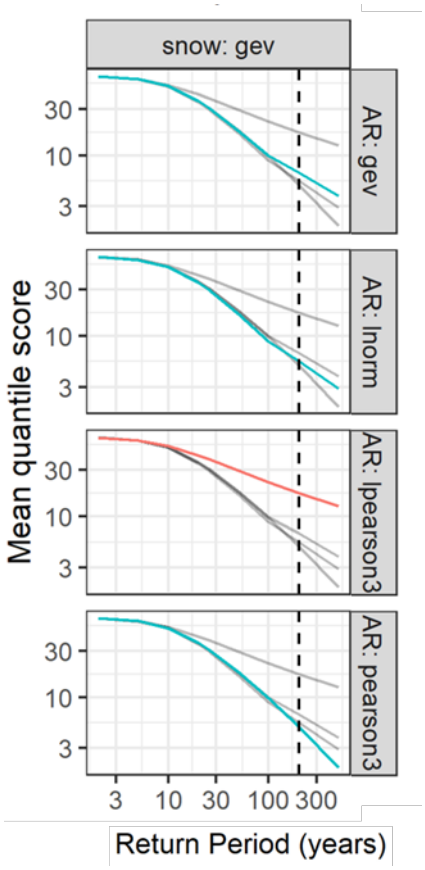

Figure 4-5. Mean quantile scores comparing each DMS model combination, plotted for each return period (% AEP) on a log-10 scale. The dashed line shows the 200-year (0.5% AEP) event. Smaller scores indicate a better model. Comparisons are only meaningful within each return period (% AEP).

The maximum likelihood estimate (MLE) fit method was used to estimate the parameters of the GEV and Log Normal distributions. The maximum goodness-of-fit estimates (MGE) method was used to fit the Pearson Type III distribution for the AR-related floods due to convergence issues during the iterative procedure with the MLE.

The stationary 200-year (0.5% AEP) event is estimated to be 1380 m^3/s in the lower watershed, with a 10^{th} and 90^{th} percentile confidence interval (CI) range of 975 to 2075 m^3/s (Table 4-3). This

best estimate is based on the assumption that the November 15, 2021 flood was 1100 m^3/s. Correspondingly, the return period (% AEP) of the November 15, 2021 event is approximately 100 years (1% AEP).

Table 4-3. Stationary FM relationship for the lower Coquihalla River watershed (08MF003/08MF068). The 10th and 90th percentiles are included as the lower and upper confidence interval (CI).

Return Period (% AEP)	Combined Approach with November 15, 2021 (m^3/s)		
	Estimate	Lower CI	Upper CI
2 (50% AEP)	240	220	265
5 (20% AEP)	395	335	450
10 (10% AEP)	540	445	645
20 (5% AEP)	700	555	860
50 (2% AEP)	930	705	1225
100 (1% AEP)	1135	835	1595
200 (0.5% AEP)	1380	975	2075
500 (0.2% AEP)	1785	1185	3170

In the upper Coquihalla watershed, the stationary 200-year (0.5% AEP) event is estimated at 115 m^3/s with 10th and 90th percentile estimates of 85 and 165 m^3/s (Table 4-4). This estimate is based on the gauged November 15, 2021 peak flow of 135 m^3/s for the upper Coquihalla River watershed (08MF062). The corresponding return period (% AEP) of the November 15, 2021 flood is between a 100 (1% AEP) and 200-year (0.5% AEP) event.

Table 4-4. Stationary FM relationship in the upper Coquihalla River watershed (02MF062). The 10th and 90th percentiles are included as the lower and upper confidence interval (CI).

Return Period (% AEP)	Combined Approach with November 15, 2021 (m^3/s)		
	Estimate	Lower CI	Upper CI
2 (50% AEP)	30	25	30
5 (20% AEP)	40	35	45
10 (10% AEP)	50	40	60
20 (5% AEP)	65	20	85
50 (2% AEP)	80	60	110
100 (1% AEP)	95	70	135
200 (0.5% AEP)	115	85	165
500 (0.2% AEP)	150	105	220

4.5. Sensitivity Analysis

The influence of the November 15, 2021 flood magnitude on the FM relationship is summarized over a range of return periods (% AEP) in the lower (Table 4-5) and upper (Table 4-6) watershed. Results show that as the estimate of the November 12, 2021 flood increases, the FM relationship shifts upwards with higher flood magnitudes. For example, the estimate of the 200-year (0.5% AEP) flood ranges from 1335 m^3/s (assuming 900 m^3/s) to 1425 m^3/s (assuming 1300 m^3/s). However, when compared to the 10^{th} and 90^{th} percentile confidence intervals, all three estimates fall with the range of uncertainty.

Table 4-5. Select flood quantiles based on a range of estimates for the November 15, 2021 event in the lower watershed (08MF003/08MF068).

November 15, 2021 Peak Flow Estimate (m^3/s)	20-year (5% AEP) Peak Flow (m^3/s)			50-year (2% AEP) Peak Flow (m^3/s)			200-year (0.5% AEP) Peak Flow (m^3/s)		
	estimate	Lower CI	Upper CI	estimate	Lower CI	Upper CI	estimate	Lower CI	Upper CI
900	690	550	845	915	700	1190	1335	970	1980
1100	700	555	860	930	705	1225	1380	975	2075
1300	705	555	880	950	705	1260	1425	985	2180
Range	15	5	35	35	5	70	90	15	200

Table 4-6. Select flood quantiles based on a range of estimates for the November 15, 2021 event in the upper watershed (02MF062).

November 15, 2021 Peak Flow Estimate (m^3/s)	20-year (5% AEP) Peak Flow (m^3/s)			50-year (2% AEP) Peak Flow (m^3/s)			200-year (0.5% AEP) Peak Flow (m^3/s)		
	estimate	Lower CI	Upper CI	estimate	Lower CI	Upper CI	estimate	Lower CI	Upper CI
100	60	50	80	80	60	105	110	85	155
135	60	50	80	80	60	110	115	85	165
150	65	50	80	80	60	110	115	85	165
Range	5	0	0	0	0	5	5	0	10

4.6. Climate-adjusted FM Relationship

The rainfall-related (AR and non-AR) floods are projected to increase over time (Figure 4-6a) while the snowmelt-related floods are projected to decrease over time (Figure 4-6b).

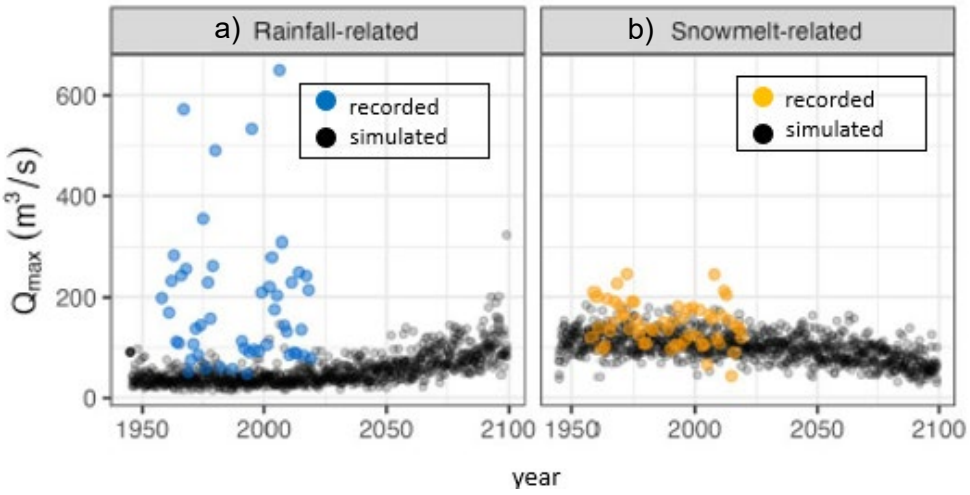

Figure 4-6. Time series for a) Q_{IPF} for rainfall-related (AR and non-AR) floods, and (b) Q_{IPF} for snowmelt-related floods in the lower watershed as recorded by WSC (coloured circles) and modelled by PCIC using six GCMs (black circles).

Return period (% AEP) projections based on dimensionless scaling factors see an immediate and rapid positive increase in the lower (Figure 4-7) and upper (Figure 4-8) watershed.

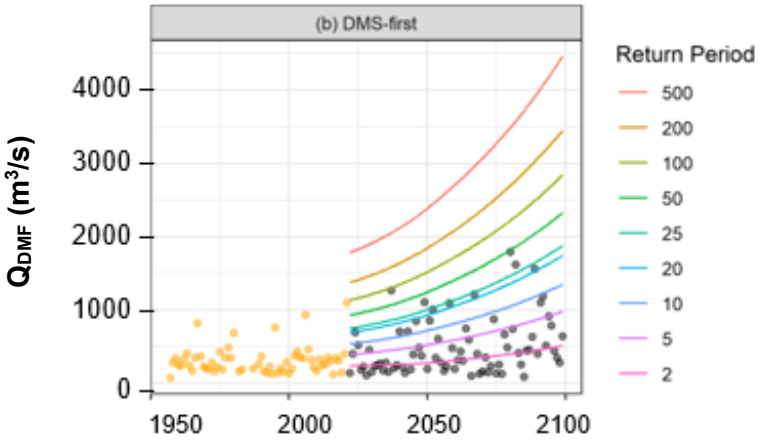

Figure 4-7. Return period (% AEP) projections in the lower watershed (08MF003/08MF068). Historical recorded data are in yellow; simulated data from the PCIC model are in black.

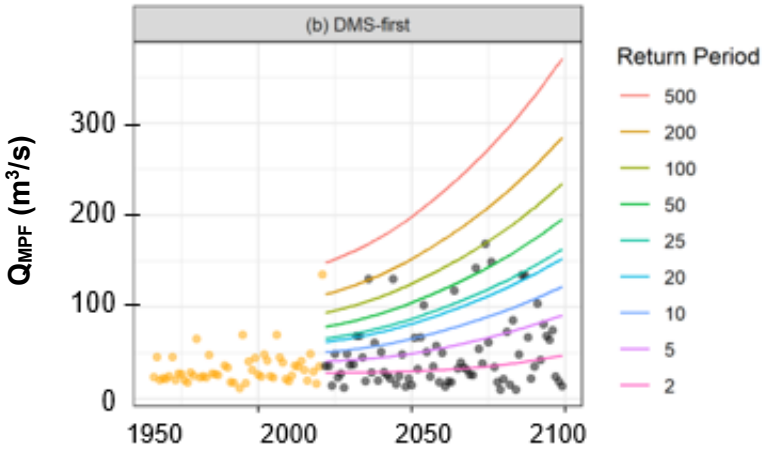

Figure 4-8. Return period (% AEP) projections in the upper watershed (02MF062). Historical recorded data are in yellow; simulated data from the PCIC model are in black.

In a non-stationary context, the FM relationship requires explicit definition because the exceedance probability associated with a flood magnitude changes with each consecutive year. The FM relationship can be defined as the flood that is exceeded once every 2, 5, 10, 20, 50, 100, 200, and 500 years on average. The climate adjusted FM relationship over the next 75 years can be defined as the flood that is exceeded 75/200 (0.5% AEP) times on average over the next 75 years.

Based on this definition, the climate-adjusted 200-year (0.5% AEP) flood in the lower watershed is estimated to be 2345 m^3/s – a 70% increase from to the stationary case (i.e., 1380 m^3/s). The stationary 200-year (0.5% AEP) flood (e.g., 1380 m^3/s) is projected to become approximately the 30-year flood in 75 years (Figure 4-7). The climate-adjusted 200-year (0.5% AEP) flood in the upper watershed is estimated to be 195 m^3/s – a 70% increase compared to the stationary case (i.e., 115 m^3/s). The stationary 200-year (0.5% AEP) flood event (e.g., 115 m^3/s) is also projected to become approximately the 30-year flood in 75 years.

The climate-adjusted FM relationship for the lower and upper watershed is provided in Table 4-7 and Table 4-8.

Table 4-7. Climate-adjusted FM relationship for the lower Coquihalla River watershed (08MF003/08MF068).

Return Period (% AEP)	Combined Approach with November 15, 2021 (m^3/s)		
	Estimate	Lower CI	Upper CI
2 (50% AEP)	310	265	365
5 (20% AEP)	615	525	735
10 (10% AEP)	865	720	1085
20 (5% AEP)	1140	930	1470
50 (2% AEP)	1556	1190	2105
100 (1% AEP)	1920	1410	2690
200 (0.5% AEP)	2345	1665	3565
500 (0.2% AEP)	3035	2030	5145

Table 4-8. Climate adjusted FM relationship for the upper Coquihalla River watershed (08MF062).

Return Period (% AEP)	Combined Approach with November 15, 2021 (m^3/s)		
	Estimate	Lower CI	Upper CI
2 (50% AEP)	30	25	35
5 (20% AEP)	60	50	70
10 (10% AEP)	75	65	100
20 (5% AEP)	100	80	125
50 (2% AEP)	135	100	180
100 (1% AEP)	160	120	225
200 (0.5% AEP)	195	140	280
500 (0.2% AEP)	250	180	365

4.7. Transfer to Ungauged Watersheds

The Jessica Bridge is located on the Coquihalla River approximately halfway up the watershed between both hydrometric stations with a watershed area of 373 km^2. Using Equation 3-4 and an n value of 1, the pro-rated 200-year (0.5% AEP) at Jessica Bridge using the lower and upper watershed FM relationships varies by more than 30% for the stationary and climate-adjusted cases (Table 4-9).

Table 4-9. Stationary and climate-adjusted 200-year (0.5% AEP) at Jessica Bridge using the lower (08MF003/08MF068) and upper (08MF062) watershed FM relationship.

Location	Watershed Area (km2)	Stationary (m3/s)	Climate-adjusted (m3/s)
Jessica Bridge based on lower watershed FM relationship	373	710	1200
Jessica Bridge based on upper watershed FM relationship	373	500	1660

The weighting factors show that the flood magnitude at Jessica bridge is influenced 70% by the downstream hydrometric station and 30% by the upstream hydrometric station based on watershed area (Table 4-10).

Table 4-10. Weighting factors.

Variable	Result
log (watershed area) at downstream hydrometric station (08MF003 / 08MF068)	2.86
log (watershed area) at upstream hydrometric station (08MF062)	1.93
log (watershed area) at Jessica Bridge	2.57
α	0.69
β	0.31

The stationary and climate-adjusted 200-year (0.5% AEP) at Jessica bridge as calculated using a weighted function based on watershed area is listed in Table 4-11. The November 15, 2021, event was estimated to be 560 m^3/s using this weighted function.

Table 4-11. Stationary and climate-adjusted 200-year (0.5% AEP) the lower (08MF003/08MF068) and upper watershed (08MF062).

Location	Watershed Area (km^2)	Stationary (m^3/s)	Climate-adjusted (m^3/s)
Jessica Bridge	373	640	1090

5.0 DISCUSSION

The combined FM relationship shows that the higher return period (% AEP) floods are AR-related while the lower return period (% AEP) events are snowmelt-related in the Coquihalla River watershed. The 200-year (0.5% AEP) flood can be expected to occur in the fall and winter, with a quick hydrological response occurring over several days. Snow on the ground in the watershed could exacerbate the flood if present (Gillett at al., 2022).

Climate change projections show that the rainfall-related (AR and non-AR) floods will increase over time while the snowmelt-related floods will decrease over time. Because the 200-year (0.5% AEP) flood is AR-related, we can expect this event to increase in magnitude in the

Coquihalla River. For example, the 200-year (0.5% AEP) is projected to become the 30-year (33% AEP) by the end of the century in the lower Coquihalla River watershed. A similar increase in floods has been shown for the Fraser River (Curry, Islan, Zwiers, and Déry, 2019).

In the FFA for the Coldwater River (BGC, May 20, 2022), the following topics were addressed:

- To include or not include the November 15, 2021 event in the analysis?
- Is the FM relationship “right”?
- Is the projected trend in rainfall-related (AR and non-AR) floods realistic?

The reader is referred to that report for a detailed discussion of these topics.

6.0 LIMITATIONS, ASSUMPTIONS, AND UNCERTAINTY

Limitations, assumptions, and sources of uncertainty in this study are listed below:

- The role of ARs on snowmelt in the spring contributing to rain-on-snow events is not considered explicitly in the statistical model for the following reasons:
    - There is only one of these events in the dataset.
    - The flood magnitude seems to be in between snowmelt-related and AR-related.
    - The AR frequency is typically lowest in the spring.
- The stationary FM relationship is based on the historical floods. Large magnitude floods control the statistical distribution, especially if AR-related. The FM relationship may require a re-calculation following a large (greater than 50-year, 2% AEP) flood.
- It is assumed that projected trends in Q_{DMF} apply to Q_{IPF}, which is a realistic assumption given these two quantities are highly correlated.
- The FM relationship should be interpreted in context of the confidence intervals, which highlight increased uncertainty with increasing return period (% AEP) events.
- The climate-adjusted FM relationship is based on the projection information available at this time. The assumptions made on changes to floods due to climate change should be revised in the future as scientific understanding of AR and snowmelt processes evolve. Human decisions and assumptions on behaviour today determines the rate of climate change in the future.
- Watershed disturbances such as land use change (e.g., conversion to agriculture), forestry (e.g., logging), insect infestations (e.g., mountain pine beetle), and wildfires may increase peak flows due to changes to hydrological processes. The projected increase in the frequency of watershed disturbances imply that the floods will likely be higher in the future. Detailed analyses on the extent of disturbance in the Coquihalla River watershed was beyond the scope of this work. As a result, the historical and projected influence of disturbances to peak flows in the Coquihalla River watershed is unknown.

7.0 CONCLUSIONS

- BGC considers the DMS approach as the preferred methodology to establish a FM relationship in the Coquihalla River.
- The 200-year (0.5% AEP) flood is AR-related and is projected to increase in magnitude over time (lower return period [higher %AEP]) due to climate change in the Coquihalla River watershed.
- The 200-year (0.5% AEP) flood in the lower watershed (08MF003/08MF068) is estimated to be 1380 m^3/s (with 10^{th} and 90^{th} percentile confidence intervals ranging from 975 to 2075 m^3/s). This estimate is based on the combined approach and assuming the November 15, 2021, event was 1100 m^3/s. The climate-adjusted 200-year (0.5% AEP) flood is estimated to be 2345 m^3/s – a 70% increase compared to the stationary case (i.e., 1380 m^3/s).
- The 200-year (0.5% AEP) flood in the upper watershed (08MF62) is estimated to be 115 m^3/s with 10^{th} and 90^{th} confidence intervals of 85 and 165 m^3/s. The climate-adjusted 200-year (0.5% AEP) flood is estimated to be 195 m^3/s – a 70% increase compared to the stationary case (i.e., 115 m^3/s).

8.0 CLOSURE

The material in this document reflects the judgment of BGC staff in light of the information available to BGC at the time of document preparation. Any use which a third party makes of this document or any reliance on decisions to be based on it is the responsibility of such third parties. BGC accepts no responsibility for damages, if any, suffered by any third party as a result of decisions made or actions based on this document.

As a mutual protection to our client, the public, and ourselves all documents and drawings are submitted for the confidential information of our client for a specific project. Authorization for any use and/or publication of this document or any data, statements, conclusions or abstracts from or regarding our documents and drawings, through any form of print or electronic media, including without limitation, posting or reproduction of same on any website, is reserved pending BGC's written approval. A record copy of this document is on file at BGC. That copy takes precedence over any other copy or reproduction of this document.

Yours sincerely,

BGC ENGINEERING INC.
per:

Melissa Hairabedian, M.Sc., P.Geo.
Hydrologist

Reviewed by:

Hamish Weatherly, M.Sc., P.Geo.
Principal Hydrologist

EGBC Permit To Practice: 1000944

KH/HW/rm/syt

Attachment I: HEC-RAS Modelling

REFERENCES

BGC Engineering Inc. (2021, June 4). *Merritt Detailed Flood Mapping Study, Nicola and Coldwater Rivers* [Report]. Prepared for Fraser Basin Council.

BGC Engineering Inc. (2022, May 20). *Frequency-Magnitude Relationship for the Coldwater River* [Report]. Prepared for Fraser Basin Council.

Bobotas, P., & Koutras, M.V. (2019). Distributions of the minimum and the maximum of a random number of random variables. *Statistics & Probability Letters, 146*, 57–64. https://doi.org/10.1016/j.spl.2018.10.023.

Coia, V., Joshi, A., Tan, S., & Zhu, Z. (2022). distplyr: Manipulation of Univariate Distributions. R package version 0.1.2.9000.

Curry, C.L., Islam, S.U., Zwiers, F.W., & Déry, S.J. (2019). Atmospheric rivers increase future flood risk in Western Canada's largest Pacific River. *Geophysical Research Letters, 46*, 1651–1661. https://doi.org/10.1029/2018GL080720

England, J.F., Jr., Cohn, T.A., Faber, B.A., Stedinger, J.R., Thomas, W.O., Jr., Veilleux, A.G., Kiang, J.E., & Mason, R.R., Jr. (2018). Guidelines for determining flood flow frequency—Bulletin 17C (ver. 1.1, May 2019). U.S. Geological Survey Techniques and Methods, book 4, chap. B5, 148 p. https://doi.org/10.3133/tm4B5

Gershunov, A., Shulgina, T., Ralph, F.M., Lavers, D.A., & Rutz, J.J. (2017). Assessing the climate-scale variability of atmospheric rivers affecting western North America. *Geophysical Research Letters, 44*(15), 7900-7908. https://doi.org/10.1002/2017GL074175

Gillett, N., Cannon, A., Malinina, E., Schnorbus, M., Anslow, F., Sun, Q., Kirchmeier-Young, M., Zwiers, F., Seiler, C., Zhang, X., Flato, G., Wan, H., Li, G., & Castellan, A. (2022). Human influence on the 2021 British Columbia floods. *Weather and Climate Extremes, 36*, 1000441 https://doi.org/10.1016/j.wace.2022.100441

Northwest Hydraulics Consultants Ltd. (NHC). (1994). *Coquihalla River Flood Hazard Management Study* [Report]. Prepared for District of Hope.

Pacific Climate Impacts Consortium (PCIC), University of Victoria. (2020, February). VIC-GL BCCAQ CMIP5 RVIC: Station Hydrologic Model Output. Downloaded from https://pacificclimate.org/data/station-hydrologic-model-output on February 15, 2022.

Sharma, A.R., & Déry, S.J. (2019). Variability and trends of landfalling atmospheric rivers along the Pacific Coast of northwestern North America. *International Journal of Climatology, 40*, 544–558. https://doi.org/10.1002/joc.6227

Sharma, A.R., & Déry, S.J. (2020a). Contribution of atmospheric rivers to annual, seasonal, and extreme precipitation across British Columbia and southeastern Alaska. *Journal of Geophysical Research: Atmospheres, 123*. https://doi.org/10.1029/ 2019JD031823

Sharma, A.R., & Déry, S.J. (2020b). Linking atmospheric rivers to annual and extreme river runoff in British Columbia and southeastern Alaska. *Journal of Hydrometeorology, 21*(11), 2457-2472. https://doi.org/10.1175/JHM-D-19-0281.1.

Wang, T., Hamann, A., Spittlehouse, D., & Carroll, C. (2016). Locally Downscaled and Spatially Customizable Climate Data for Historical and Future Periods for North America. *PLoS ONE 11*(6): e0156720. https://doi.org/10.1371/journal.pone.0156720

Watt, W.E. (Ed.). (1989). *Hydrology of floods in Canada: a guide to planning and design*. Ottawa, Canada: National Research Council Canada, Associate Committee on Hydrology.

Waylen, P., & Woo, M-K. (1982). Prediction of annual floods generated by mixed processes. *Water Resources Research, 18*(4), 1283-1286. https://doi.org/10.1029/WR018i004p01283

Waylen, P., & Woo, M-K. (1983). Annual floods in Southwestern British Columbia, Canada. *Journal of Hydrology, 62*, 95-105. https://doi.org/10.1016/0022-1694(83)90096-3

Zhang, Z., Stadnyk, T.A., & Burn, D.H. (2020). *Identification of a preferred statistical distribution for at-site flood frequency analysis in Canada.* Canadian Water Resources Journal, 45(1), 43-58. https://doi.org/10.1080/07011784.2019.1691942

ATTACHMENT I
HEC-RAS MODELLING

1.0 INTRODUCTION

As an independent effort from the WSC, the magnitude of the November 15, 2021, flood at the *Coquihalla River above Alexander Creek* (08MF068) hydrometric station was estimated using high water marks (HWMs) observed on a reach of the river in the vicinity of Othello Road. This site is located approximately 2.8 km upstream of the Alexander Creek station and has a drainage area of 602 km^2, compared to 730 km^2 at the WSC station.

HEC-RAS (version 6.2) modelling software was used to relate the HWMs to a range of discharges. HEC-RAS is a public domain hydraulic modelling program developed and supported by the United States Army Corps of Engineers (USACE) (Brunner & CEIWR-HEC, 2021). For this study, a two-dimensional (2D) hydraulic model was developed. The 2D model provides more detailed information on the flow depths and velocities than a one-dimensional (1D) model. A 2D model also removes some of the subjective modelling techniques which are involved in the development of 1D models such as defining ineffective flow areas, levee markers and cross-section orientation.

Detailed topographic data of the floodplain for the Coquihalla River at Othello Road are available from a high-resolution lidar dataset obtained by BGC from McElhaney. The lidar was acquired on December 3, 2021. HWM locations were geolocated by BGC on December 2, 2021 (Figure 1-1). The highwater marks collected by BGC staff had an uncertainty associated with the geographic coordinates of typically +/- 4 m from the accuracy of the GPS of the devices used to take the photos (phones and tablets). As a result of the uncertainty in the coordinates of the HWMs and the large elevation gradients at many of the locations measured only three of the collected HWMs were able to determined with enough certainty to be used for the present analysis.

Figure 1-1. Example of a HWM from the Coquihalla River flooding. Sediment deposited along Othello Road is clearly visible. Photo: BGC, December 2, 2021.

2.0 HYDRAULIC MODELLING

2.1. Model Domain and Boundary Conditions

The model domain covers an approximately 4.5 km stretch of the Coquihalla River ending 6.5 km upstream of Kawkawa Lake Road in Hope (Figure 2-1).

The upstream boundary of the Coquihalla River was set as steady inflow hydrograph. Flow hydrograph boundary conditions comprise of an inflow value and a hydraulic gradient to distribute this inflow along the length of the boundary condition line. The gradient used across the upstream boundary condition was measured from the lidar Digital Elevation Model (DEM) (0.8%).

A normal depth assumption was used as the downstream boundary for the Coquihalla River using a gradient measured from the lidar DEM (1.6%).

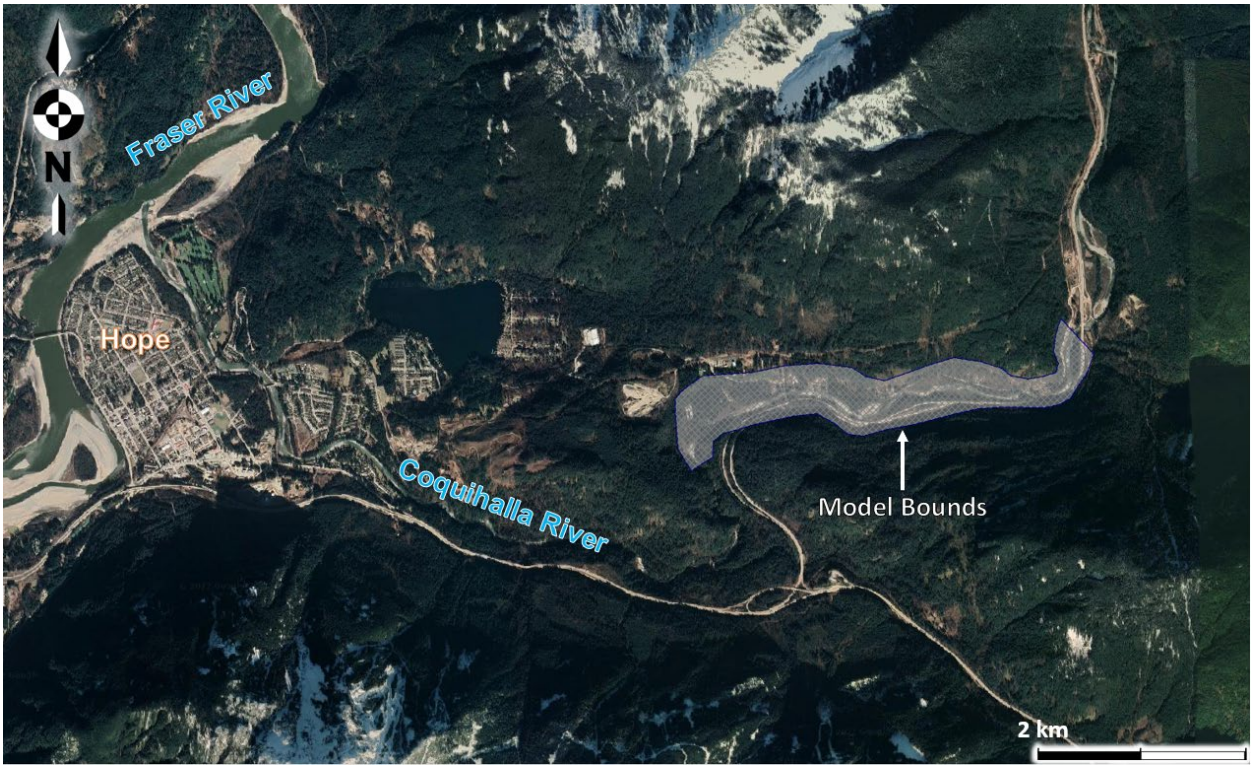

Figure 2-1. Overview of modelling location.

2.2. Manning's Roughness Values

Manning's roughness values (n)[1] were assigned by land cover type. A Manning's n of 0.1 was used for forested regions and 0.025 for roads. As it was not possible to calibrate the Manning's n value for the main channel (due to a lack of preflood bathymetry), a sensitivity analysis was instead performed. Manning's n for the main channel was varied between 0.035, based on the bed material, to 0.55, as calculated using Jarrett's equation (Jarrett, 1985). This range in

[1] Manning's n is a coefficient representing the friction applied to flow by the channel it is passing through.

roughness produced an average 0.3 m change in water surface elevation (WSE) for the modelled discharges. A value of 0.035 was ultimately selected for the channel as it produced regions of supercritical flow that best matched those observed by BGC staff when visiting the site.

The Manning's n values used for the present work are shown in Table 2-1 and Figure 2-2.

Table 2-1. Associating land class with Manning's n.

Land Class	Manning's n	Color
1. Roads	0.025	
2. Forest	0.1	
3. Main Channel	0.035	

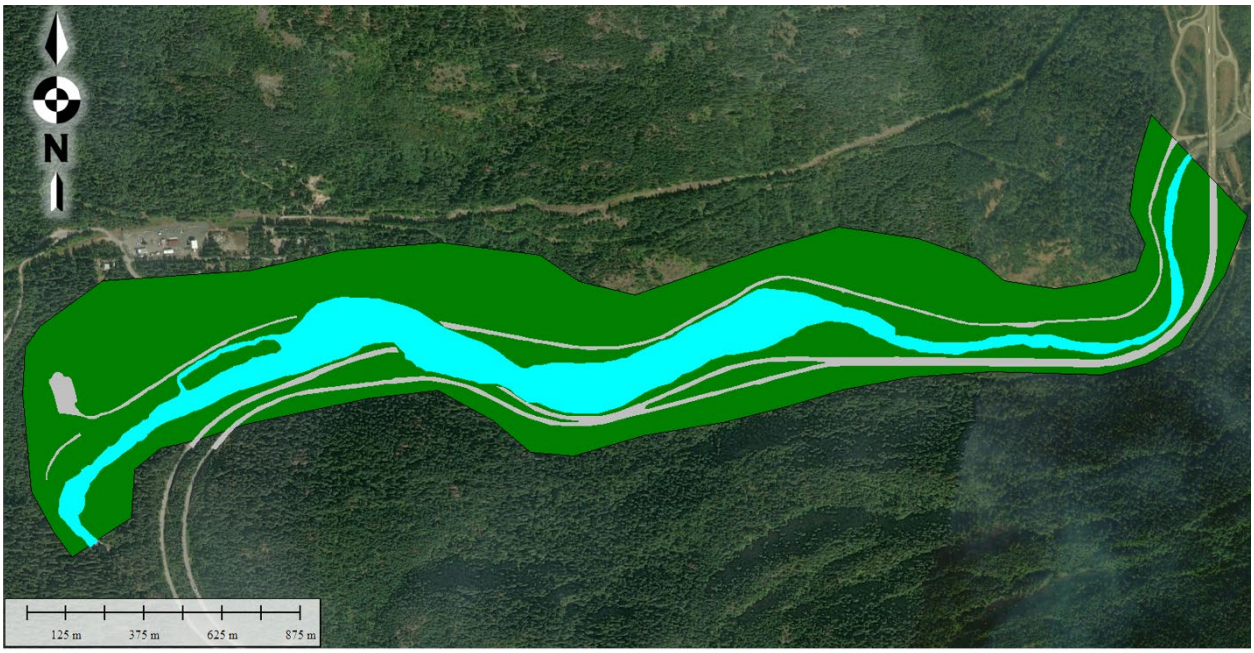

Figure 2-2. Manning's n roughness layer defined for the model.

2.3. HEC-RAS Model Meshing

The HEC-RAS software for 2D modelling uses an irregular mesh to simulate the flow of water over the terrain. Irregular meshes are useful for the development of numerically efficient 2D models to allow refinement of the model in locations where the flow is changing rapidly and/or where additional resolution is desired. With 2D models, the objective of mesh development is to use the coarsest mesh possible to reduce model runtime, while preserving the desired level of accuracy in the hydraulic results.

The default cell geometries created by HEC-RAS are rectangular, but other geometries can be selected to suit the problem under consideration. Within HEC-RAS, a 2D mesh is generated based on:

- Refinement areas to define sub-domains where the mesh properties (e.g., mesh resolution) are adjusted.
- Breaklines to align the mesh with terrain features which influence the flow such as dikes, ditches, terraces, and embankments. HEC-RAS provides options to adjust the mesh resolution along breaklines.

From these inputs, HEC-RAS generates the mesh consisting of interconnected grid cells with computational points at the cell centroids and along the faces of the cells (i.e., along the cell sides). The mesh was cleaned and checked for errors, such as a cell having more than 8 faces and gaps in the mesh.

2.4. Initial Mesh Development

For the Coquihalla River study area, a base mesh resolution of 25 m was selected. Breaklines were placed along the channel centerline, and along terrain features such as natural ridges and road embankments. Cell resolution on either side of breaklines was 5 m with 0 – 5 repeats.[2] An example of the mesh developed is provided in Figure 2-3.

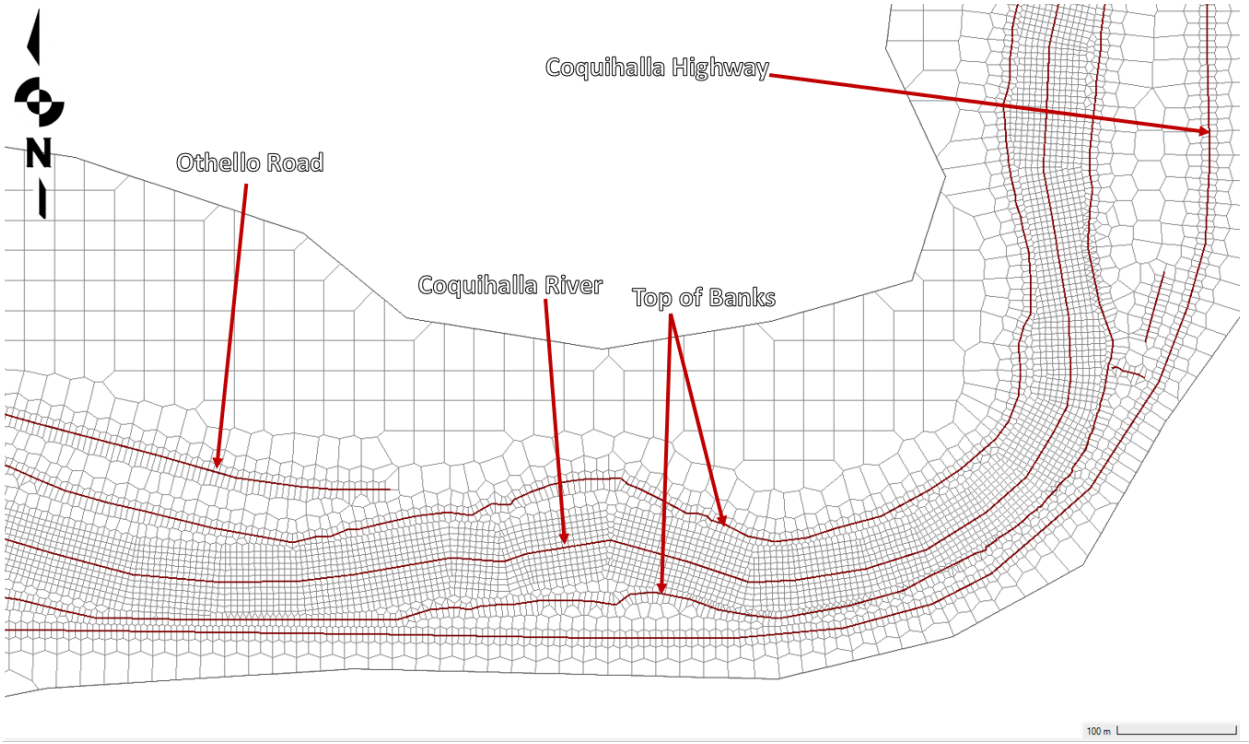

Figure 2-3. Manning's n roughness layer defined for the model.

[2] Repeats are rows of cells adjacent to those along the breakline using the same resolution and orientation defined by the breakline. As an example, a breakline with a 1 m resolution and 1 repeat would have 2 rows of 1x1 m cells on either side of it.

2.5. Simulation Settings

The HEC-RAS 2D model was run using the shallow water equations with a Courant-controlled time step[3]. The shallow-water equations provide an accurate representation of vertically-averaged flow dynamics, especially where sharp constrictions/expansions/changes in direction of flow are observed (e.g., meander bends, bridges, etc.). The initial time step was six seconds, and the maximum Courant number was 2. The model was run to simulate a 48-hour period to reach steady flow within the model domain.

2.6. Sensitivity Analysis

Five different discharge scenarios for the Coquihalla River were run to compare against the HWMs: 850, 900, 950, and 1050 and 1150 m^3/s. As there was no channel bathymetry surveyed, the lost capacity of the channel was accounted for by subtracting the flow measured at the *Coquihalla River above Alexander Creek gauge* the date the lidar was captured, 150 m^3/s, from the modelled scenarios (i.e., 700, 750, 800, and 900 and 1000 m^3/s were the modelled discharges). This work around is an approximation as the cross-sectional area that conveyed the 150 m^3/s discharge on the date the lidar was flown would be able to convey a higher flow at higher discharges (i.e., the same cross-sectional area would be inundated but the average channel velocity would be higher). Each scenario was run for 6 hours with the model reaching steady state after 3 hours.

3.0 MODEL CALIBRATION

The model was calibrated to three key areas of interest adjacent to where Othello Road was washed out:

1. Water cannot overtop the right bank of the river at the residential area location shown in Figure 3-1. There was no evidence of inundation in that area.
2. The water needs to overtop the road at the location shown in Figure 3-2. This area had sediment deposited over Othello Road and corresponds to the photo shown in Figure 1-1.
3. The WSE should match the HWM recorded by BGC at the location shown in Figure 3-3.

For area of interest one, the model shows overtopping of the banks for the 1150, 1050 and 950 m^3/s runs suggesting that flood flows were likely under 950 m^3/s. Likewise for area of interest two, inundation onto Othello Road was not observed for the 850 m^3/s case suggesting that flood flows were likely above 850 m^3/s. The HWM in area of interest is most closely aligned with the 900 m^3/s run. As such a peak flow of 900 m^3/s is the best estimate for the November 15, 2021 flood on the Coquihalla River at Othello Road. When prorated downstream to the *Coquihalla River above Alexander Creek* gauge, this yields an estimate of 1100 m^3/s.

[3] The Courant number is the product of the velocity and the time step divided by the distance step. For a Courant-controlled time step, the time step is halved if the Courant number for any cell exceeds the maximum Courant number set by the user. A maximum Courant number of up to 5 is recommended by the HECRAS 2D User Manual when using the Diffusion Wave equations, 3 when using the Shallow Water Equations, Eulerian-Lagrangian Method and 1 when using the Shallow Water Equations, Eulerian Method (Brunner & CEIWR-HEC, 2021).

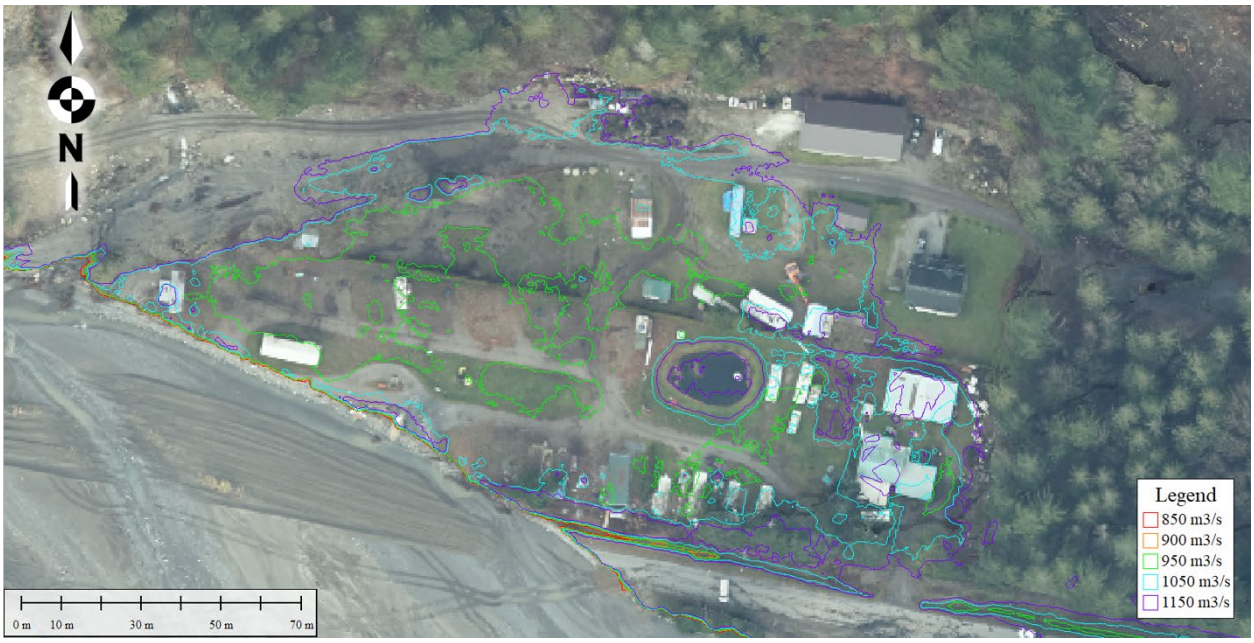

Figure 3-1. Modelled flooding extents at area of interest one.

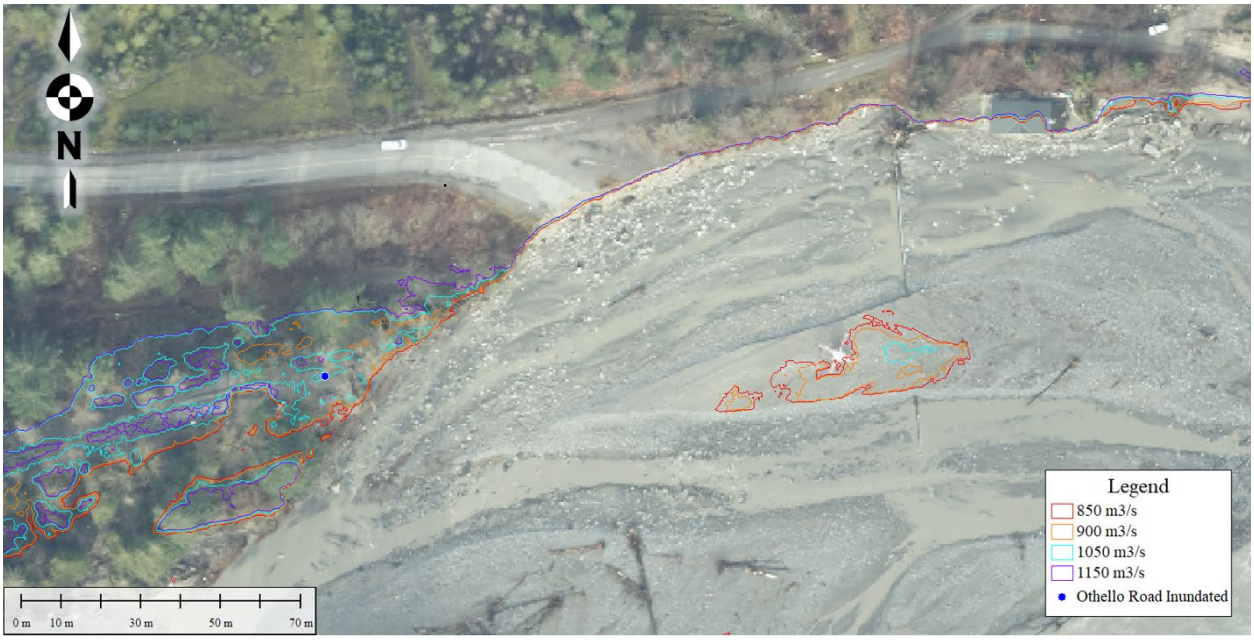

Figure 3-2. Modelled flooding extents at area of interest two.

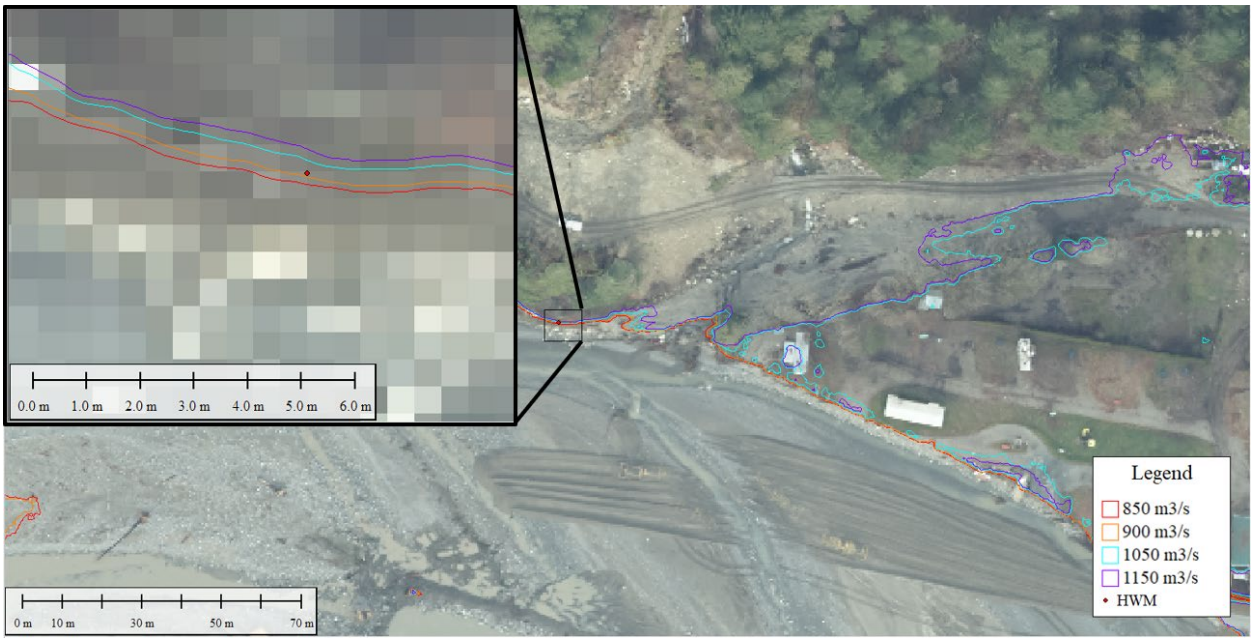

Figure 3-3. Modelled flooding extents at area of interest three.

4.0 SUMMARY AND LIMITATIONS

Using a 2D hydraulic model of the Coquihalla River and observed HWMs, BGC's estimated the magnitude of the November 15, 2021 flood on the Coquihalla River at Othello Road. The results are sensitive to the selected Manning's n value used in the hydraulic model. An average difference of 0.15 m exists in WSEs measured for the 850 and 950 m^3/s model runs. However, an increase to the Manning's n value from 0.035 to 0.055 produces a 0.3 m change to WSE, double that difference. No supercritical flow was shown in the model results when using an n value of 0.055 which does not match with the observed site conditions indicating the lower value is more accurate. There is a continuum of Manning's n and discharge values that would produce the observed HWMs, but based on the information currently available, 900 m^3/s is BGC's best estimate of the peak flow for the November 15, 2021 flood on the Coquihalla River at Othello. When prorated downstream to the *Coquihalla River above Alexander Creek* gauge, this yields an estimate of 1100 m^3/s.

REFERENCES

Brunner, G. W., & CEIWR-HEC. (2021). *HEC-RAS River Analysis System 2-D Modeling User's Manua*l. Retrieved from www.hec.usace.army.mil.

Jarrett, R.D., (1985). Determination of Roughness Coefficients for Streams in Colorado. U.S. Geological Survey. Water-Resources Investigations Report 85-4004. 60pp.

Design Criteria Sheet for Climate Change Resilience

Highway Infrastructure Engineering Design and Climate Change Adaptation
BC Ministry of Transportation and Infrastructure
(Separate Criteria Sheet per Discipline)
(Submit all sheets to the Chief Engineers Office at:
BCMoTI-ChiefEngineersOffice@gov.bc.ca)

Project:	*Peers Creek Frontage Road Washout Site*
Type of work:	*2021 Flood Recovery Repair*
Location:	*Coquihalla River at Peers Creek Frontage Road, near Hope, B.C.*
Discipline:	*Hydrotechnical*

Design Component	Design Life or Return Period	Design Criteria + (Units)	Design Value Without Climate Change	Change in Design Value from Future Climate	Design Value Including Climate Change	Adaptation Cost Estimate ($)	Comments / Notes / Deviations / Variances
Hydrotechnical design of riprap features	200-year RP	Instantaneous Flow Rate (m^3/s)	1,070 m^3/s	+69% on instantaneous flow rate	1815 m^3/s	$1,270,000	As summarized in Table 1

Explanatory Notes / Discussion:

Flooding on the Coquihalla River in November and December 2021 resulted in extensive erosion and damage to Peers Creek Frontage Rd (PCFR) and Highway 5 located near Hope, BC. The BC Ministry of Transportation and Infrastructure (MoTI) plans to reinstate PCFR adjacent to Highway 5.

The PCFR site is vulnerable to changes in future peak flows as a consequence of climate change. As requested by MOTI, an assessment was undertaken by BGC to estimate climate-adjusted design flows. The Pacific Climate Impacts Consortium (PCIC) provides daily streamflow projections for the *Coquihalla River above Alexander Creek* (08MF068) hydrometric station under naturalized conditions. The daily mean streamflow is simulated using runoff and baseflow generated with an upgraded version of the Variable Infiltration Capacity (VIC-GL) model that is coupled to a glacier model (Schnorbus, in prep) and routed with RVIC (Lohmann et al., 1998, 1996; Hamman et al., 2016).

Rainfall-related peak flows were extracted for the September to March period from the PCIC forecasted data. The snowmelt-related peaks were extracted for the April to August period. Curves were fit to the projected annual maximum flows for the three separate time series (e.g., yearly maximums, rainfall-related, and snowmelt-related). The scales were removed from each curve by dividing out the current (2022) value of the curve, capturing how many times greater each future year's geometric mean is compared to the geometric mean in 2022 – the "dimensionless scaling factors". The dimensionless scaling factors were subsequently used to re-scale the peak flow distributions (snowmelt-related and rainfall-related).

The results indicate that the climate-adjusted 200-year (0.5% AEP[1]) instantaneous peak flow increases by 69% to a value of 2345 m^3/s from the stationary case (1380 m^3/s) at the *Coquihalla River above Alexander Creek* (08MF068) hydrometric station. The instantaneous peak flows were prorated to the PCFR site, resulting in flows of 1,070 m^3/s for the stationary 200-year instantaneous peak flow and 1815 m^3/s for the climate-adjusted 200-year instantaneous peak flow.

[1] Annual exceedance probability

Proposed riprap protection works along the section of the PCFR to be reinstated include five components:

1. A 300 m long riprap revetment along Peers Creek Road.
2. An 80 m long deflection berm at the downstream end of the revetment.
3. Knick point armouring immediately downstream of the deflection berm.
4. Ditch armouring along Peers Creek Road from the proposed revetment south to the Othello interchange.
5. Road embankment armouring along Peers Creek Road from the proposed revetment south to the Othello interchange.

Differences in flood hydraulics between the climate-adjusted 200-year flow and the stationary 200-year flow results in differences in armouring requirements for the five riprap design components. The differences in design, estimated material quantities, and estimated total costs are summarized in Table 1.

Table 1. Summary of differences in design, estimated material quantities, and estimated costs for the riprap design components.

Design Component	Difference in Armouring Requirement	Material Quantity Difference	Cost Difference
Riprap Revetment	For the climate-adjusted 200-year flow, the design velocity is 5.2 m/s and the required riprap size is 2000 kg Class riprap. For the stationary 200-year flow, the design flow velocity is 4.5 m/s and the required riprap size is 1000 kg Class riprap.	**Riprap Quantity Difference ~ 1700 m^3** Climate-Adjusted Volume ~ 7600 m^3 (Class 2000 kg riprap) Stationary Volume ~ 5900 m^3 (Class 1000 kg riprap)	**Cost Difference ~ $960,000** Climate Adjusted Cost: $3,040,000 Assumed Unit Price (Class 2000 kg riprap): $400/$m^3$ Stationary Cost: $2,080,000 Assumed Unit Price (Class 1000 kg riprap): $350/$m^3$
Deflection Berm	The deflection berm is recommended for the climate-adjusted 200-year flow, but not required for the stationary 200-year flow	**Riprap Quantity Difference ~ 560 m^3** Climate-Adjusted Volume = 800 m^3 (Class 250 kg riprap) Stationary Volume = 0 m^3	**Cost Difference ~ $170,000** Climate Adjusted Cost: $170,000 Assumed Unit Price (Class 250 kg riprap): $300/$m^3$ Stationary Cost: $0
Knick Point	There is no difference between the design of the knick point armouring for the stationary or climate-adjusted 200-year flow.	-	-
Ditch Armouring	There is a small reduction in flow velocity between the climate-adjusted 200-year flow and the stationary 200-year flow, but there is no difference in the design of the ditch armouring.	-	-
Road Embankment	For the climate-adjusted 200-year flow, the design velocity is 3.5 m/s and the required riprap size is Class 100 kg riprap. For the stationary 200-year flow, the design flow velocity is 1.0 m/s and the required riprap size is Class 10 kg riprap.	**Riprap Quantity Difference ~ 500 m^3** Climate-Adjusted Volume = 1000 m^3 (Class 100 kg riprap) Stationary Volume = 500 m^3 (Class 10 kg riprap)	**Cost Difference ~ $140,000** Climate Adjusted Cost: $250,000 Assumed Unit Price (Class 100 kg riprap): $250/$m^3$ Stationary Cost: $110,000 Assumed Unit Price (Class 10 kg riprap): $220/$m^3$
			Total Cost ~ $1,270,000

The estimated cost for adapting the riprap protection to climate change is estimated to be $1,270,000. Costs of other project elements (e.g., road repair) are not considered here.

For a complete discussion of the climate change assessment and design, please refer BGC's report titled "Hydrotechnical Assessment and Design for Peers Creek Frontage Road Washout Site", dated May 23, 2023.

Recommended by: Engineer of Record: Evan Shih, P.Eng.

May 23, 2023

Date: May 23, 2023

Engineering Firm: BGC Engineering Inc.

2023.05.15

Accepted by BCMoTI Consultant Liaison: _____
(For External Design)

Deviations and Variances Approved by the Chief Engineer: _____
Program Contact: Chief Engineer BCMoTI

APPENDIX B
MEMO – PRELIMINARY HYDROTECHNICAL ASSESSMENT FOR INTERIM REPAIRS OF PEERS CREEK FRONTAGE ROAD

BGC ENGINEERING INC.
AN APPLIED EARTH SCIENCES COMPANY
Suite 500 - 980 Howe Street, Vancouver, BC Canada V6Z 0C8
Telephone (604) 684-5900 Fax (604) 684-5909

Project Memorandum

To:	**BC Ministry of Transportation and Infrastructure**		
Attention:	**Dickson Chung, Senior Highway Design Engineer; Maureen Kelly, Senior Geotechnical Engineer**	**cc:**	**Neetu Bhatti, McElhanney Senior Project Manager**
From:	**Evan Shih, BGC Engineering Inc.**	**Date:**	**October 25, 2022**
Subject:	**Preliminary Hydrotechnical Assessment for Interim Repairs of Peers Creek Frontage Road**		
Project No.:	**0272-097**		

1.0 INTRODUCTION

In November 2021, landfalling of an atmospheric river brought two days of intense rainfall to southwestern British Columbia resulting in extreme streamflow and extensive geomorphic change in watersheds across a large spatial extent of the lower Fraser River watershed, including the Coquihalla River. Flooding on the Coquihalla River in November and December 2021 resulted in extensive erosion and damage to infrastructure throughout the river valley, with washouts of Othello Road, Highway 5 (located valley-opposite to Othello Road) and Peers Creek Frontage Road near Hope, British Columbia (BC).

BGC Engineering Inc. (BGC) was retained by the BC Ministry of Transportation and Infrastructure (MoTI) to provide hydrotechnical engineering support for the long-term repair of Peers Creek Frontage Road in coordination with MoTI's road design and project management consultant, McElhanney Consulting Services Ltd (McElhanney). Design for long-term repair of the road is currently in the conceptual phase; however, BGC understands that Kiewit Corporation (Kiewit) intends to complete interim repairs of the road to provide construction access for the Trans Mountain Expansion Project until a long-term solution can be implemented by MoTI. Construction of the interim works is expected to initiate sometime between late October and early November 2022 pending acquisition of permits and approvals. On September 30, 2022, Kiewit requested that BGC provide recommendations to inform hydrotechnical design of a section of the road that washed out during the November 2021 flood and where instream works (i.e., riprap armouring) will be required for the interim repairs. McElhanney is providing design recommendations from a highway design perspective.

This memo provides an overview of BGC's preliminary hydrotechnical assessment and recommendations for Kiewit's proposed interim instream works. Key hydrotechnical design parameters were estimated including the design water surface elevation, riprap size, and scour depth. All work was conducted in accordance with the existing As & When Geotechnical Engineering and Design Services contract (Contract No. 861CS1183) between BGC and MoTI, dated September 16, 2021. BGC understands that MoTI will share this memo will Kiewit.

2.0 HYDROTECHNICAL ASSESSMENT

2.1. General

The preliminary hydrotechnical assessment was conducted to support Kiewit's design of interim repairs to Peers Creek Frontage Road. The assessment utilizes a two-dimensional (2D) hydrodynamic model of the Coquihalla River prepared by BGC using HEC-RAS (Hydrologic Engineering Center – River Analysis System). The hydrodynamic model was originally prepared to support design of the Othello Rd washout site (i.e., Othello Road Site B). The model domain was subsequently extended upstream to encompass the river reach adjacent to Peers Creek Frontage Road. Due to the urgency of this assessment, calibration and validation of the model has not been completed. Therefore, the results presented herein are considered preliminary and may vary from those reported following detailed assessment and design of the long-term repair works.

2.2. Design Flood Event

As part of the Othello Road Site B project, BGC conducted a detailed analysis to estimate flood magnitudes for a range of return periods. Details of that analysis are summarized in BGC (July 13, 2022). The estimated quantiles were prorated by drainage area to the Peers Creek Frontage Road site (Table 2-2). BGC understands that MoTI typically requires temporary flood protection works to be designed to the 10-year return period peak flow. Recommendations within this memo are provided in consideration of this flood magnitude (i.e., 420 m^3/s)

Table 2-1. Peak flow estimates for a range of return periods at Peers Creek Frontage Road site.

Return Period	Peers Creek Washout Site Flow (m^3/s)
2	190
5	305
10	420
20	500
50	720
100	880
200	1070

2.3. Flood Hydraulics

The 2D hydrodynamic model was developed using a digital elevation model (DEM) that combined bathymetric survey data collected by McElhanney from August 29-31 and September 16, 2022 with lidar data collected by McElhanney on April 22, 2022. The upstream model boundary was located approximately 1.5 km upstream of the project area. The downstream model boundary was set approximately 5 km downstream of the project area, just upstream of the Coquihalla River

canyon. The parameters used in the 2D model simulations are summarized in Table 2-3. Water surface elevations (WSE), flow velocities and flow depths were extracted from the model at the location shown in Figure 2-1, where the road washed out during the November 2021 flood and where instream installation of a temporary riprap revetment is proposed.

During the 10-year peak flow event, the channel is estimated to have an average flow depth of approximately 3 m and flow velocity of approximately 4 m/s at the area of interest. A profile of the modelled WSE along the blue line shown in Figure 2-1 is illustrated in Figure 2-2.

Table 2-2. Parameters used for 2D hydrodynamic modelling using HEC-RAS.

Hydraulic Parameter	Value
Manning's n roughness coefficient in the channel	0.035
Manning's n roughness coefficient in the floodplain	0.1
Slope at the downstream model boundary (m/m)	0.016
General mesh spacing (m)	25 m x 25 m
Grid spacing at breaklines (m)	5 m x 5 m
Model time step	Variable based on Courant condition

Figure 2-1 Location of hydraulic parameter estimation. WSEs, flow velocity and flow depth were estimated along the blue line. A scour analysis was conducted using a typical cross section along the red line.

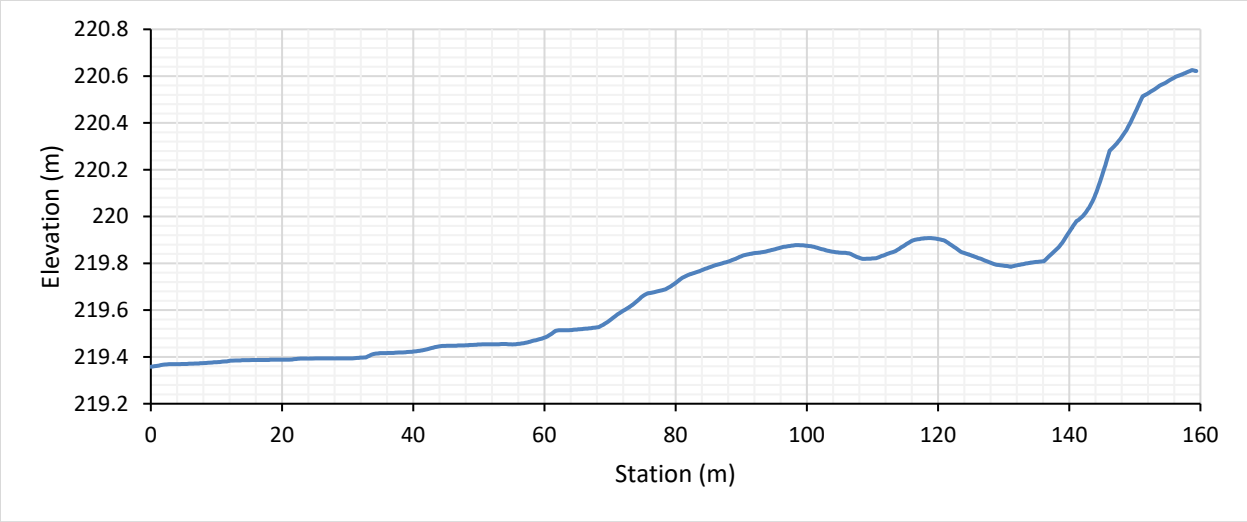

Figure 2-2 Modelled WSE profile for 10-year return period peak flow. The WSE was extracted from the 2D model along the blue line shown in Figure 2-1 with station 0 located at the downstream extent of the line.

2.4. Scour Assessment

A scour assessment was completed using outputs from the hydraulic model taken along a typical cross section at the area of interest (red line shown in Figure 2-1). Natural scour was estimated using the Blench Regime method (Blench, 1969). Results of the analysis indicate that limited scour is expected to occur below the channel thalweg elevation (216.7 m) during the 10-year peak flow event.

Immediately following the November 2021 flood event, considerable sediment aggradation was observed along the project reach. In the period following, the channel bed was observed to have degraded considerably; potentially up to 2 m in areas. The morphology of the project reach and potential for additional channel degradation had not been reviewed at the time of preparation of this memo. Although limited scour is predicted during the 10-year peak flow event, keying the riprap revetment into the channel bed to an elevation of 216.0 m, or approximately 0.7 m below the surveyed channel thalweg, would provide an allowance for uncertainty in the analysis and the potential for ongoing degradation.

2.5. Riprap Sizing

Riprap sizing for the proposed riprap revetment was estimated based on methods provided in USACE EM 1110-2-1601 (USACE 1994). Design flow velocity and depth were estimated from the 2D modelling results as discussed in Section 2.3. Assuming a 2H:1V bank slope, the analysis indicates that a minimum riprap size of 500 kg Class (D_{50} = 725 mm) would be required to maintain hydraulic stability during the 10-year peak flow event.

3.0 RECOMMENDATIONS

Based on the preliminary hydrotechnical analysis, BGC's recommendations are summarized as follows:

- Ideally, the top elevation of the riprap revetment would be installed above the 10-year WSE, although this may not be feasible given site constraints. Based on discussions with McElhanney, BGC understands that overtopping of the revetment may be tolerated given that the interim works will repair the site to an improved condition from what presently exits.
- A minimum riprap size of 500 kg Class is required for hydraulic stability of the proposed riprap revetment. BGC has not estimated the gradation of riprap that was installed onsite immediately following the November 2021 flood. However, based on visual inspection, the riprap appeared to consist of a range of sizes of approximately 500 kg Class and larger. BGC understands that Kiewit will be repurposing existing riprap onsite to construct the temporary revetment. BGC recommends that a sorting of riprap onsite be completed to the extent possible such that the temporary revetment is constructed of 500 kg Class riprap or larger, while meeting the gradation specifications provided in Section 205 of the MoTI Standard Specifications (MoTI, 2020). The revetment should be constructed at slopes no steeper than 2H:1V and the minimum thickness of the riprap should align with the riprap size selected (i.e., if a larger class of riprap is used, it should match the corresponding thickness indicated in Table 205-D of MoTI (2020)).
- Geotextile filter fabric should be installed beneath all riprap to reduce the potential for migration of soil particles from the underlying in-situ soils. Mirafi 1100N or equivalent is recommended and overlain with a 150 mm gravel bedding layer.
- The riprap revetment should be blended into the existing revetments upstream and downstream to provide smooth transitions, and keyed into the channel bed to an elevation of 216.0 m.

4.0 CLOSURE

BGC Engineering Inc. (BGC) prepared this document for the account of BC Ministry of Transportation and Infrastructure. The material in it reflects the judgment of BGC staff in light of the information available to BGC at the time of document preparation. Any use which a third party makes of this document or any reliance on decisions to be based on it is the responsibility of such third parties. BGC accepts no responsibility for damages, if any, suffered by any third party as a result of decisions made or actions based on this document.

As a mutual protection to our client, the public, and ourselves all documents and drawings are submitted for the confidential information of our client for a specific project. Authorization for any use and/or publication of this document or any data, statements, conclusions or abstracts from or regarding our documents and drawings, through any form of print or electronic media, including without limitation, posting or reproduction of same on any website, is reserved pending BGC's written approval. A record copy of this document is on file at BGC. That copy takes precedence over any other copy or reproduction of this document.

Yours sincerely,

BGC ENGINEERING INC.
per:

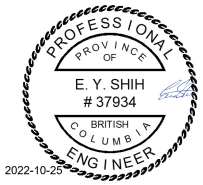

Evan Shih, M.Eng., P.Eng.
Senior Hydrotechnical Engineer

Reviewed by:

Rob Millar, Ph.D., P.Eng., P.Geo.
Principal Hydrotechnical Engineer

EGBC Permit To Practice: 1000944

ES/RM/md/th

REFERENCES

BC Ministry of Transportation and Infrastructure (MoTI). (2020). 2020 Standard Specifications for Highway Construction. Volume 1 of 2.

BGC Engineering Inc. (July 13, 2022). *Hydrotechnical Design Basis for Othello Road Washout Site – Interim Report* [Draft Report]. Prepared for BC Ministry of Transportation and Infrastructure.

Blench, T. (1969). *Mobile-bed fluviology.* Edmonton, AB: University of Alberta Press.

US Army Corps of Engineers (USACE). (1994). *Hydraulic Design of Flood Control Channels. Engineering Manual* (EM) 1110-2-1601. June 30, 1994.

APPENDIX C
STABILITY SEEDING MEMO FROM DR. BRETT EATON

Habitat benefits of using a stability seeding approach to channel stabilization

Brett Eaton

2023-03-08

1 executive summary

New proof-of-concept experiments demonstrate the potential impact of the "stability seeding" approach to channel stabilization. This approach involves introducing sediment (typically in the boulder size class range) that is consistent with the largest sediment transported by the river at the site requiring stabilization. This stabilizing sediment includes sediment ranging from 50% to 100% of the largest mobile particle at the site. This size of sediment has been shown to control the stability of the banks, bars, pools and riffles in gravel bed streams by controlling the deposition of the rest of the sediment found in the bed of the river.

There are a range of methods for implementing stability seeding, including: positioning the stabilizing sediment on the floodplain surface adjacent to the channel banks and relying on bank erosion to recruit them; placing stabilizing sediment directly on the channel banks (either on top of existing riprap or on top of an eroding cut-bank) so that high flows can recruit the sediment before bank erosion occurs; and placing the stabilizing sediment on the channel bed at key locations to mimic the redistribution of these sediments that naturally occur during high flows. While the nature of the potential habitat impacts produced by stability seeding are well defined, the degree to which they can be realized in a real-world implementation depends on how well the stabilizing sediment can be recruited by the river and transported to key locations that control the channel morphology. Therefore, it is important to remember that the extent of the habitat improvement that will result remains to be demonstrated in the field.

Relative to standard riprap designs, channel rehabilitation using stability seeding approaches has the potential to retain a diverse set of physical habitats (including riffles, pools and bars) within the stabilized reach, and to maintain the exchange of water between the stream and the river bed (which is key to maintaining potential spawning habitat quality associated with riffles).

When used to stabilize actively retreating meander bends, the stability seeding approach will help offset the reduction in bed sediment supply associated with stabilizing the bank, thereby reducing the potential for degradation of the riffles downstream of the bend. This should reduce the potential for the bank stabilization activities to have negative impacts on downstream habitat quality.

Stability seeding also limits the potential for vertical bed scour, which not only simplifies the channel morphology and degrades the physical habitat, but can expose and damage buried infrastructure (which can obviously have negative effects on the local riverine ecology). The degree to which this effect can be realized depends on how much of the stabilizing sediment can be entrained by the flow and transported to key locations (such as riffles) that control the stability of the stream bed. In situations where vertical scour is an imminent threat to infrastructure and physical habitat, direct placement of stabilizing sediment in the stream channel may be preferable to a standard riprap installation.

2 stability seeding overview

The gravel bed streams found in mountainous regions like British Columbia are commonly referred to as threshold streams (Church 2006) because they seldom experience flows that are much more powerful than

those capable of eroding and transporting the median sized sediment particle on the surface of the river bed (called D_{50}).

The relative strength of a flow can be indexed using the average shear stress, which is the force per unit area exerted on the channel bed (τ). It depends primarily on the water depth, d, and the water surface gradient, S. Relative flow strength is also often indexed using the average flow velocity (U), which depends on d, S, and the roughness of the channel boundary. The key equations used to analyse sediment transport are most often constructed using τ. To more explicitly link channel stability to the hydrological events that produce channel change, specific discharge, q, (or discharge divided by the width of the river at that discharge) is used in this memo to represent the power of the river to erode and transport sediment. The threshold specific discharge, q_{c50}, is the discharge at which the median sized sediment on bed surface (D_{50}) is first entrained, and significant transport of the sediment found in the river channel begins. This typically occurs at flows less than the bank-full flow; experience in BC at Fishtrap Creek suggests that q_{c50} is about half the bank-full flow (Eaton et al. 2010).

The reason that gravel bed streams typically never experience flows that exceed q_{c50} by more than a factor of about 3 is that their banks are weak compared to the stream bed. Shortly after flows exceed q_{c50}, an unarmoured gravel bank is subject to forces capable of eroding it. While riparian vegetation can delay the onset of bank erosion in smaller rivers, the effect of riparian vegetation on bank strength disappears for rivers much deeper than 2 m at their bank-full flood stage (Eaton and Giles 2009), making large gravel bed streams particularly prone to hazardous lateral migration. Once bank erosion is initiated, gravel bed streams will widen, spreading the total flow over a greater area and maintaining specific discharge values close to about 3 times q_{c50}. This negative feedback between bank erosion and specific discharge is an important mechanism by which these systems maintain their relative stability.

Because gravel bed streams tend to respond to rare flood events by rapid bank erosion and channel widening, they often are transformed from single-threaded channels into multi-threaded (or braided) channels. In contrast, the larger sand bed streams found further downstream where valley gradients are lower typically have banks that are relatively strong due the the cohesive sediment found in them, which means they can (and do) sustain specific discharges much greater than 3 times q_{c50} (Church 2006). As a result, they are far less likely to experience extensive channel migration and seldom are transformed from single-thread to braided morphologies.

Recent research has demonstrated that, in threshold gravel bed streams, the stability of the channel is not controlled by the median sized sediment on the bed surface as has long been assumed; it is controlled by the largest grains on the bed surface, which most likely form a stable skeletal structure that traps and stores the smaller material found on the bed surface. Experiments by Eaton and Church (2004) and Eaton, MacKenzie, and Booker (2020) showed that gravel bed streams could not establish a stable, single-thread channel morphology for flow conditions during which the coarsest sediment in the stream was eroded and transported. Subsequent research demonstrated that the addition of a small quantity of sediment from the coarse tail of the bed surface grain size distribution was sufficient to prevent significant lateral migration of an experimental stream channel during bank-full flows (MacKenzie and Eaton 2017); the channels with and without the additional stabilizing sediment are shown in Fig. 1. Booker and Eaton (2020) similarly showed that the coarse tail of the bed sediment distribution controlled the stable gradient for in-channel sediment deposits at near-threshold flow conditions.

These findings indicate that there is the potential to modulate erosion and transport in gravel bed streams with only minor additions of stabilizing coarse sediment to the system. Eaton, MacKenzie, and Tatham (2022) tested one possible means of implementing a stability seeding approach that relies on bank erosion to recruit stabilizing sediment from the floodplain and high flows to redistribute the material within the channel. The stabilizing sediment used in these proof-of-concept experiments is close to the 90th percentile of the bed surface sediment size distribution, as shown in Fig. 2. The stabilizing sediments are mobilized during the highest flows but they are entrained less frequently and move shorter distances than do the majority of the sediment sizes on the bed surface.

More generally, sediment ranging from 50% to 100% of the largest mobilized particle in the stream can be used as stabilizing sediment. This corresponds approximately to sediment coarser than the 84th percentile of

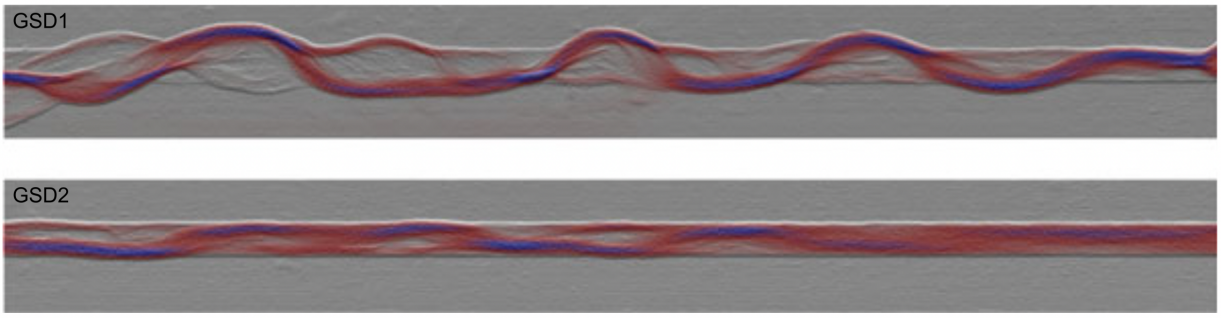

Figure 1: Maps of specific discharge are presented for two channels with nearly identical bed sediment distributions. The upper panel shows the channel pattern formed in the original bed material. The lower panel shows the morphology of a stream with a small addition of coarse sediment to the bed material. Figure taken from MacKenzie and Eaton, 2017.

the bed surface grain size distribution. Ideally, it should be rounded to sub-rounded in shape, consistent with sediment naturally found within the river. In most gravel bed streams, this will include sediment in the boulder size range, though some large cobbles will also act as stabilizing sediment in some gravel bed rivers.

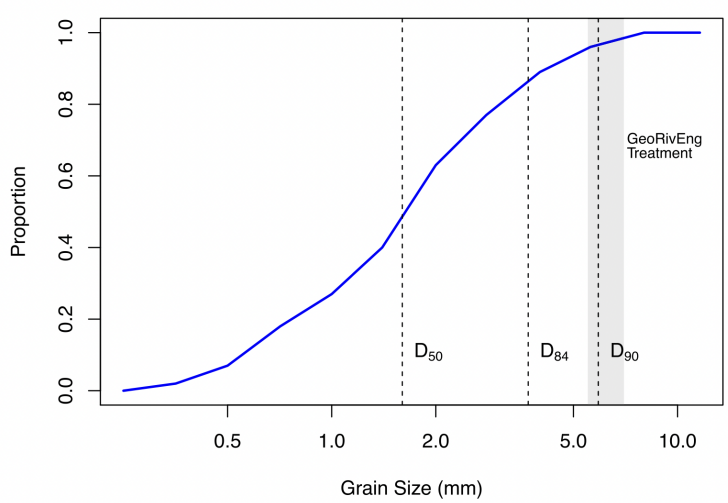

Figure 2: Experimental sediment size distribution and stabilizing sediment size range (GeoRivEng Treatment) for the proof-of-concept experiments by Eaton, MacKenzie and Tatham, 2022.

The treatment using this size of sediment will be referred to as the "stability seeding" experiments. Fig. 3. shows the channel morphology at the beginning of each experiment (top panel), the morphology after three floods of increasing magnitude (the largest of which is 3 times larger than the bank-full flood) for an untreated reach (second panel), the morphology after three floods for the reach with stability seeding (third panel), and the morphology for a reach with standard class 3 riprap (bottom panel).

The detailed post-flood morphology of the stability seeding treatment reach is shown in Fig. 4. The treatment involved placing a layer of stabilizing sediment one grain diameter thick on the bank top, right up to the edge of the channel but not within the channel. Fig. 5 presents the same information for the riprap treatment. Riprap was installed following the conventional design, including toeing the installation into the channel bed.

Briefly, the stability seeding treatment was able to modulate the rate of bank erosion during a range of flood events. As a result, the natural channel morphology comprising cut-banks, bars, pools and riffles was maintained throughout the experiment, although the channel was prevented from widening so much

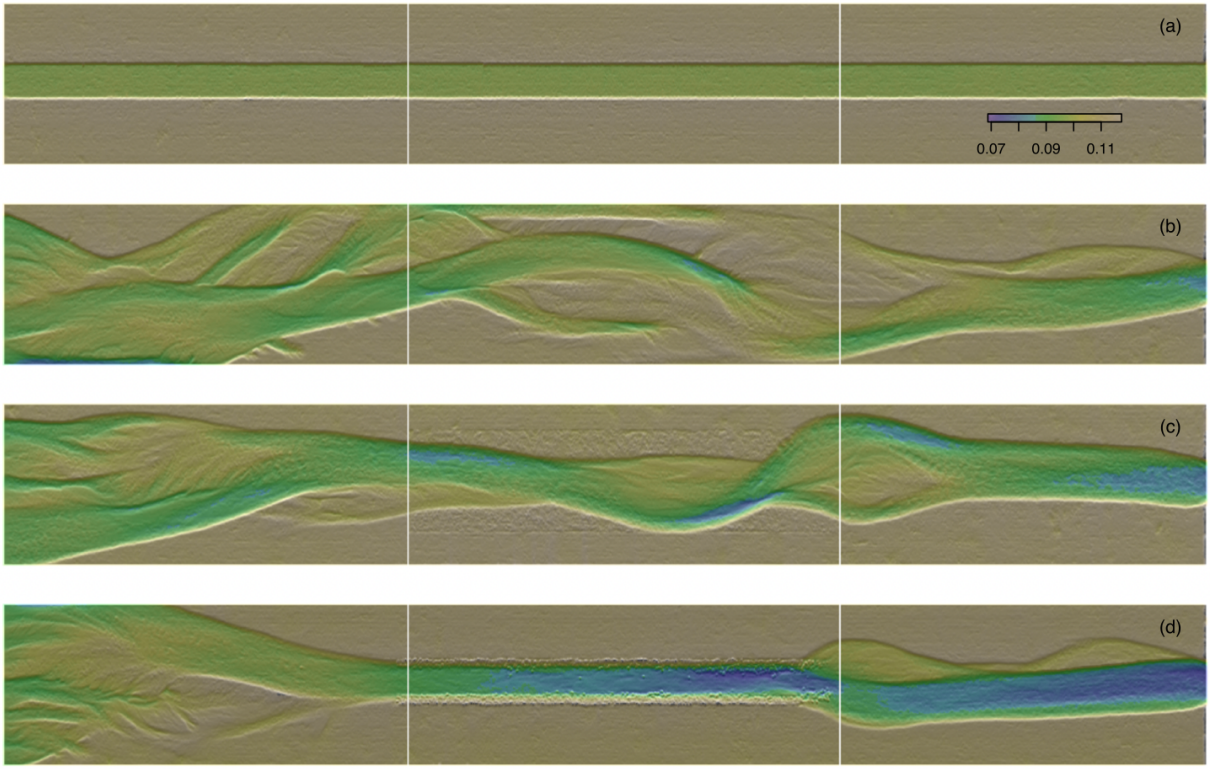

Figure 3: Hillshade images of channel morphology (a) at the beginning of each run; (b) with no stabilizing treatment; (c) with stability seeding treatment; and (d) with standard class 3 riprap treatment. Each experiment involved three floods of increasing magnitude, with the largest flood reaching 3 times the size of the bankful flood. Flow direction is from right to left. Only the middle sections of the experimental channels were stabilized; the upstream and downstream sections were left unprotected.

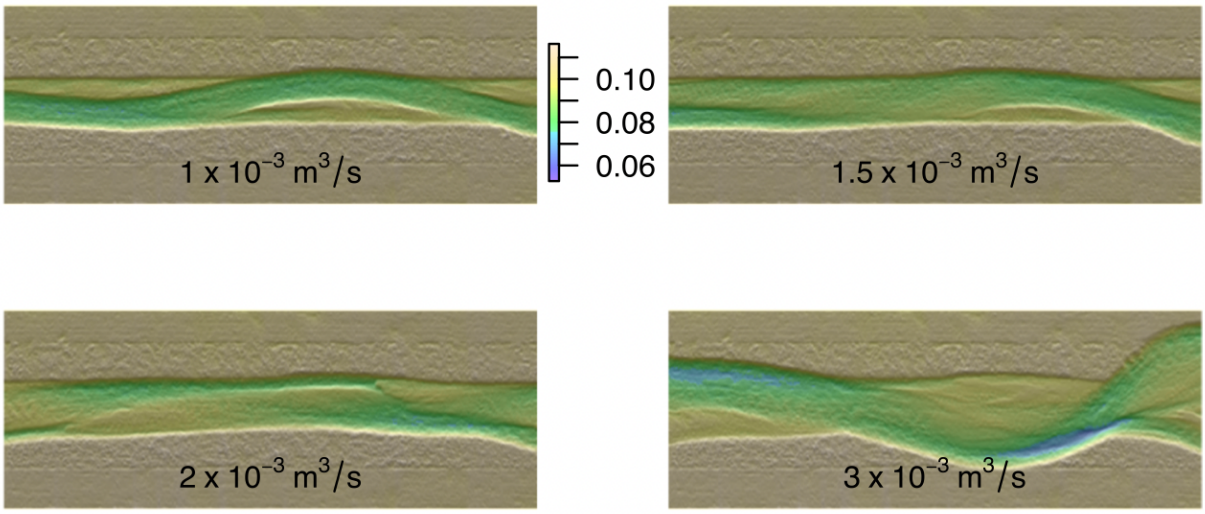

Figure 4: Morphology of the treated reach with stability seeding after four floods, ranging from the bankfull flow to 3 times the bankfull flow.

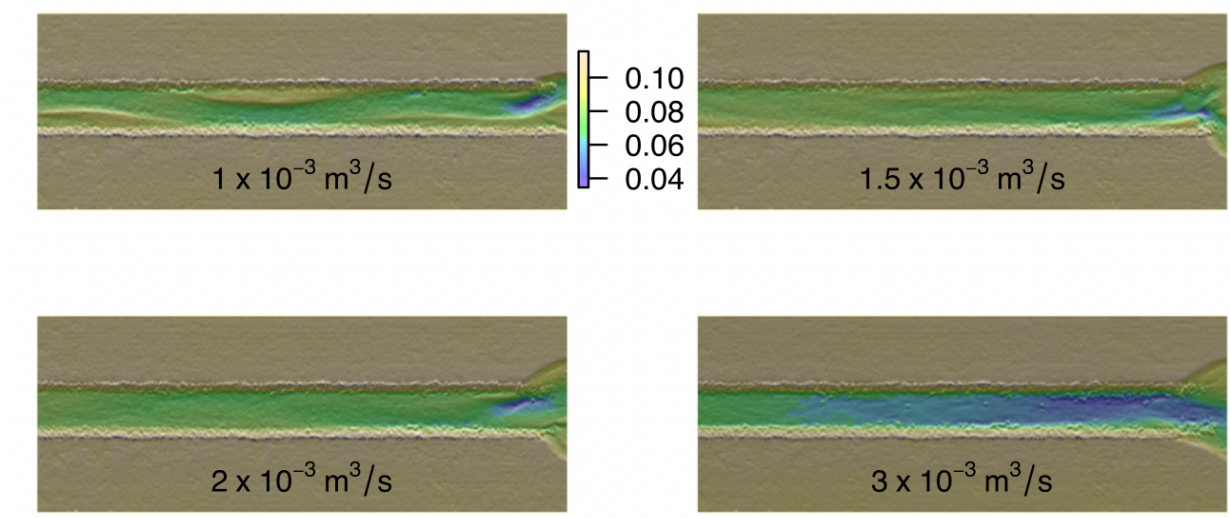

Figure 5: Morphology of the treated reach with class 3 riprap after four floods, ranging from the bankfull flow to 3 times the bankfull flow.

that it would transition to a braided channel pattern. As a result, a diverse suite of physical habitats was maintained, and the topographic variations responsible for generating flow into and out of the stream bed were maintained, thereby maintaining the quality of the potential spawning habitat associated with these hyporheic exchange patterns.

In contrast, standard riprap prevented any lateral channel migration, and prevented the stabilizing feedback between channel widening and specific discharge reduction from occurring. As a consequence, the riprap reach was subject to excessively high shear stresses and high rates of sediment transport, which produced significant vertical bed degradation, and the loss of channel complexity; by the end of the last flood, no bars, pools or riffles remained in the riprap reach. Over 75% of the channel bed in the riprap reach experienced net vertical bed scour that exceeded the mean bank-full water depth, which could pose a significant risk to buried linear infrastructure beneath the stream bed.

3 geomorphic effects and habitat benefits

There are several ways in which the stabilizing sediment could be delivered to the stream channel. The potential habitat benefits of each approach are slightly different and are described separately below. The actual habitat benefits of stability seeding in the field have not yet been studied, so the discussion below is speculative. The actual benefits that will occur in the field will depend largely on (a) how much of the stabilizing sediment is recruited by the river; and (b) where on the river bed it is deposited. Furthermore, the recruitment and redistribution of these stabilizing sediments only happens during floods capable of producing wide-spread bank erosion and channel widening (e.g. 50-year return period floods), so they would have no direct (negative or positive) effects on river habitat until after a rare flood event occurred.

3.1 stability seeding on the channel floodplain

The placement of a layer of stabilizing sediment on the floodplain adjacent to the channel banks has been tested experimentally (Eaton, MacKenzie, and Tatham 2022) and the potential benefits of this approach are reasonably well documented. It can be applied to both banks and in straight reaches where a straight channel alignment needs to be maintained (as in Figs 3, 4 and 5), to both banks of a sinuous, meandering channel (tested by Eaton, MacKenzie, and Tatham 2022 but not shown), or along a single eroding meander bend (tested in the lab, but not yet published).

(1) The first benefit of this approach is that it involves the minimum possible disturbance to the treated reach. No sediment is placed directly on the stream bed or banks, and sediment only enters the channel when it is recruited by bank erosion. In addition, the added material is indistinguishable from the bed material in terms of size and roundness. As a result, the effects on bed surface structure and porosity would be analogous to those that occur naturally.

(2) This approach could also be combined with riparian planting in and around the stabilizing grains, which would increase the likelihood that the plantings would remain undisturbed for long enough to establish a mature forest cover capable of moderating bank erosion rates on its own. This combination of stabilization and revegetation would help restore the natural linkages between the river and the rehabilitated riparian forest. This approach is likely to be particularly successful on streams with average bank heights of 1 m or less, since root reinforcement can be moderately to highly effective in streams of this size (Eaton 2006).

(3) If/when stabilizing sediments are introduced to the treated reach via bank erosion, it is likely that the natural sequences of bars, pools, and riffles will be maintained to a greater degree than if traditional riprap were used. This could help maintain more diverse physical habitat comprising slow and deep pools, and shallow and rapid riffles. It may also help maintain the topographic variability necessary to drive hyporheic exchanges between the stream the the river bed.

(4) Transitions from stable single-thread channels to multiple-thread braided channels during future rare floods will be less likely to occur. Braided streams are highly complex, but they often have little in the way of vegetative cover, and they may experience de-watering during low flows and/or elevated stream temperatures due to a lack of shade. Maintaining a single-thread channel reduces the potential magnitude of such impacts, even if some widening and channel modification does occur in the treated reach.

(5) Minor bank erosion may continue to occur within the treated reach, preventing a static channel bed from developing and maintaining the disturbance regime upon which the aquatic ecosystem depends.

(6) Stabilization of the channel bed (and in particular, of the riffles downstream of the treatment, where the treatment is installed on an active meander) could potentially modulate the amount of vertical scour that occurs, preventing the exposure of buried infrastructure. Where meander bends must be stabilized, it is often the case that the local reduction in sediment supply can cause the downstream riffle to degrade, steepening the gradient along the meander bend and possibly threatening the stabilization works. When the riffle degrades, the potential spawning habitat associated with the riffle is lost, and the riffle/pool morphology is replaced by a more uniform run or glide. Since the stabilizing sediment is mobile, it can be transported to the riffle, where it can potentially counter-balance the reduction in sediment supply due to meander stabilization.

3.2 stability seeding on channel banks

Where it is not feasible/desirable to stage the stabilizing sediment on the bank tops and to allow the river to recruit it when and where the banks experience migration, it is possible to add the stabilizing sediment as a facing on the toe of channel bank. Typically, such sediment additions will be placed upon an existing riprap installation where vertical degradation is a concern, or where the integrity of the riprap is compromised, but full-scale replacement is not feasible/necessary. This approach has not yet been tested experimentally (but will be soon). The benefits will be similar to those for the bank-top stability seeding approach, and it is likely that recruitment of the stabilizing sediment will require rare floods capable of eroding unprotected channel banks.

(1) The natural processes of erosion, transport and deposition will distribute the stabilizing grains within the channel when and where the channel becomes unstable.

(2) The addition of stabilizing grains to the face of a cut-bank along a meander bend will potentially off-set the sediment reduction associated with stabilizing the bend, and could help maintain the downstream riffle. This will likely help maintain diverse riffle /pool morphology and hyporheic exchange patterns while still preventing any lateral migration of the river from occurring.

(3) If stabilizing grains are introduced along the entire meander bend, then the stabilizing grains could reduce the potential for vertical incision along the channel, protecting buried infrastructure. The stabilizing grains could also help create complex sedimentary habitats by triggering the formation of stone lines, clusters and cells, which can provide important interstitial habitat for invertebrates and small/young fishes. The same features that reduce the potential for vertical incision create valuable benthic habitat.

3.3 stability seeding on the channel bed

In sections where vertical degradation of the channel is an imminent concern (e.g. at bridge crossings, or buried linear infrastructure crossings), it may be advantageous to place stabilizing sediment on the stream bed. The degree to which this (untested) stabilization approach will have the desired effect depends on how well the placements mimic the redistribution processes that have been produced in the laboratory experiments. Therefore the potential habitat benefits are less clear and are more likely to vary from site to site, depending on the details of the stabilization design.

(1) The stabilizing grains could potentially provide important interstitial habitat for invertebrates and small/young fishes by promoting the formation of stone lines, clusters and cells.

(2) Depending on the design, in-stream placement of stabilizing sediment could create/maintain sequences of bars, pools, and riffles. This could help maintain more diverse physical habitat and help promote hyporheic exchanges between the stream the the river bed.

4 monitoring

After implementing a stability seeding project, it is appropriate to conduct a monitoring program to document its effects. The stability seeding approach is relatively new, and post-implementation monitoring will yield important insights into its long-term effects. The precise nature of the monitoring will depend on the project design and the goals of the project, but overall, monitoring should seek to:

(1) collect annual or biannual (meaning every two years) aerial surveys of the project reach during low-flow conditions using an unmanned aerial vehicle (UAV) to document the post-implementation adjustment of the channel morphology, as well as the progressive re-vegetation of the channel where stability seeding has been combined with riparian planting;

(2) tag and trace a sample of boulder sized sediment used in the stability seeding to better understand where they are moving and how they are contributing to channel stability; and

(3) implement more detailed surveys, hydraulic modelling and sediment transport analysis following subsequent large floods that have the potential to mobilize and transport the stabilizing grains.

Because only floods with return periods of 10 years (or higher) will likely be capable of mobilizing and transporting the sediment grains used for stability seeding, the approach to monitoring needs to be opportunistic. That is, data should be collected regularly, while detailed analysis need only be conducted after a significant flood event has occurred. Fortunately, recent advances in data collection and analysis make this a cost-effective option. Nearly all the necessary data can be collected by conducting an aerial survey using a UAV.

4.1 Aerial surveys

Using UAVs, an aerial survey of a 500 m length of stream can be conducted in about the same amount of time as would be required to survey a single cross section using traditional methods. These surveys should be conducted during low flow conditions when as much of the channel as practical is exposed, and when the water turbidity is low.

Each survey will produce a high resolution orthophoto image of the study stream showing vegetation, large wood, bed sediment texture, and all other visible hydraulic and geomorphic features; and a geo-registered

digital elevation model of the reach (including the topography of the submerged parts of the stream) with a positional accuracy of about 2 to 5 cm. Following some recently developed procedures (Tamminga et al. 2014; Tamminga, Eaton, and Hugenholtz 2015; Tamminga and Eaton 2018), a wide range of physical and ecological assessments can be made using the orthophoto image and DEM, including:

(1) mapping riparian vegetation (considering density, type, health), bed surface grain sizes, and accumulations of large wood;
(2) estimating the water depth and bathymetry of the river system using the ratio of the red and green colour channels on the orthophoto image (as described by Tamminga, Eaton, and Hugenholtz 2015) and some calibration depths measured in the field on the date of the aerial survey;
(3) modelling the flow conditions relevant to fish habitat; and
(4) documenting the geomorphic effects of extreme flood events on channel morphology.

While the data collection process is relatively straightforward and efficient, it takes a much greater investment of time to perform the analyses outlined above. Therefore, the recommended approach to monitoring involves:

(1) collecting baseline data annually/biannually, generating orthophoto images of the project reach, and calculating a few simple metrics of channel change (such as change in vegetated area, vegetation type, and bank erosion near the project), which requires about 3 days of work per year by a team of two; and
(2) triggering an in-depth analysis of the data only once a significant flood has occurred (including mapping sediment texture, large wood position and abundance, changes to the project area, and hydraulic modelling of the the project reach at several reference flow levels), which requires about 2 months of work by an intern such as a MITACS-funded graduate or undergraduate student under the supervision of senior geoscientist.

If a period of 5 years passes without the occurrence of a flood large enough to trigger an in-depth analysis of the data (e.g. a 10-year return period flood or higher), it may be worth conducting an in-depth analysis anyway, if only to refresh the baseline data and to identify any subtle changes that may have occurred.

4.2 sediment tracking

One thing that UAV surveys cannot tell us about is the typical transport distances for stabilizing sediment once it is eroded from the bed. A key scientific question relevant to the stability seeding approach is: "where do the stabilizing grains go, once they are eroded, and how do they help stabilize the channel morphology?" Tracking the movement of the stabilizing grains following a large flood will help answer these questions.

The best way to track the movement of the stabilizing grains is to tag them with passive integrated transponders. These are tracking tags that require no power source, which were originally developed to track the movements of anadromous fish such as salmon. The transponder is activated when it is in close proximity to a specialized antenna, at which point it broadcasts a unique identity code. These have been used to track the movement of sediment along a river system (Lamarre, MacVicar, and Roy 2005; Wilcock, Pitlick, and Cui 2009). A suitable approach would be to tag 50 to 100 boulders installed as part of the stability seeding project, and track their movement during periodic re-surveys.

Because the erosion and transport of stabilizing grains occurs only rarely, re-surveys of the boulder locations should be conducted once a detailed assessment of the UAV imagery has been triggered (either by a flood with a return period of 10 years or higher, or after a period of 5 years with no detailed analysis). The re-survey should be conducted during low flows when as much of the project reach as possible can be waded safely. These surveys can be time-consuming if the sediment has traveled a long way from where they were installed, and may take a week to complete for a team of two people in the field.

4.3 ground surveys

When a detailed analysis of the UAV survey data is triggered, it is worth considering a direct survey of the channel bathymetry and the water depths in the project reach. These data can be used to verify the water depth estimates based on UAV imagery. Such a survey could be combined with a survey of the stabilizing sediment movement during low flow conditions.

references

Booker, WH, and BC Eaton. 2020. "Stabilising Large Grains in Self-Forming Steep Channels." *Earth Surface Dynamics* 8 (1): 51–67. https://doi.org/10.5194/esurf-8-51-2020.

Church, M. 2006. "Bed Material Transport and the Morphology of Alluvial River Channels." *Annual Review of Earth and Planetary Sciences* 34 (1): 325–54. https://doi.org/10.1146/annurev.earth.33.092203.122721.

Eaton, BC. 2006. "Bank Stability Analysis for Regime Models of Vegetated Gravel Bed Rivers." *Earth Surface Processes and Landforms* 31 (11): 1438–44. https://doi.org/10.1002/esp.1364.

Eaton, BC, CAE Andrews, TR Giles, and JC Phillips. 2010. "Wildfire, Morphologic Change and Bed Material Transport at Fishtrap Creek, British Columbia." *Geomorphology* 118 (3-4): 409–24. https://doi.org/10.1016/j.geomorph.2010.02.008.

Eaton, BC, and M Church. 2004. "A Graded Stream Response Relation for Bed Load–dominated Streams." *Journal of Geophysical Research* 109 (F3). https://doi.org/10.1029/2003jf000062.

Eaton, BC, and TR Giles. 2009. "Assessing the Effect of Vegetation-Related Bank Strength on Channel Morphology and Stability in Gravel-Bed Streams Using Numerical Models." *Earth Surface Processes and Landforms* 34 (5): 712–24. https://doi.org/10.1002/esp.1768.

Eaton, BC, LG MacKenzie, and WH Booker. 2020. "Channel Stability in Steep Gravel–cobble Streams Is Controlled by the Coarse Tail of the Bed Material Distribution." *Earth Surface Processes and Landforms* 45 (14): 3639–52. https://doi.org/10.1002/esp.4994.

Eaton, BC, LG MacKenzie, and C Tatham. 2022. "Modulating the Lateral Migration of a Gravel Bed Channel Using the Coarse Tail of the Bed Material Distribution." *Earth Surface Processes and Landforms* 47 (5): 1304–21. https://doi.org/10.1002/esp.5318.

Lamarre, H., B. MacVicar, and A. G. Roy. 2005. "Using Passive Integrated Transponder (PIT) Tags to Investigate Sediment Transport in Gravel-Bed Rivers." *Journal of Sedimentary Research* 75 (4): 736–41. https://doi.org/10.2110/jsr.2005.059.

MacKenzie, LG, and BC Eaton. 2017. "Large Grains Matter: Contrasting Bed Stability and Morphodynamics During Two Nearly Identical Experiments." *Earth Surface Processes and Landforms* 42 (8): 1287–95. https://doi.org/10.1002/esp.4122.

Tamminga, AD, and BC Eaton. 2018. "Linking Geomorphic Change Due to Floods to Spatial Hydraulic Habitat Dynamics." *Ecohydrology* 11 (8): e2018. https://doi.org/10.1002/eco.2018.

Tamminga, AD, BC Eaton, and CH Hugenholtz. 2015. "UAS-Based Remote Sensing of Fluvial Change Following an Extreme Flood Event." *Earth Surface Processes and Landforms* 40 (11): 1464–76. https://doi.org/10.1002/esp.3728.

Tamminga, AD, C Hugenholtz, BC Eaton, and MF Lapointe. 2014. "Hyperspatial Remote Sensing of Channel Reach Morphology and Hydraulic Fish Habitat Using an Unmanned Aerial Vehicle (UAV): A First Assessment in the Context of River Research and Management." *River Research and Applications* 31 (3): 379–91. https://doi.org/10.1002/rra.2743.

Wilcock, Peter, John Pitlick, and Yantao Cui. 2009. "Sediment Transport Primer: Estimating Bed-Material Transport in Gravel-Bed Rivers." https://doi.org/10.2737/rmrs-gtr-226.